Charles University in Prague
Faculty of Mathematics and Physics

DIPLOMA THESIS

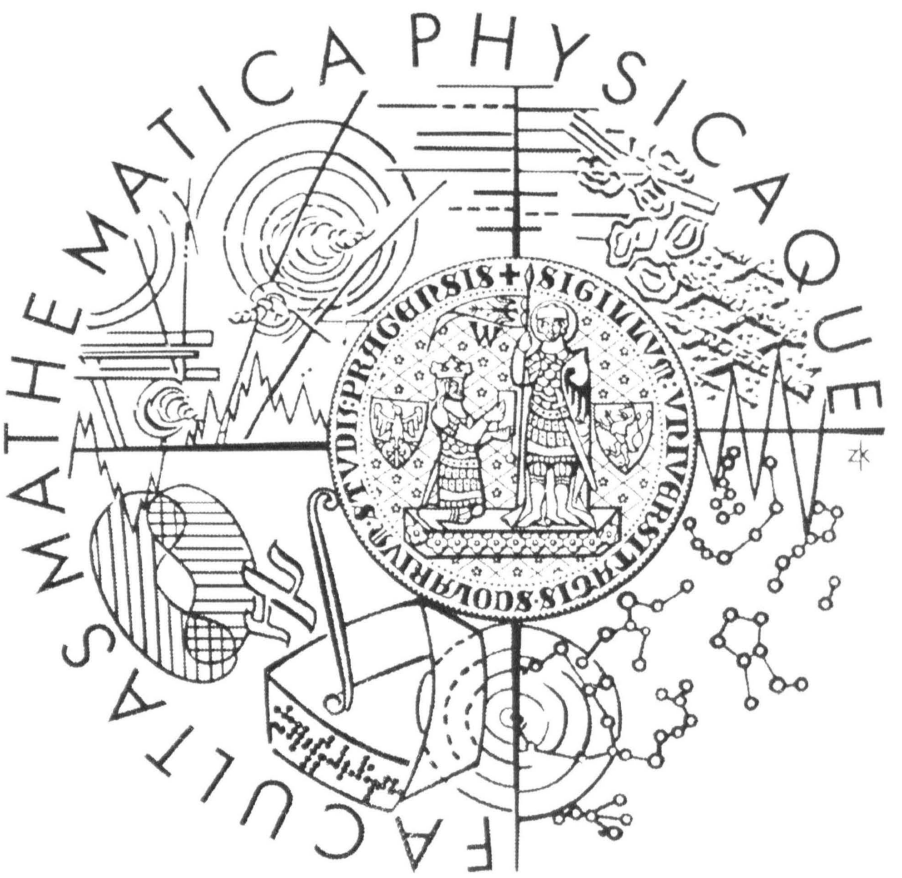

Miroslava Fraňová

Interaction of β-cyclodextrine with biologically active molecules

Department of Chemical Physics and Optics
Diploma Thesis Supervisor: Prof. RNDr. Pavla Čapková, DrSc.
Study Field: Biophysics

ACKNOWLEDGEMENT

I would like to thank to Prof. RNDr. Pavla Čapková DrSc. for supervising my Diploma thesis, to Zentiva for providing the experimental back-up for this study and to the dean of the faculty for enabling together with Zentiva the participation at the 12th cyclodextrine symposium where most of backround information for this thesis was gained.

Hereby I confirm that I wrote this Diploma Thesis entirely by myself and with the use of listed references. I agree with lending this Diploma Thesis.

Prague, March 29th 2005

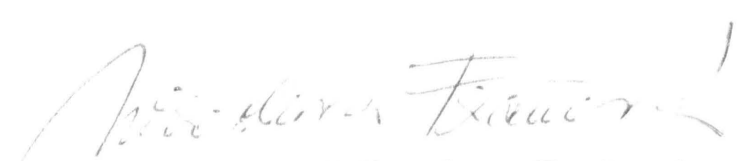

Miroslava Fraňová

CONTENTS

LIST OF FIGURES

Title: *Interaction of β-cyclodextrine with biologically active molecules*
Author: *Miroslava Fraňová*
Department: *Department of Chemical Physics and Optics*
Supervisor: *Prof. RNDr. Pavla Čapková, DrSc.*
Supervisor's e-mail address: *capkova@karlov.mff.cuni.cz*
Abstract:
New compound containing tibolone (TB) and β-CD in ratio 1:20 was experimentally prepared. Its structure could not be determined from X-ray diffraction pattern itself. With the help of molecular simulations we found that the new entity is TB-β-CD complex and that TB can be immersed into the β-CD cavity in two ways, OH group inside and outside the basket, and that the host-guest interaction energy is in both cases nearly the same. We used classical molecular dynamic simulations in NVT ensemble and cff91 force field to study the stability of tibolone versus isotibolone at room temperature and at temperature of 340K. Molecular dynamics showed that isotibolone is more stable than tibolone and that tibolone prefers the conformation with negative inversion angle (angle between the bond C_2-C_4 and the plane defined by atoms C_1, C_2 and C_5). Stability of inclusion complex TB-β-CD was studied for TB being immersed into the CD with OH group inside and outside the basket. Model with C_2-C_4 bond inside the basket (OH group outside the basket) was found to be relatively stable whereas the model with C_2-C_4 bond outside the basket was found less stable, considering the statistical inversion angle distribution and its change with temperature.

Keywords: cyclodextrine, complex, conformational behaviour, molecular simulation

Názov práce: *Interakcia β-cyklodextrínu s biologicky aktívnymi molekulami*
Autor: *Miroslava Fraňová*
Katedra: *Katedra chemickej fyziky a optiky*
Vedúci diplomovej práce: *Prof. RNDr. Pavla Čapková, DrSc.*
e-mail vedúceho: *capkova@karlov.mff.cuni.cz*
Abstrakt:
Zmiešaním tibolónu a β-CD v pomere 1:20 sa experimentálne pripravil produkt, ktorého štruktúra sa použitím samotného difraktogramu nedala jednoznačne určiť. S pomocou molekulárnych simulácií sme zistili, že tento produkt tvorí TB-β-CD complex, a že tibolón môže byť do dutiny β-CD vložený dvoma spôsobmi, a to OH skupinou smerom dovnútra a OH skupinou smerom von. V oboch prípadoch je interakčná energia hosť-hostiteľ skoro rovnaká. Pre štúdium stability tibolónu v porovnaní so stabilitou isotibolónu pri izbovej teplote a teplote 340K sme použili klasickú molekulárnu dynamiku so súborom NVT a silovým poľom cff91. Výsledky molekulárnej dynamiky ukázali, že isotibolón je stabilnejší, a že tibolón preferuje konformáciu so záporným inverzným uhlom (uhol medzi väzbou C_2-C_4 a rovinou definovanou atómami C_1, C_2 a C_5). Stabilitu inklúzneho komplexu TB-β-CD sme študovali pre prípad tibolónu vloženého do dutiny CD OH skupinou smerom von a OH skupinou smerom dnu. Model s väzbou C_2-C_4 vo vnútri košíka (a teda s OH skupinou smerom von) sa javil ako relatívne stabilný, zatiaľ čo model s väzbou mimo košíka sa javil ako menej stabilný, berúc v úvahu štatistické rozloženie inverzného uhlu, ktoré je závislé na teplote.

Kľúčové slová: cyklodextrín, komplex, konformačné zmeny, molekulárne simulácie

INTRODUCTION

Drug design is an iterative process which begins when a chemist identifies a compound that displays an interesting biological profile and ends when both the activity profile and the chemical synthesis of the new chemical entity are optimized. Traditional approaches to drug discovery rely on a step-wise synthesis and screening program for large numbers of compounds to optimize activity profiles. Biological activity is dependent on the three-dimensional placement of specific functional groups. Computational tools are being successfully used, in conjunction with traditional research techniques, to examine the structural properties of existing compounds, develop and quantify a hypothesis which relates these properties to observed activity and utilize these "rules" to predict properties and activities for new chemical entities. [1]

Computational chemistry/molecular modeling is the science of representing molecular structures numerically and simulating their behaviour with the equations of quantum and classical physics. Computational chemistry programs allow scientists to generate and present molecular data including geometries (bond lengths, bond angles, torsion angles), energies (heat of formation, activation energy, etc.), electronic properties (moments, charges, ionization potential, electron affinity), spectroscopic properties (vibrational modes, chemical shifts) and bulk properties (volumes, surface areas, diffusion, viscosity, etc.). As with all models however, the chemist's intuition and training is necessary to interpret the results appropriately. Comparison to experimental data, where available, is also important to guide both laboratory and computational work.[1]

Interaction of β-cyclodextrine with biologically active molecule tibolone has been studied. In the present work, the experimental data provided by pharmaceutical company Zentiva have been compared and complemented with the results of molecular modeling in order to obtain important information about the structure and stability of a β-cyclodextrine-tibolone inclusion complex as the structure could not have been identified only from experimental data itself. New compound might either have been a new chemical entity or it could have just been a mixture of already known compounds.

All experimental and computational methods used in this study are described in the theoretical part of this work, as well as there is the information about cyclodextrines and tibolone. Second part of the work describes the strategy and particular steps of molecular simulations together with the results achieved. The main goal of the work was to find out the structure of the new compound and to study conformational behaviour of tibolone molecule at room temperature and 340K using the molecular dynamics and both these missions were successfully accomplished.

1. THEORY

1.1 CYCLODEXTRINES

1.1.1 General Information about Cyclodextrines

Cyclodextrines, sometimes also named cyclomaltoses or cycloamyloses are macrocyclic oligosaccharides obtained from the enzymatic degradation of starch. When glucosyltransferase enzyme (CGT) degrades starch, the primary product from the splitting of the glycosidic linkage undergoes an intramolecular reaction without water molecule involved in it. D-glucose units linked by α–(1–> 4) glycosidic bonds are formed. Three major cyclodextrines; α-cyclodextrine, β-cyclodextrine and γ-cyclodextrine comprises 6,7,8 of these units respectively (see Figure 1).

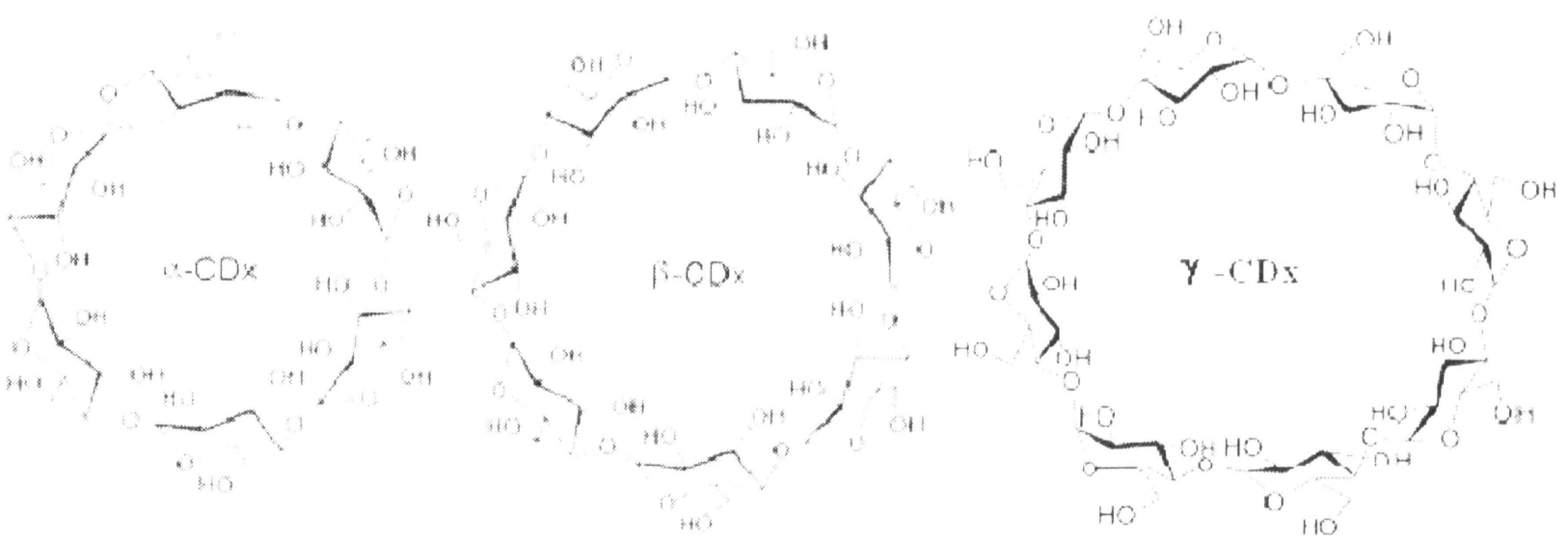

Figure 1: α-cyclodextrine, β-cyclodextrine and γ-cyclodextrine [2]

Cyclodextrines were isolated for the first time by Villiers over 100 years ago from a culture medium of Bacillus macerans. The foundation of the cyclodextrine chemistry was laid down by Schardinger who discovered their cyclic structure. Therefore cyclodextrines are sometimes called Schardinger's dextrins. [3]

Commercially, cyclodextrines are still produced from starch, but more specific enzymes are used to selectively produce consistently pure, or -cyclodextrine, as desired.[4]

1.1.2 Cyclodextrine Inclusion Complexes

In water the cavity of cyclodextrines (CD) can not be considered as an empty space, as it is filled with water molecules. When the cavity of cyclodextrines is occupied by a molecule(s) of another substance an inclusion complex is formed. Inclusion complex always consists of at least two molecules, one being a "host" molecule (in this case cyclodextrines) and other(s) being "guest" molecules(s), which are partly or totally included in the host molecule strictly by physical forces, without covalent bonding.

Chemical factors include the character of the host-guest interaction and mutual relation between the host-guest and guest-guest interaction energy. The inclusion of guest molecule in a CD cavity is energetically favoured process, as the water molecules originally included in hydrophobic CD cavity are replaced by a less polar guest. The complex formation depends on the polarity of the guest molecule. Strongly hydrophilic molecules, strongly hydrated and ionized groups are not, or only very weakly complex able. That means that only molecules which are less polar than water can be complexed by cyclodextrines. Consequently the host-guest interaction between the apolar CD cavity and apolar guest molecule is mainly ruled by Van der Waals forces. The effect of guest-guest interaction is important in case of an excessively strong cohesive forces between the guest molecules. The strong guest-guest interactions obstruct their separation, which is a precondition for the inclusion. Consequently the crystals with the melting point higher than 200 °C can not be complexed.[5]

The cavity of cyclodextrines can embrace molecule(s) of approximate size of two benzene rings to form crystalline inclusion complexes. The usual stoichiometry of the inclusion complexes is 1:1, 1:2 and 2:1, depending on the size of the guest molecules.

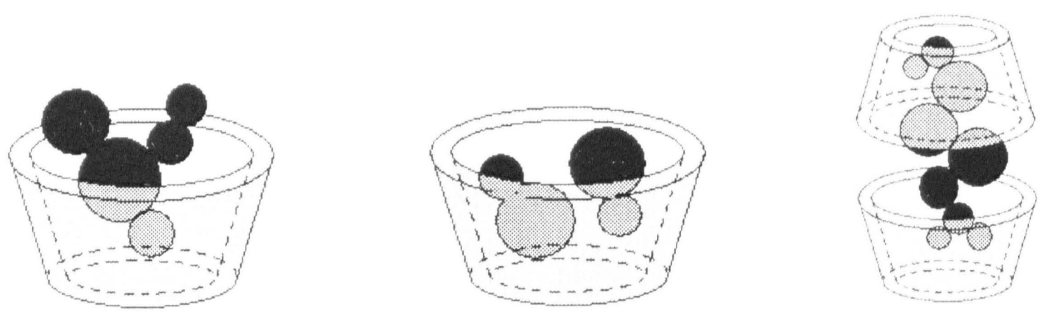

Figure 2: Example of inclusion complexes with stoichiometry 1:1 (A), 1:2 (B) and 2:1 (C)

1.1.3 Structure of Cyclodextrine Inclusion Complexes

Cyclodextrine inclusion complexes may crystallize in three different forms, depending on the nature and size of guest molecules: Herringbone-type cage; Brick-type cage and Channel-type with either head-to-head or head-to-tail arrangement of CD molecules. In the cage-type crystal structure the cavity of each CD molecule is blocked on both sides by the adjacent CD molecules. In this type of arrangement the CD molecules can be packed crosswise in a herringbone fashion or in a brick-wall fashion. In the channel-type crystal structures the CD baskets are stacked in a roll so that the cavities form infinite channels. The guest molecules are embedded into endless channels, formed by aligned cavities. This alignment can be either head-to-head or head-to-tail.See Figure 3.[5]

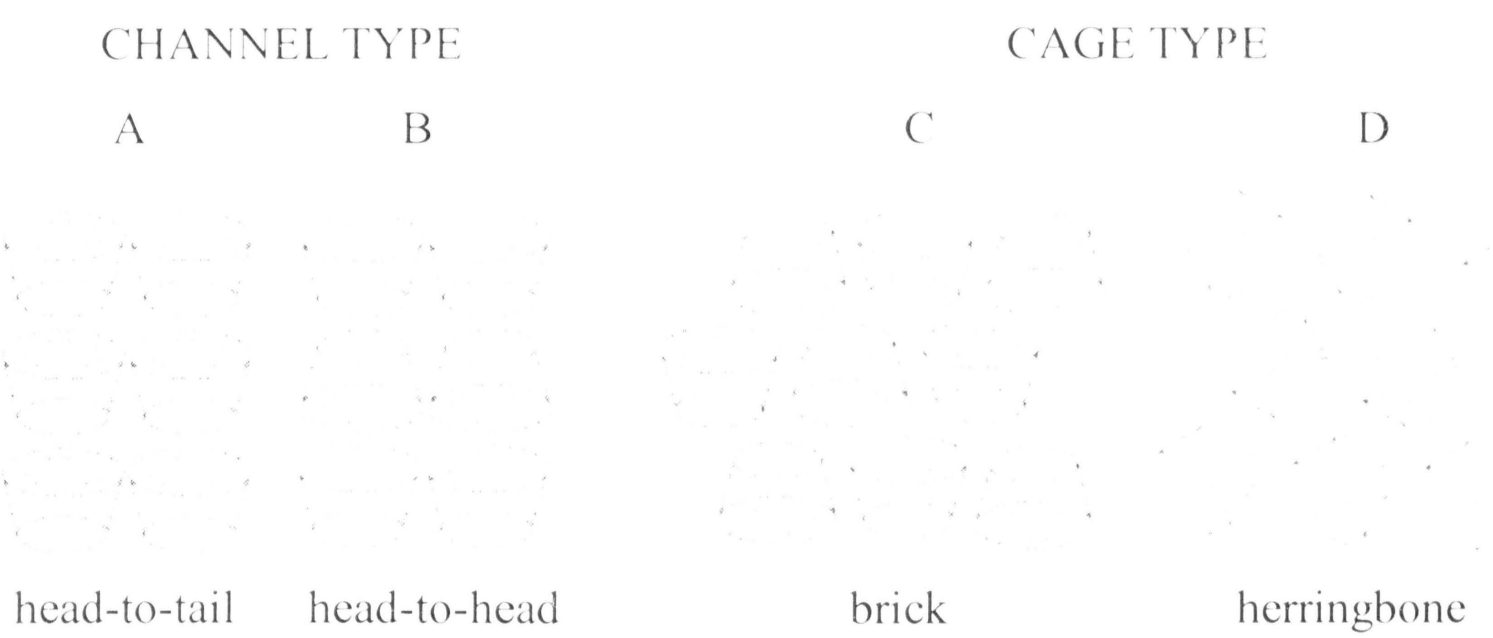

Figure 3: Channel (A,B) and cage (C,D) alignment of cyclodexrin molecules in crystal structure

Crystal packing of inclusion complexes in case of α-CD with small guests like iodine, methanol to 1-butanol is cage-type with herringbone motif. With larger guests α-CD prefers channel-type crystal structure; α-CDs complexes with small aromatic guests have slightly distorted baskets due to the benzene ring inside the cavity packed in the brick-type cage structure. β-CD forms herringbone-type cage complexes with small guests. Larger guests are located within double baskets formed between two CD molecules. These CD dimmers can be stacked either collinearly to form channel-type structure, or can be displaced sideways to different degrees. γ-CD forms herringbone

type cage structure only with water. γ-CD complexes with other guests crystallize in channel-type structures.[5]

In some cases, guest molecules are also found co crystallized between the CD molecules, that means guest molecules are not included, but bound by hydrogen bonding to CD hydroxyl, forming an non-inclusion "outer sphere complex". The complex formation, structure type, stability and solubility are the result of geometrical and chemical factors which determine the host-guest complementarity. Geometry and size of the guest molecule in relation to the size of CD basket is naturally the crucial factor in the complex formation. The α-, β- and γ-CDs with different internal cavity diameter (see Figure 4) are able to accommodate molecules of different size (α-, β- and γ-CD has 6-,7- and 8-membered ring respectivelly). For example naphtalen is too bulky for α-CD and anthracene fits only into γ-CD. The included molecules are normally oriented in the CD basket in such a position as to achieve the maximum contact between the hydrophobic part of the guest and the apolar CD cavity. The hydrophilic part of the guest remains as far as possible at the outer face of the complex. Too small guest molecules can be statistically disordered in the cavity volume, so that it is sometimes impossible to locate them properly. [5, 6, 7]

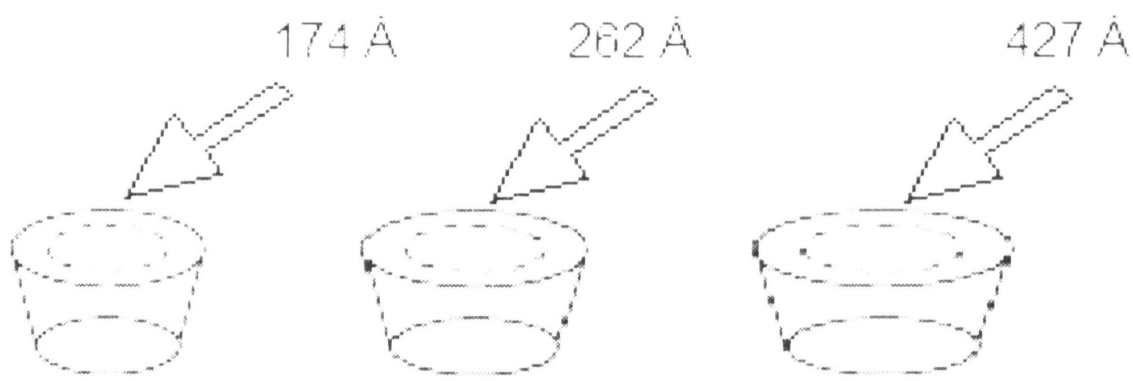

Figure 4: Cavity volume of α-CD, β-CD and γ-CD respectively.

1.1.4 β-cyclodextrine

β-cyclodextrine (β-CD) is also known as cycloheptaamylose, betadex, kleptose or Schardinger B-dextrin. Its seven glucopyranose units form a truncated cone with a hydrophilic pherifery and hydrophobic cavity in the center. All secondary hydroxyl groups are situated at the wider edge of the ring, and all the primary hydroxyl groups at

the other one. The rotation of primary hydroxyl groups decreases the effective diameter of the narrower side of the cavity. The structure and approximate dimensions of β-CD are shown in Figure 5.

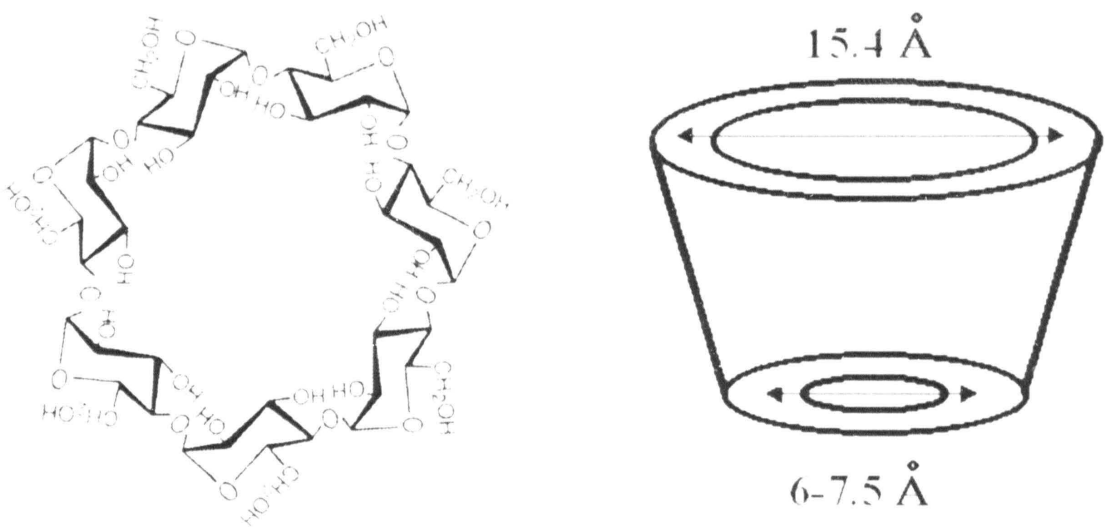

Figure 5: Structure and dimensions of BCD [8, 9]

The C_2-OH groups of the glucose units can form a hydrogen bond with the C_3-OH groups of the adjacent glucose unit. [6] These hydrogen bonds make β-CD a rigid structure with the lowest solubility in water of all cyclodextrine.

Clean β-CD was discovered to crystallize only in herringbone cage type fashion. Hydrated β-CD has 2 crystal forms: β-CD11H_2O (known from X-ray) and β-D12H_2O (known from neutron diffraction studies). These two forms differ mainly in the distribution of water molecules inside the cavity. Small differences in crystal lattice parameters are also being observed. β-CD11H_2O contains 11 water molecules (6.12 in the cavity and 4.88 in the interstices). They are distributed together over 16 positions (8 in the cavity, 8 in the interstices). Cavity water forms only two hydrogen bonds to the host β-CD, and 6 contacts to neighbouring β-CDs. Positions of these molecules are more ordered than those of crystal water* (water in the interstices). β-CD12H_2O contains 12 water molecules (6.5 in the cavity and 5.5 in the interstices).[6]
Characteristics of β-CD are summarised in table 1.

** Cyclodextrines crystallised from water are not pure but contain water molecules. Some water molecules become integral parts of the crystal structure (known as crystal water) and others are placed inside the cavity of cyclodextrine.[6]*

The intensity of reflections in the X-ray powder diagrams of cyclodextrines is very dependant on number and position of water molecules. Elimination of water by drying decreases the intensity of reflections, finally resulting in an amorphous structure. The change in crystallinity of β-CD as a funcion of dehydration and mechanical grinding is reflected in the X-ray diffraction pattern.

The degree of hydration of β-CD is dependant on relative humidity (RH). While at 100% RH the degree of hydration is 11 water molecules/molecule of β-CD, below 20% RH it is only about 4 molecules of water/molecule β-CD. [6]

No. of glucose units	7
Mol. wt.	1135
Solubility in water g 100 ml $^{-1}$ at room temp.	1.85
$[\alpha]^{25}_{D}$	162.5+-0.5
Cavity diameter Å	6.0-6.5
Height of torus Å	7.9+-0.1
Diameter of outer periphery Å	15.4+-0.4
Approx. volume of cavity Å^3	262
Approx. cavity volume in 1 mol CD (ml)	157
in 1 g CD (ml)	0.14
Crystal forms (from water)	Monoclinic parallelograms
Crystallographic parameters:	
C'_1- O_4- C_4 angle	117.7 °
Φ°/ Ψ°	169°/-172°
O_4...O'_4 distance Å	4.39
O_2...O'_3 distance Å	2.86
Crystal water wt. %	13.2-14.5
Diffusion constant at 40 °C	3.223
Partial molar volumes in solution (ml mol $^{-1}$)	703.8
Adiabatic compressibility in aqeuous solutions (ml mol $^{-1}$ x 10^4)	0.4

Table 1: Characteristics of β-CD,[6]

1.1.5 Use of β-cyclodextrine

Controlled release - BCD can be used to control the release of active ingredients, such as drugs, flavors and so on.

Stabilization - Many active ingredients such as flavors are sensitive to light, heat or air. Encapsulation of a 'guest' substance in cyclodextrine provides protection, resulting in increased shelf-life and a reduced loss of active ingredients owing to degradation or evaporation.

Increased solubility - BCD is itself soluble in water, and can greatly increase the solubility of highly water insoluble substances.

Protection against volatilization - Volatilization causes products to lose flavour and other qualities over time. When complexed with BCD, the volatile components display high stability.

Taste modification - BCD can improve the taste of foods or drugs by masking unpleasant odors through complex formation.

β-CD Application in pharmaceuticalindustry - A drug substance has to have a certain level of water solubility to be readily delivered to the cellular membrane, but it needs to be hydrophobic enough to cross the membrane. The majority of pharmaceutical active agents do not have sufficient solubility in water and traditional formulation systems for insoluble drugs involve a combination of organic solvents, surfactants, and extreme PH conditions, which often cause irritation or other adverse reactions. BCD is not irritant and offer distinct advantages such as the stabilization of active compounds, reduction in volatility of drug molecules, and masking malodors and bitter tastes. [10]

1.2 BIOLOGICALLY ACTIVE MOLECULES

1.2.1 Choice of the Biologically Active Molecules

The biologically active molecules for this study were chosen in cooperation with the pharmaceutical company (Zentiva). The choice was done according to the availability of the experimental measurements, problems raised during structure determination and according to the usefulness in the future production of this drug for human use.

1.2.2 Tibolone as the Biologically Active Molecule

What is tibolone?

Tibolone (figure 6, 7 and 8) is a synthetic steroid that combines progestogenic and androgenic properties as well as oestrogenic effects. These three groups of hormones are naturally produced by the ovaries (the female gonads).

What is tibolone used for?

Tibolone is a compound that can be selectively metabolized by individual tissues to its estrogenic, progestogenic, or androgenic metabolites and hence exhibits tissue-specific hormonal effects. Women treated with tibolone report significant reductions in vaginal dryness and dyspareunia, effects that may be secondary to both estrogenic and androgenic actions.

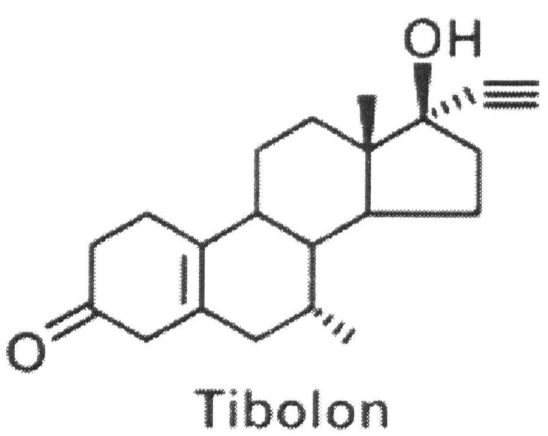

Figure 6: Structure of tibolone [11]

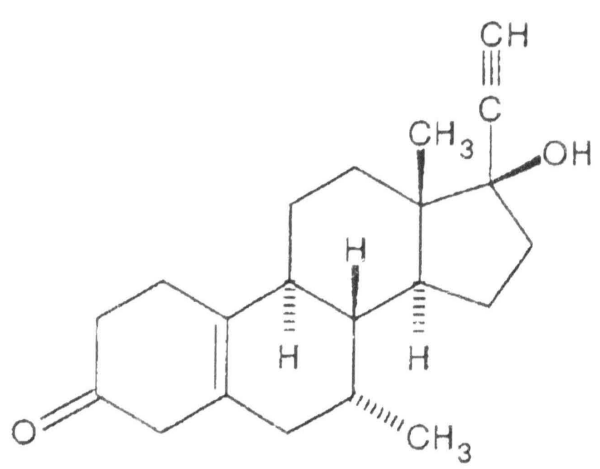

Figure 7: Structure of tibolone [12]

Tibolone is licensed for the treatment of menopausal symptoms e.g. hot flushes and also for decreased libido at this time. Since March 1997, it has been licensed to be used in the prevention of osteoporosis in post menopausal women. Since tibolone does not stimulate endometrial tissue at any site, it is particularly useful in patients with a past history of endometriosis.[13]

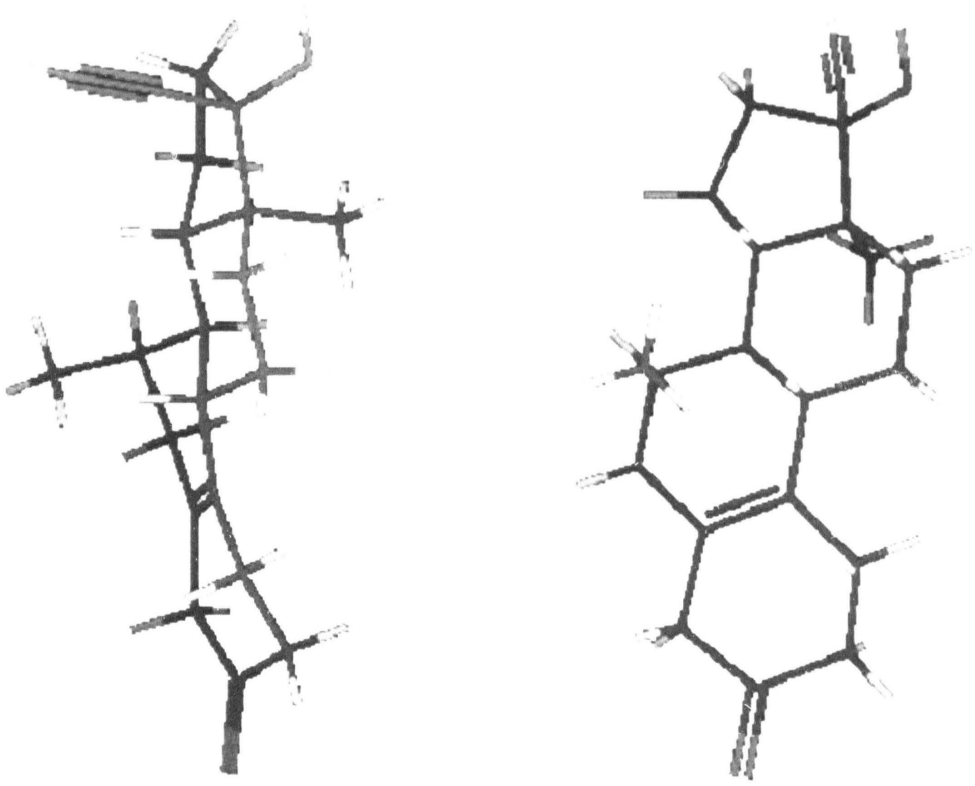

Figure 8: Pictures of tibolone made in Cerius

1.2.3 Tibolone and its Metabolites

Tibolone itself does not have the typical characteristics for estradiol receptor bonding and therefore it is not responsible for the estrogenic impacts on bones, vagina, etc. Tibolone first has to metabolise in the woman's body before it takes this effective form (figure 9).

After oral administration tibolone quickly metabolises with the help of 3α and 3β hydroxysteroiddehydrogenase (HSD) into 3α– and 3β–hydroxy-tibolone (-OH-tibolone). Both metabolites have the half life of about 7 hours however 4 times more 3α-hydroxy-tibolone than 3β–hydroxy-tibolone is found in the circulation. These two metabolites are responsible for the estrogenic activity.

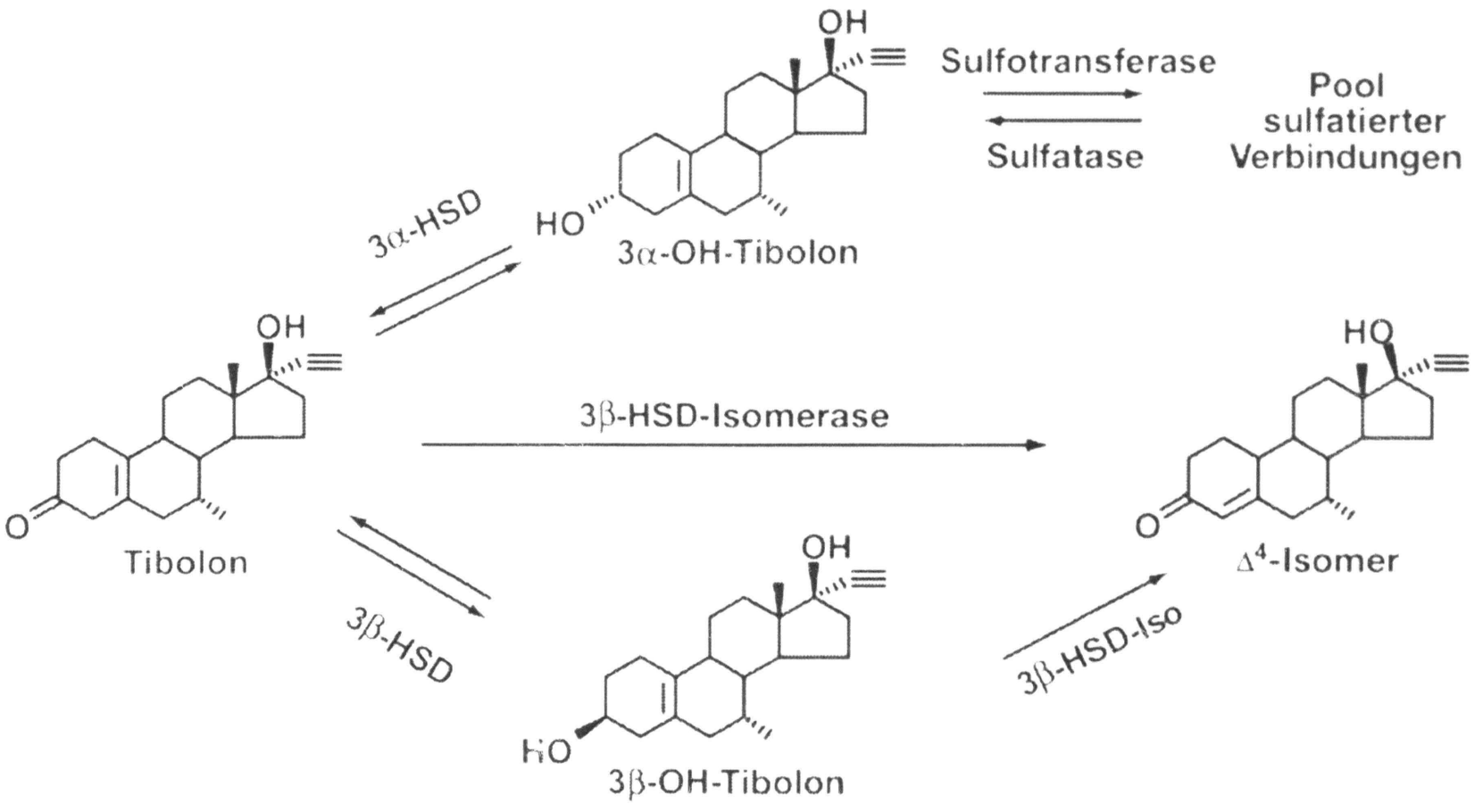

Kloosterboer HJ Journal fur Menopause 2003; 10 (Sonderheft 3): 2 8. (Ausgabe fur Osterreich) ©

Figure 9: Schematic illustration of tibolone, active enzymes and metabolites produced. [11]

During the activity of 3β-HSD- isomerase the third metabolite Delta-4-isomer (Δ^4 isomer, isotibolone) directly from tibolone is formed. The potential substrate for it is also 3β-hydroxy-tibolone. In this case it can not be overseen that the OH metabolites formation is reversible process apart from double bond overleaping on 4^{th} and 5^{th} carbon atom. Delta 4 Isomer is from circulation quickly eliminated and its half life can not be measured. [11]

1.3 MOLECULAR SIMULATIONS

1.3.1 Molecular Mechanics and Energy Minimization

Molecular mechanics can be considered to arise from the Born-Oppenheimer approximation, which assumes that the motions of the nuclei of a molecule are independent of the motions of the electrons. In molecular mechanics calculations, the arrangement of the electrons is assumed to be fixed and the positions of the nuclei are calculated. Molecular mechanics is a mathematical formalism which attempts to reproduce molecular geometries, energies and other features by adjusting bond lengths, bond angles and torsion angles to equilibrium values that are dependent on the hybridization of an atom and its bonding scheme. Rather than utilizing quantum physics, the method relies on the laws of classical Newtonian physics and experimentally derived parameters to calculate geometry as a function of steric energy. The general form of the molecular mechanics equation is

$$U_{total} = \sum \left(E_b + E_\theta + E_\phi + E_{nb} + E_\delta + E_{Coul} + E_{hb} \right) \qquad (1)$$

where $\sum E_b$ is the total bond deformation energy, $\sum E_\theta$ the total valence angle deformation energy (sometimes a supplemental term E_{UB} Urey Bradley potential is calculated), $\sum E_\phi$ the total torsional angle deformation energy, $\sum E_{nb}$ the total non-bonded (van der Waals) interaction energy, $\sum E_\delta$ the out-of-plane bending component of the steric energy, $\sum E_{Coul}$ the electrostatic interaction energy and $\sum E_{hb}$ the hydrogen bonding interaction energy. The individual energy terms were calculated using simple functions. [1]

Bonds were modelled as springs that obey Hooke's law (eq. 2), where k_b is the force constant or spring "strength" and r_0 is the ideal bond length or the length the spring wants to be. Anharmonicity can be included using cubic or higher terms (eq 3), or Morse potential (eq 4). Figure 10 shows the harmonic, cubic and Morse potential functions.

Harmonic potential $$E_{bh} = k_b\left(r_{ij} - r_0\right)^2 \quad (2)$$

Cubic term $$E_{bc} = \frac{1}{2}k_b\left(r - r_0\right)^2 + x\left(r - r_0\right)^3 \quad (3)$$

Morse potential $$E_{bm} = D_0\left[\exp\left(-\sqrt{\frac{k_b}{2D_0}}\left(r_{ij} - r_0\right)\right) - 1\right]^2 \quad (4)$$

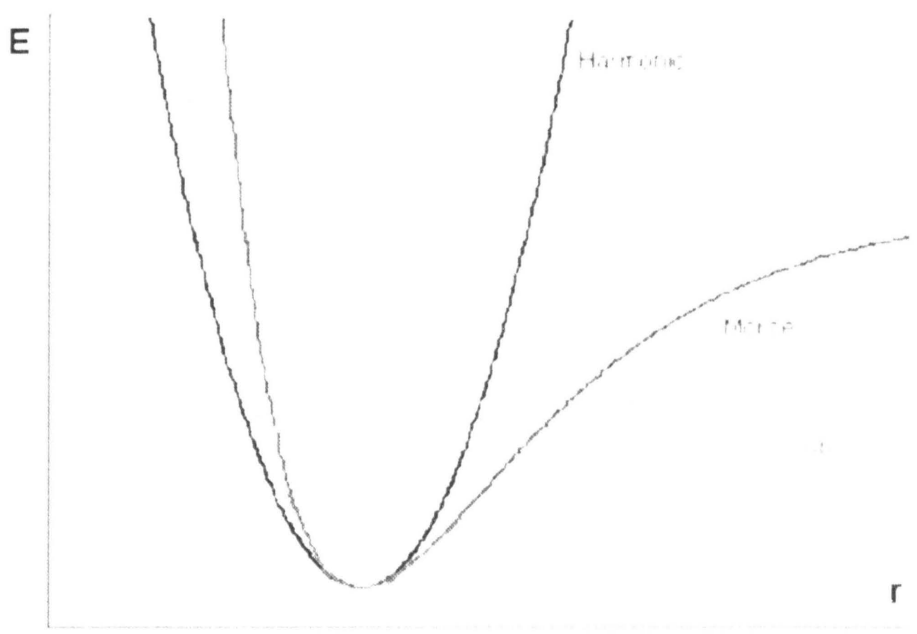

Figure 10: Harmonic, Cubic and Morse potential

Valence angles were modelled in a similar way (eq 5, eq 6), where k_θ is the strength of the "spring" holding the angle at its ideal value of θ_0.

$$E_\theta = \frac{1}{2}k_\theta\left(\theta_{ijk} - \theta_0\right)^2 \quad (5)$$

$$E_\theta = \frac{1}{2}k_\theta\left(\cos\theta_{ijk} - \cos\theta_0\right)^2 \quad (6)$$

Eq 7 shows Urey Bradle potential between two atoms *i* and *j* bonded to atom *k*.

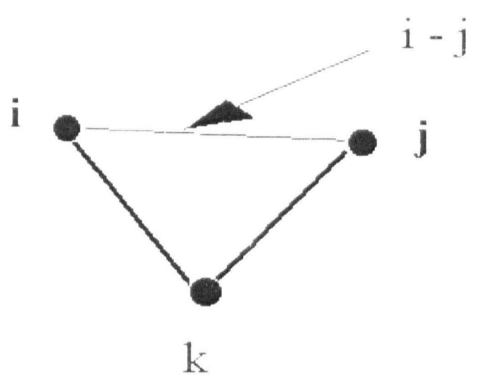

$$E_{UB} = \frac{1}{2}k_{UB_0}\left(r_{ij} - r_0\right)^2 + k_{UB_1}\left(r_{ij} - r_0\right) \quad (7)$$

Figure 11: Atoms *i* and *j* bonded to atom *k* [5]

Torsion or dihedral angles could not be modeled in the same manner since a periodic function is required (Eq 8), where k_ϕ is the height of the barrier to rotation

about the torsion angle ϕ_{ijkl}, m is the periodicity and ϕ_{offset} is the offset of the minimum energy from a staggered arrangement.

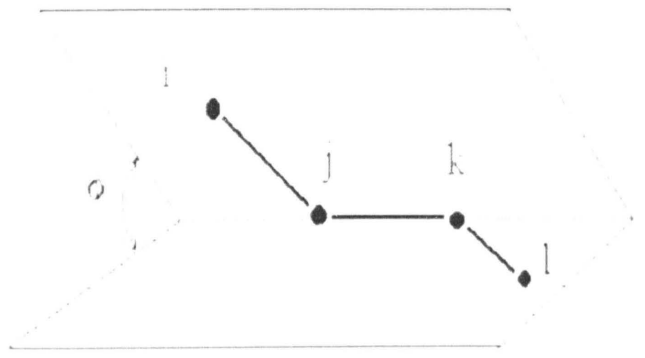

$$E_{\phi} = \frac{1}{2} k_{\phi} \left\{1 + \cos\left[m\left(\phi_{ijkl} + \phi_{offset}\right)\right]\right\} \qquad (8)$$

Figure 12: Schematic illustration of torsion angle ϕ between two planes defined by atoms *ijk* and *jkl* [5]

Nonbonded interactions are calculated using a function that includes a repulsive and an attractive (London dispersion) component as Buckingham (eq 9) or Lenard-Jones potential (eq 10) where d_{ij} is the distance between the two nuclei and A, B, and C are atom-based constants.

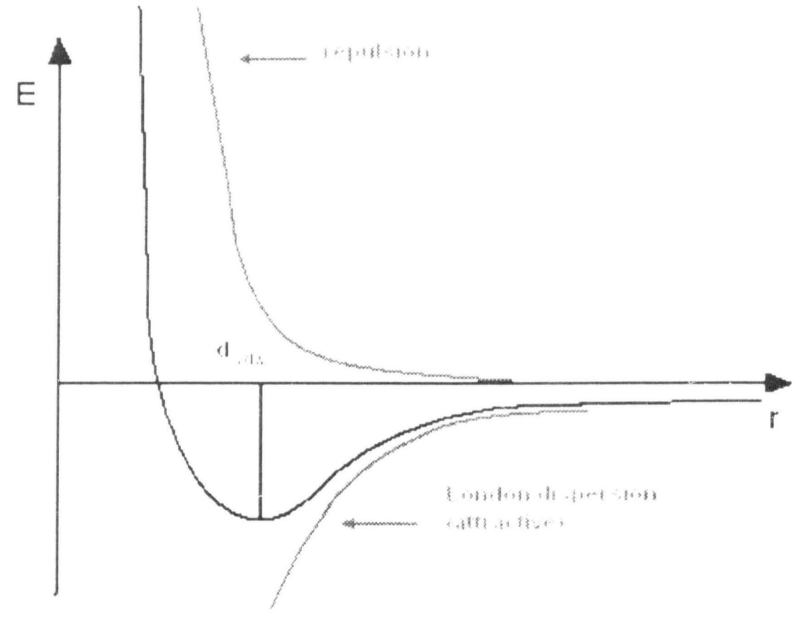

$$E_{nb} = Ae^{-Bd_{ij}} - Cd_{ij}^{-6} \qquad (9)$$

$$E_{nb} = Ad_{ij}^{-12} - Cd_{ij}^{-6} \qquad (10)$$

Figure 13: Lenard-Jones potential curve

Out-of-plane deformation terms E_{δ} have been included in models of aromatic or sp^2 hybridized systems (Eq 11), where δ is the angle between the plane defined by three atoms and the vector from the centre of these atoms to a fourth bonded atom, and k_{δ} is the corresponding force constant.

$$E_{\delta} = \frac{1}{2} k_{\delta} \delta^2 \qquad (11)$$

There are three different types of out-of-plane deformation:

AMBER:

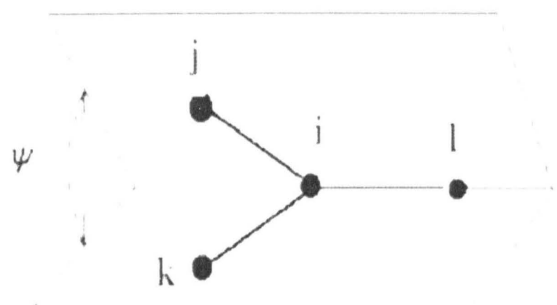

$$E_\delta = \frac{1}{2} k_\psi \cos\left[n(\psi - \psi_0)\right] \tag{12}$$

Figure 14: Schematic illustration of angle ψ between two planes defined by atoms *jil* and *kil* [5]

UMBRELLA:

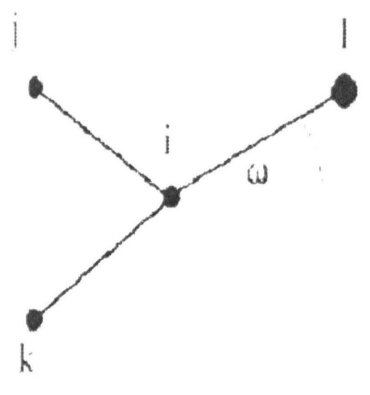

$$E_\delta = \frac{1}{2} k_\omega \left(\cos\omega - \cos\omega_0\right)^2 \tag{13}$$

Figure 15: Schematic illustration of angle ω between the bond *il* and the plane defined by atoms *ijk* [5]

CHARMM:

$$E_\delta = \frac{1}{2} k_{\psi'} \left(\psi' - \psi'_0\right)^2 \tag{14}$$

Electrostatic interactions are modelled based on the Coulomb law (eq 15), where q_i and q_j are the partial charges on atoms i and j, ε is the dielectric constant and d_{ij} is the inter-atomic separation.

$$E_{Coul} = \frac{q_i q_j}{d_{ij}\varepsilon} \tag{15}$$

Hydrogen bonding interactions are generally modelled using a function of the type given in (eq 16), where F and G are empirically derived constants that reproduce the energy of a hydrogen bond and d_{ij} is the donor-acceptor distance.

$$E_{hb} = F d_{ij}^{-12} - G d_{ij}^{-10} \tag{16}$$

The force constants and equilibrium values are atomic parameters which are experimentally derived from X-ray, NMR, IR, microwave, Raman spectroscopy and *ab initio* calculations on a given class of molecules. The set of functions together with the force constants is referred to as the force field. The energy terms describing the valence interactions and force field parameters may differ in various force fields and it is evident that the choice and test of the force field belong to the most important part of the modeling strategy. Once a model and a force field have been chosen for a particular problem, the goal of molecular mechanics is to find the geometry with the minimum strain energy. [1, 14]

1.3.2 Molecular Dynamics

Molecular dynamics combines energy calculations from force field methodology with the laws of Newtonian mechanics. The simulation is performed by numerically integrating Newton's equation of motion over a small time steps (usually 10^{-15} sec or 1 fsec). The simulation is initialised by providing the location and assigning a force vector for each atom in the molecule. The acceleration of each atom is then calculated

Newton's equation of motion:
$$m_i \frac{\partial^2 \mathbf{r}_i}{\partial t^2} = \mathbf{F}_i, \quad i = 1 \ldots N \tag{17}$$

where m is the mass of the atom and F the negative gradient of the potential energy function (the mathematical description of the potential energy surface). The Verlet algorithm is used to compute the velocities of the atoms from the forces and atom locations. Once the velocities are computed, new atom locations and the temperature of the assembly can be calculated. These values then are used to calculate trajectories, or time dependant locations, for each atom. [1]

The temperature and the distribution of atomic velocities in a system are related through the Maxwell-Boltzmann equation:

$$f(v)dv = \left(\frac{m}{2\pi kt}\right)^{\frac{3}{2}} e^{-\frac{mv^2}{2kT}} 4\pi v^2 dv \tag{18}$$

where $f(v)$ is a probability that a molecule of mass m has a velocity of v when it is at temperature T. Figure 16 shows the Maxwell-Boltzmann distribution at various temperatures.[15]

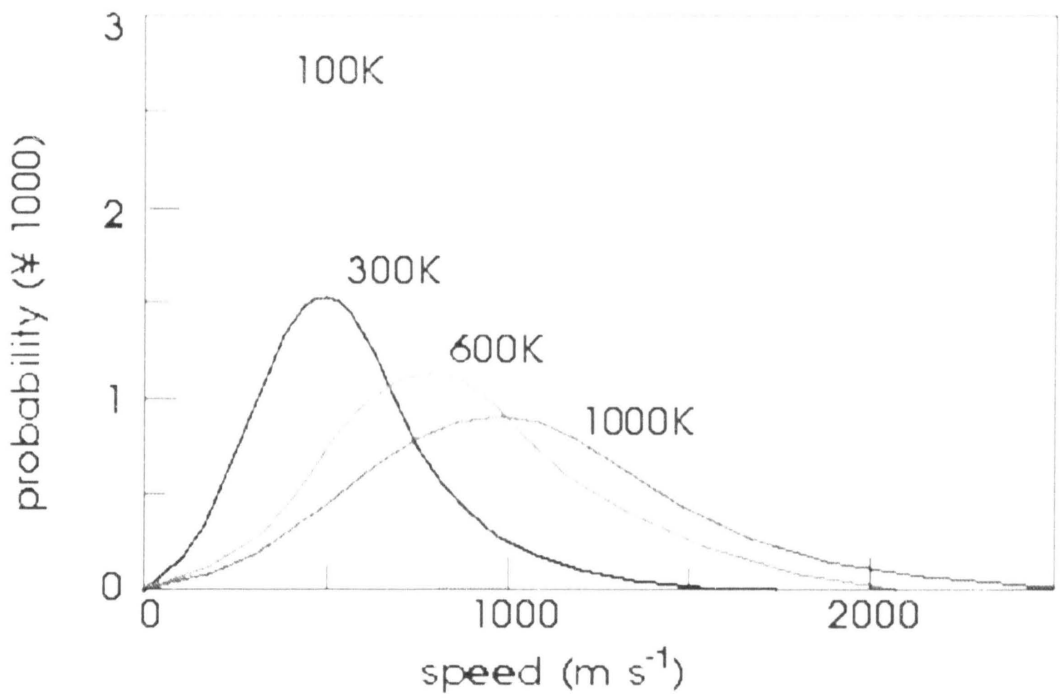

Figure 16: Maxwell-Boltzmann distribution at various temperatures [15]

Temperature and kinetic energy of the system are linked together by the following formula:

$$T = \frac{2}{N_f k} \sum_i m_i v_i^2 \qquad (19)$$

where N_f is number of degrees of freedom.

Molecular dynamics has proved to be an optimum numerical recipe applicable to problems with many degrees of freedom from quite different fields of science. The knowledge of the energy or potential landscape of interacting particles, like electrons and atoms, enables one to calculate the forces acting on the particles and to study the evolution of the system with time. [16]

1.3.3 Algorithms Used in Molecular Simulations

Charge Equilibration (QEq)

Knowledge of the charge distribution within molecules is essentials for determining the electrostatic energies in molecular mechanics and molecular dynamics calculations QEq is a general method for calculation of charge distribution on different types of molecules. The main characteristic of this method is the charges reliance on geometry of

molecules, which can change during the simulation. The approximation is based on the expression of energy of isolated atom as a function of its charge. The energy of isolated atom A as a function of charge Q can be expressed through second order of Taylor expansion as follows:

$$E_A(Q) = E_{A0} + Q_A\left(\frac{\partial E}{\partial Q}\right)_{A0} + \frac{1}{2}Q_A^2\left(\frac{\partial^2 E}{\partial Q^2}\right)_{A0} + \ldots \tag{20}$$

For $Q = 0, +1, -1$ the equation (20) takes the following forms:

$$E_A(0) = E_{A0} \tag{21}$$

$$E_A(+1) = E_{A0} + \left(\frac{\partial E}{\partial Q}\right)_{A0} + \frac{1}{2}\left(\frac{\partial^2 E}{\partial Q^2}\right)_{A0} \tag{22}$$

$$E_A(-1) = E_{A0} - \left(\frac{\partial E}{\partial Q}\right)_{A0} + \frac{1}{2}\left(\frac{\partial^2 E}{\partial Q^2}\right)_{A0} \tag{23}$$

Adding and subtracting (22) and (23) leads to

$$\left(\frac{\partial E}{\partial Q}\right)_{A0} = \frac{1}{2}(I_A + E_A) = \chi_A^0 \tag{24}$$

$$\left(\frac{\partial^2 E}{\partial Q^2}\right)_{A0} = I_A - E_A \tag{25}$$

where χ_A^0 is the atom electronegativity (ability of atom to attract electrons), I_A is the ionization energy (the energy needed for separation of an electron from an isolated atom), E_A is the electron affinity (the energy released when an anion from an electroneutral atom is created).

To understand the physical significance of the second-derivative quantity $\left(\frac{\partial^2 E}{\partial Q^2}\right)$, consider the simple case of a neutral atom with a single occupied orbital, ϕ_A, that is empty for the positive ion and doubly occupied for the negative ion. The difference between the I_A and E_A for this system is

$$I_A - E_A = J_{AA}^0 \tag{26}$$

where J_{AA}^0 is the Coulomb repulsion between two electrons in the ϕ_A orbital.

Using (24) and (26) leads to

$$E_A(Q) = E_{A0} + \chi_A^0 Q_A + \frac{1}{2} J_{AA}^0 \tag{27}$$

The total energy of the system is calculated as follows

$$\chi_A(Q_1 \ldots Q_N) = \frac{\partial E}{\partial Q_A} = \chi_A^0 + Q_A J_{AA}^0 + \sum_{B=1, B \neq A}^{N} Q_B J_{AB} \tag{28}$$

where χ_A is a function of the charges on all the atoms. For equilibrium it is required that the atomic chemical potentials be equal, leading to $N-1$ conditions

$$\chi_1 = \chi_2 = \ldots = \chi_N \tag{29}$$

Adding the condition on total charge

$$Q_{tot} = \sum_{i=1}^{N} Q_i \tag{30}$$

leads to a total of N simultaneous equations for the equilibrium self-consistent charges that are solved one for a given structure. [17]

Newton's equations of motion

For numerical integration of Newton's equations of motion Leap Frog variant of Verlet algorithm is used. The equation (17) can be rearranged into (31),(32) in order to get all the atomic positions $\mathbf{r}_i$ in times t_n and all velocities $\mathbf{v}_i$ in times $t_{n+\frac{1}{2}}$

$$\frac{d\mathbf{v}}{dt}(t) = \mathbf{a}(t) \frac{\mathbf{F}(t)}{m} \tag{31}$$

$$\frac{d\mathbf{r}}{dt}\left(t + \frac{\Delta t}{2}\right) = \mathbf{v}\left(t + \frac{\Delta t}{2}\right) \tag{32}$$

Leap Frog variant of Verlet algorithm got its name from specific calculation of atomic positions and velocities, which are determined by overleaping each other as it is shown in the algorithm beneath:

1. Generate the initial positions (in $t = 0$) and velocities (in $t = 0 - \frac{\Delta t}{2}$)
2. According to the actual position calculate the force F in time t
3. Calculate the velocity in time $\left(t + \frac{\Delta t}{2}\right)$ using the following equation:

$$\mathbf{v}\left(t+\frac{\Delta t}{2}\right)=\mathbf{v}\left(t-\frac{\Delta t}{2}\right)+\frac{\mathbf{F}(t)}{m}\Delta t \tag{33}$$

4. Calculate the position using the velocity from step 3 as follows:

$$\mathbf{r}(t+\Delta t)=\mathbf{r}(t)+\mathbf{v}\left(t+\frac{\Delta t}{2}\right)\Delta t \tag{34}$$

5. Change the time $t = t + \Delta t$ and go to step 2

There are certain disadvantages of this method like that the time and velocity are not known at once what can be a problem while generating velocities and calculating energy. The force can not rely on velocities as they are not known in each step. In this case the elacie Verlet method can be used. The advantage is that for derivation of a function in time t both values calculated in $t-\frac{\Delta t}{2}$ and in $t+\frac{\Delta t}{2}$ are used with the same account (weight). [18]

NVT ensemble

Integrating Newton's equation of motion allows exploring the constant-energy surface of a system. However, most natural phenomena occur under conditions where a system is exposed to external pressure and/or exchange heat with the environment. Under these conditions, the total energy of the system is no longer conserved, and extended forms of molecular dynamics are required. Several methods are available for controlling temperature and pressure. Depending on which state variables are kept fixed, different statistical ensembles can be generated. A variety of stuctural, energetic, and dynamic properties can then be calculated from the averages or the fluctuations of these quantities over the ensemble generated.

The constant-temperature, constant-volume ensemble NVT, also referred to as the *canonical ensemble*, is obtained by controlling the thermodynamic temperature. This is the appropriate choice when conformational searches of molecules are carried out in vacuum without periodic boundary conditions.[15]

$$\mathbf{v}\left(t+\frac{\Delta t}{2}\right)=\mathbf{v}\left(t-\frac{\Delta t}{2}\right)+\frac{\mathbf{F}(t)}{m}\Delta t \tag{33}$$

4. Calculate the position using the velocity from step 3 as follows:

$$\mathbf{r}(t+\Delta t)=\mathbf{r}(t)+\mathbf{v}\left(t+\frac{\Delta t}{2}\right)\Delta t \tag{34}$$

5. Change the time $t = t + \Delta t$ and go to step 2

There are certain disadvantages of this method like that the time and velocity are not known at once what can be a problem while generating velocities and calculating energy. The force can not rely on velocities as they are not known in each step. In this case the clacic Verlet method can be used. The advantage is that for derivation of a function in time t both values calculated in $t-\frac{\Delta t}{2}$ and in $t+\frac{\Delta t}{2}$ are used with the same account (weight). [18]

NVT ensemble

Integrating Newton's equation of motion allows exploring the constant-energy surface of a system. However, most natural phenomena occur under conditions where a system is exposed to external pressure and/or exchange heat with the environment. Under these conditions, the total energy of the system is no longer conserved, and extended forms of molecular dynamics are required. Several methods are available for controlling temperature and pressure. Depending on which state variables are kept fixed, different statistical ensembles can be generated. A variety of stuctural, energetic, and dynamic properties can then be calculated from the averages or the fluctuations of these quantities over the ensemble generated.

The constant-temperature, constant-volume ensemble NVT, also referred to as the *canonical ensemble*, is obtained by controlling the thermodynamic temperature. This is the appropriate choice when conformational searches of molecules are carried out in vacuum without periodic boundary conditions.[15]

Berendsen Thermostat

Molecular dynamics methods are temperature dependant. For maintaining the constant temperature in simulations the Berendsen thermostat is used. This method corrects the difference between the temperature of the simulated system and the temperature required. The deviation from required temperature T_0 is corrected according to the following equation:

$$\frac{dT}{dt} = \frac{T_0 - T}{\tau} \tag{35}$$

The temperature drops exponentially with the time constant τ. T characterizes the exchange rate between the heat and the heat bath. The advantage of this method is that the time constant can be changed according to the requirements. For fast equilibrium establishment the time constant can be 0.01 ps, for more accurate equilibrium establishment the time constant has to be greater, appoximately 0.5 ps. The atomic velocity is in each step scaled by the factor λ

$$\lambda = \sqrt{1 + \frac{\Delta t}{\tau_T}\left(\frac{T_0}{T\left(t - \frac{\Delta t}{2}\right)} - 1\right)} \tag{36}$$

where τ_T is proportional to the time constant

$$\tau = \frac{2C_V \tau_T}{N_f k} \tag{37}$$

where C_V is heat capacity of the system, k is the Boltzmann constant and N_f is the number of degrees of freedom of the system. [18]

1.4 X-RAY DIFFRACTION

1.4.1 X- ray Crystallography

X- rays are electromagnetic radiation discovered in 1895. It occurs in the part of the electromagnetic spectrum between the ultraviolet and gamma rays. X-rays have energies in the range of approximately 100 eV – 100 keV that corresponds to the wavelength of approximately several angstroms to 0.1 angstrom. X- rays are produced generally by either x-ray tubes or synchrotron radiation.[19]

1.4.2 X- ray Diffraction

Diffraction occurs as the X- rays interact with crystals which have regularly repeating atomic structures. Typical inter-atomic distances in crystalline solids are few angstroms therefore the wavelengths comparable to the size of atoms are used.

Diffracted waves from different atoms interfere with each other and the resultant intensity distribution is strongly modulated by this interaction. Positions and intensities of interference maxima (peaks) are strongly related to the distribution of atoms. Measuring the diffraction pattern therefore allows us to deduce the distribution of atoms in a material.

X- rays scattered from a crystalline solid can constructively interfere producing a diffracted beam only when certain geometric requirements are met. In 1912 W. L. Bragg recognized a predictable relationship among several factors.

1) The distance between atomic planes in a mineral (the inter-atomic spacing) which we call the d-spacing and measure in angstroms (Figure 17)

2) The angle of diffraction which we call the theta angle and measure in degrees. For practical reasons the diffractometer measures an angle twice that of the theta angle. Not surprisingly, we call the measured angle "2-theta" (Figure 18)

3) The wavelength of the incident X-radiation, symbolized by the Greek letter lambda λ (Figure 18)

Lattice Planes

Figure 17: Lattice planes [20]

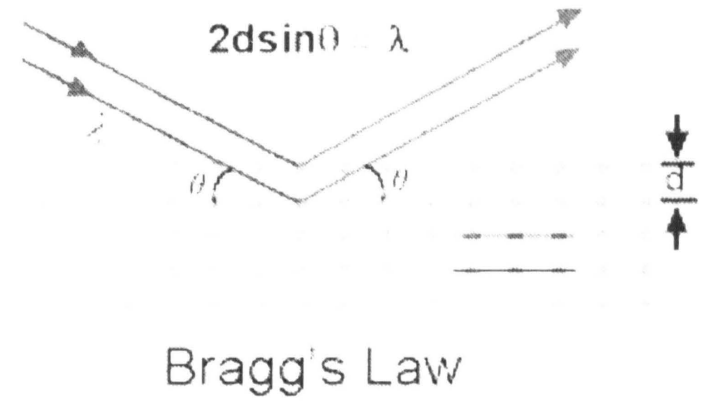

Bragg's Law

Figure 18: Bragg's Law [20]

These factors are combined in Bragg's Law

$$n\lambda = 2d\sin\theta \tag{38}$$

where n = an integer, λ (lambda) = wavelength in angstroms, d (d-spacing) = inter-atomic spacing in angstroms, θ (theta) = diffraction angle in degrees.[19, 20, 21]

1.4.3 Powder X ray Diffraction

Powder XRD (X-ray diffraction) is perhaps the most widely used X- ray diffraction technique for characterizing materials. Each crystalline solid has its unique characteristic X- ray powder pattern which may be used as a "fingerprint" for its identification. Once the material has been identified, X- ray crystallography may be used to determine its structure, i.e. how the atoms pack together in the crystalline state and what the inter-atomic distance and angle are etc. As the name suggests, the sample is usually in a powder form, consisting of fine grains of single crystalline material to be studied.

The term powder really means that the crystalline domains are randomly oriented in the sample. Therefore when the 2D diffraction pattern is recorded, it shows concentric rings of scattering peaks corresponding to the various d-spacings in the crystal lattice. The positions and the intensities of the peaks are used for identifying the underlying structure (or phase) of the material. For example, the diffraction lines of graphite would be different from diamond even though they both are made of carbon atoms. This phase

identification is important because the material properties are highly dependent on structure.

Powder diffraction data can be collected using either transmission or reflection geometry. Because the particles in the powder sample are randomly oriented, these two methods will yield the same data (Figure 19). [20]

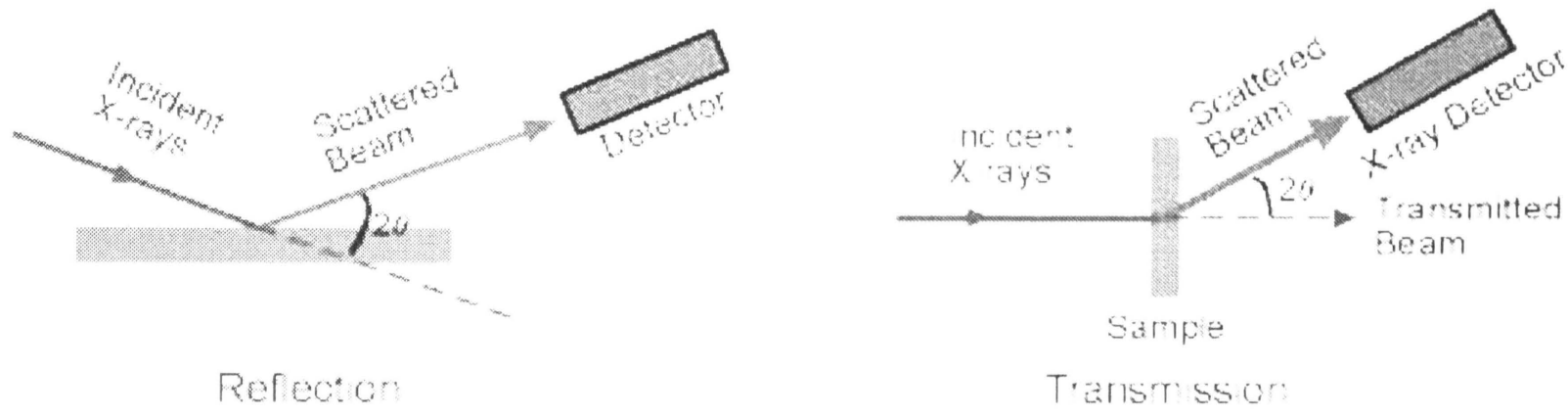

Figure 19: Schematic illustration of detecting reflected and transmitted beams [20]

1.4.4 Evaluation of Diffraction Data

In a diffraction experiment the intensities and the position of reflections are measured. From the position of the reflection its index triple (h,k,l) can be determined and the appropriate intensity assigned to it. This intensity is proportional to the square of the structure factor – amplitude diffracted by one unit cell $F_{(h,k,l)}$. $I_{h,k,l} \approx F_{h,k,l} F^*_{h,k,l}$

The structure factor $F_{(h,k,l)}$ for a reflection h,k,l itself is a complex number derived quite straightforward as follows :

$$F_{(h,k,l)} = \sum_{j=1}^{atoms} f_{(j)} \exp\left[2\pi \cdot i\left(hx_{(j)} + ky_{(j)} + lz_{(j)}\right)\right] \qquad (39a)$$

This is a simple summation which extends over all atoms j, with $x,y,$ and z their fractional coordinates. The $f_{(j)}$ is the scattering factor of atom j and depends on the kind of atom and the diffraction angle of the corresponding reflection (h,k,l). For $h,k,l = 0$, f equals the atom's number of electrons. It can be immediately seen that the

dimension of $F_{(h,k,l)}$ then must be electrons. The exponent is complex with x,y,z the fractional coordinates of each atom in the summation, and h, k, l the three indices of the corresponding reflection. Formula (39a) shows that if the structure is known, structure factors can be easily calculated. Structure factor can be expressed also using electron density in unit cell $\rho(\vec{r})$ (eq 39b), where $\vec{H} = ha^* + kb^* + lc^*$ is a reciprocal lattice vector.

$$F_{h,k,l} = \int_{Vofunitcell} \rho(\vec{r}) e^{2\pi i \vec{H}\vec{r}} dV \qquad (39b)$$

The crystallographic studies are in fact dealing with the inverse problem, structure factors (or, to be precise, their amplitude or magnitude only from the measured intensities) are known and the structure need to be determined.. How to do that?

Fourier transformation

The complex exponential function is periodic, and with the above parameters it is limited between -1,1 for its real part and -i, i for the imaginary part (its elementary strip). In such cases of periodic functions a Fourier transformation (FT) can be applied and for formula (1) the following FT obtained, which has now the $F_{(h,k,l)}$s as its Fourier coefficients:

$$\rho_{(x,y,z)} = \frac{1}{V} \sum_h \sum_k \sum_l F_{(h,k,l)} \exp[-2\pi \cdot i(hx + ky + lz)] \qquad (40)$$

From looking at the dimensions can be seen that the result of the transformation, $\rho_{(x,y,z)}$, must be an electron density: $F_{(h,k,l)}$ is in units of electrons (see above) and the sum is divided by the cell volume V. Note also the minus sign now preceding the exponent: In fact an inverse space (the h,k,l's are actually derived from fractional numbers ($1/h, 1/k, 1/l$) designating where corresponding lattice planes intersect the unit cell) is being transformed into a real or direct space (the electron density at a real point x,y,z in space). It is a general feature of the FT to transform from one space into its inverse space and vice versa. So the diffraction pattern (an image of the reciprocal space) it transformed back into the real space of electron density. This transformation is accurate and in principle complete. If the structure factors are known (inverse space

from diffraction by electrons) the actual real structure (the density of the electrons in real space) can be calculated. As formula (40) is essentially a summation over all structure factors, it is also referred to as a Fourier synthesis or Fourier summation.

Unfortunately, a closer look at formula (40) reveals a small but bothersome detail : In order to perform the FT, the complex structure factors $F_{(h,k,l)}$ are needed but only their magnitude $\left|F_{(h,k,l)}\right|$ is known. In terms of physics this means that only the absolute value of the complex vector $F_{(h,k,l)}$ is known but not its phase, $\alpha_{(h,k,l)}$. Consequently, this nuisance is called the Phase Problem. Formula (40) can be reformulated and split up so that the phase term $\alpha_{(h,k,l)}$ becomes evident :

$$\rho_{(x,y,z)} = \frac{1}{V}\sum_{h}\sum_{k}\sum_{l}\left|F_{(h,k,l)}\right|\exp\left[-2\pi\cdot i\left(hx+ky+lz-\alpha_{(h,k,l)}\right)\right] \qquad (41)$$

Hauptman and Jerome Karle won a Nobel prize in 1985 for their work in the late 1940s and early 1950s on "the direct method" -- a mathematical approach that makes it possible to glean phase data from the diffraction intensities. The key insight behind the direct method derives from the "atomicity" of molecules -- i.e., atoms are small, discrete points relative to the spaces between them -- which limits the possible relationships between phase and intensity to a range of probabilities.

The direct method has made it relatively routine to determine structure for molecules of 100 or fewer atoms. As molecular size increases, however, the probability relationships become weaker, and the direct method breaks down for molecules larger than about 150 non-hydrogen atoms. Another method, based on inserting heavy metal atoms into the crystal structure, has worked reasonably well for very large molecules -- more than about 600 atoms. But for molecules in-between, ranging from about 200 to 500 atoms, structure determination remains a hit-and-miss proposition that takes months or years if it succeeds at all.[22, 23]

1.4.5 Some of the Facts and Settings Affecting the Diffraction Pattern

Preferred orientation/Texture

Preferred orientation usually occurs with rod or plate-like crystallites. For example, plate-like crystallites tend to lie flat on the sample holder; very few will have a perpendicular orientation. As there is no longer a random orientation of crystallites some of the x-ray reflections that would be expected are unusually weak or missing altogether.[24] In general powder diffraction data, preferred orientation is probably the most common cause of deviation of experimental diffractometer data from the ideal intensity pattern for the phase(s) analysed. Preferred orientation can be recognised and compensated for when identifying crystalline phases in a specimen, but is much more difficult to deal with when attempting to do quantitative analysis or precise unit cell calculations. [25]

Speed of rotation of detector and **time constant**

Speed of rotation of detector and time constant of integrator are two parameters that have to be chosen carefully in order to prevent from distortion of peaks' profiles and positions in diffraction pattern. Examples of diffraction patterns made with different settings of these parameters are shown in figure 20 and 21.

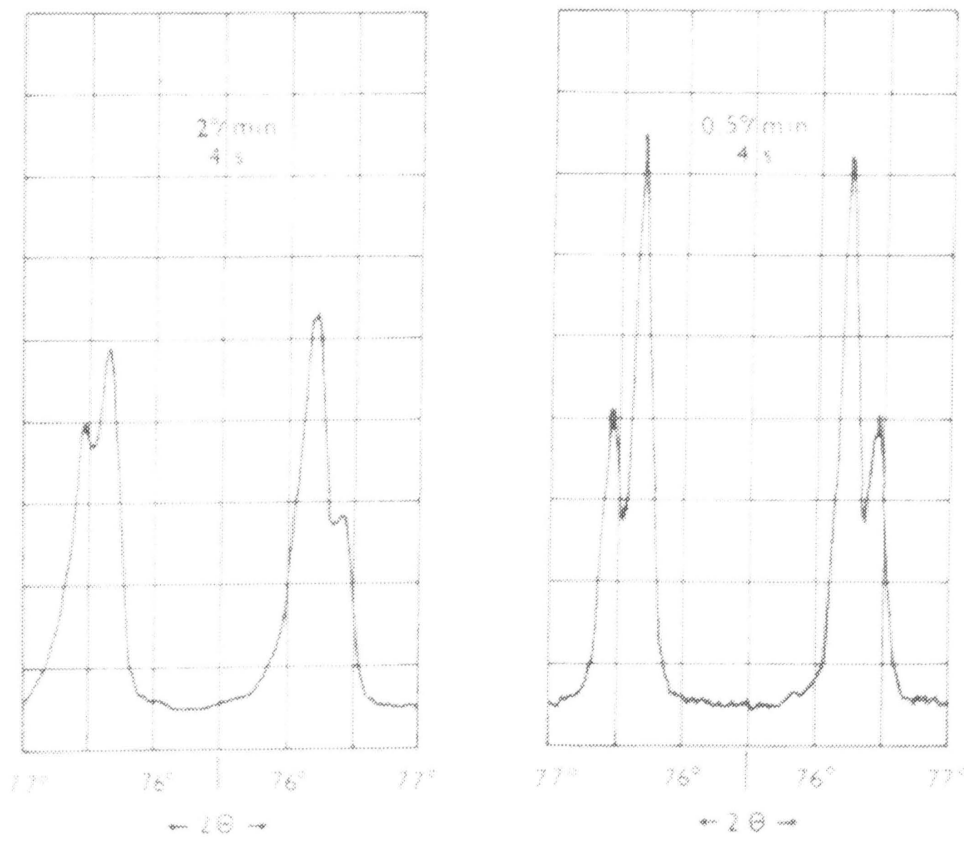

Figure 20: Two diffraction patterns, both made with the same time step 4 seconds but with different speed of rotation of detector, the one on the left with 2°/min and the one on the right with 0,5°/min.[26]

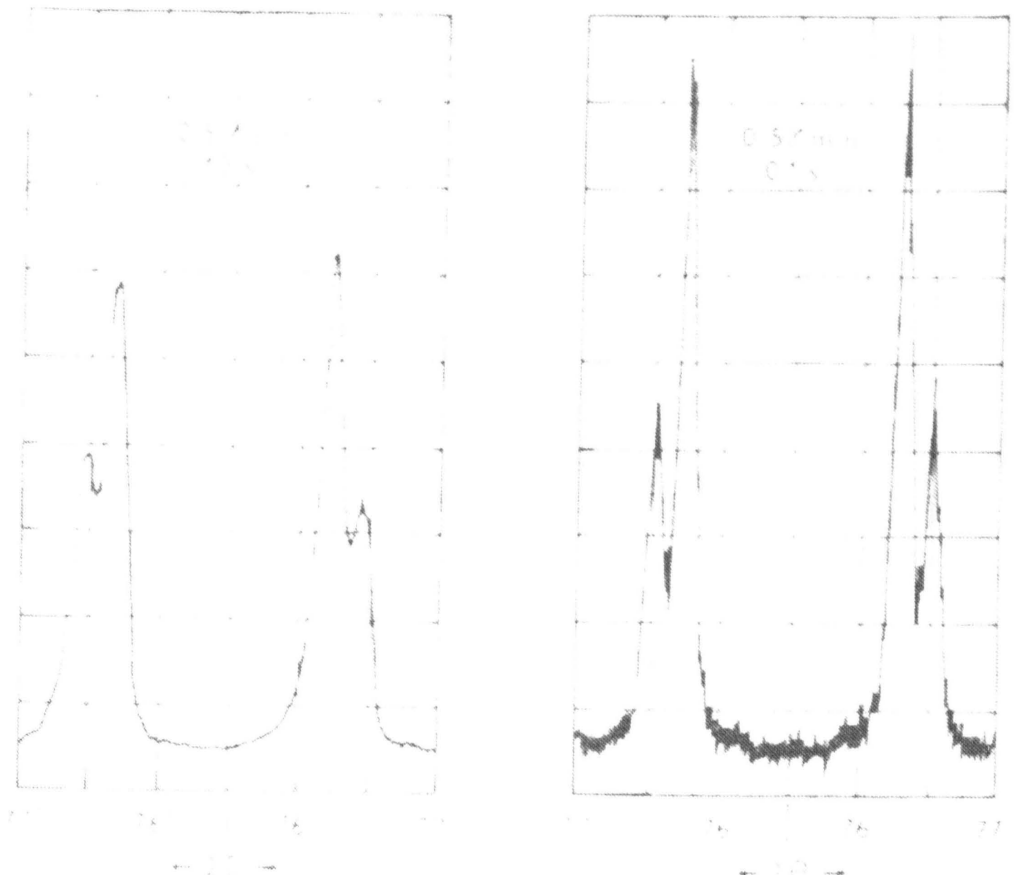

Figure 21: Two diffraction patterns, both made with the same speed of rotation of detector 0,5°/min but with the different time step, the one on the left with 10 s and the one on the right with 0,1 s [26].

Crystallite size

For crystallites of large size (i.e., thousands of unit cells), the nature diffraction will produce diffraction peaks only at the precise location of the Bragg angle. This is because of the canceling of diffraction by incoherent scattering at other angles by the lattice planes within the large crystal structure. If the particle size is smaller (such that there are insufficient lattice planes to effectively cancel all incoherent scattering at angles close to the Bragg angle the net result will be a broadening of the diffraction peak around the Bragg angle.

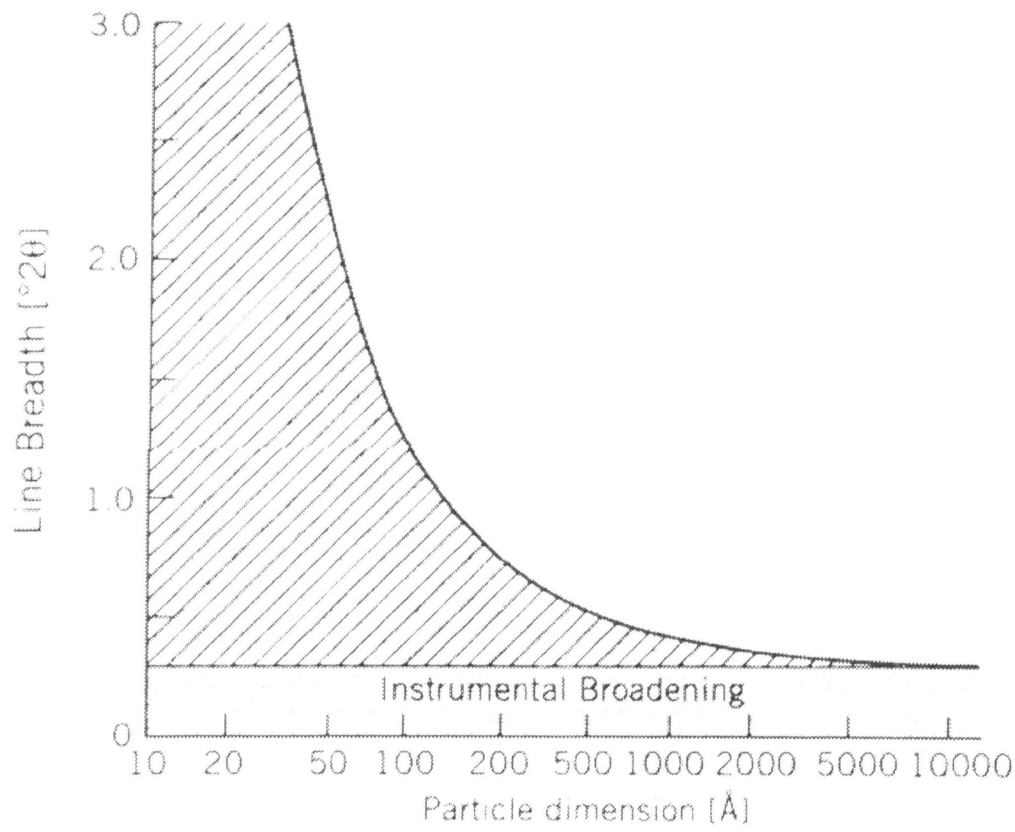

Figure 22: Line width as a function of particle dimension [24]

This phenomenon of widening of diffraction peaks is related to incomplete "canceling" of small deviations from the Bragg angle in small crystallites is known as *particle size broadening*. Particle size broadening is differentiated from the normal width of diffraction peaks related to instrumental effects. In most cases, particle size broadening will not be observed with crystallite sizes larger than 1 μm. [25]

Strain/Stress

Strain in a material can produce two types of diffraction effects. If the strain is uniform (either tensile or compressive) it is called macrostress and the unit cell distances will become either larger or smaller resulting in a shift in the diffraction peaks in the pattern. Macrostrain causes the lattice parameters to change in a permanent (but possibly reversible) manner resulting in a peak shift. Microstrains are produced by a distribution of tensile and compressive forces resulting in a broadening of the diffraction peaks. In some cases, some peak asymmetry may be the result of microstrain. Microstress in crystallites may come from dislocations, vacancies, shear planes, etc; the effect will generally be a distribution of peaks around the unstressed peak location, and a crude broadening of the peak in the resultant pattern. See figure 23.[25]

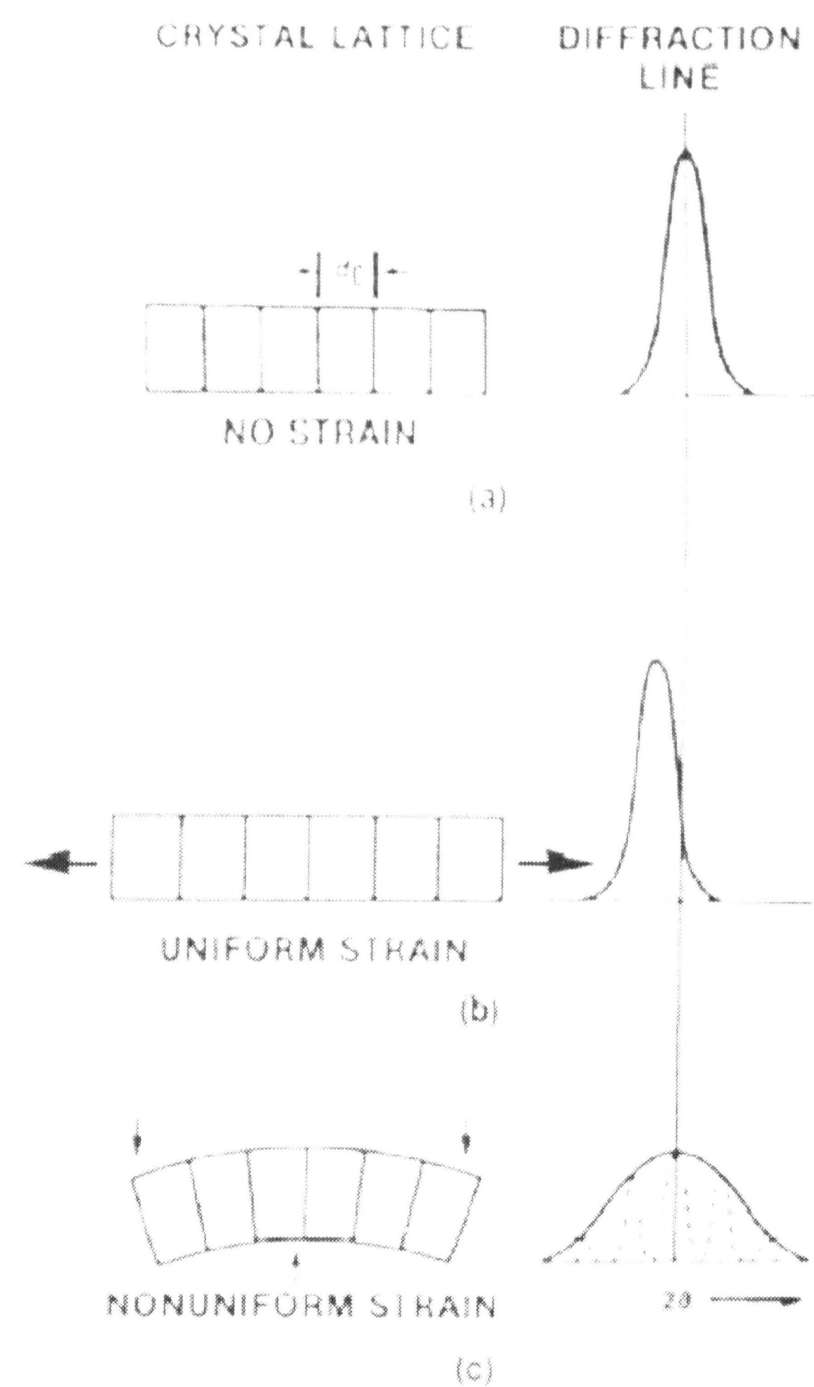

Figure 23: Example of shifting and distortion of diffraction peaks due to residual stress and strain

2. RESULTS AND DISCUSSION

2.1 TIBOLONE-β-CD COMPLEX

2.1.1 Modelling Strategy

The host-guest complementarity in case of cyclodextrine inclusion complexes is mainly given by the size factors, i.e. mutual relationship between the size of the guest molecule and CD cavity. This is the first task for molecular modeling in prediction of complex formation. In order to reach the global minimum of potential energy we use the grid search strategy creating the series of initial models with systematic rotation and translation of the guest molecule in CD basket. Our modeling strategy worked out for CD inclusion complexes consists of the following gradual steps:

- The choice of the host structure: comparing the experimental X-ray diffraction pattern of the β-CD host structure used for complexation with calculated patterns for the β-CD structures presented in structural database.
- The choice and test of the force field using similar known structure of β-CD complex from structural database.
- Modeling of one molecule of tibolone- β-CD complex: the systematic grid search is used to generate initial models for various positions and orientations of tibolone in β-CD basket. Preliminary energy minimization is carried out to search for the lowest energy structure. (Energy minimization with fixed β-CD basket and variable translation and rotation of tibolone molecule.)
- Modeling of crystal structure of tibolone - β-CD complex. Energy minimization under following conditions: variable lattice parameters, variable all atomic positions of guest molecule – tibolone, variable orientation of the CD-OH groups, variable positions and orientations of CD baskets.
- Refinement of the calculated structure. Comparison of the calculated and measured diffraction pattern of tibolone - β-CD complex.

2.1.2 β-cyclodextrine as a Host Structure

The pharmaceutical company used for experimental preparation of tibolone β-CD inclusion complex certain type of β-cyclodextrine. It was found out that in case of β-cyclodextrine all clean structures are herring-bone cage type with space group P21, and with approximately the same amount of water molecules. (see chapter ..) However, the cell parameters may be different for each structure, as well as the water molecules may occupy different positions. The diffraction pattern for one structure may therefore vary a lot from the diffraction pattern of another strucuture.

The search for the crystal structure of β-CD provided us with four clean β-CD structures and consequently with four different sets of lattice parameters. All four structures, named BCD03, BCD04, BCD05 and BCD10 were found in the Cambridge database [27] and all have the same space group P21, all are herringbone cage type and all have approximately the same amount of water molecules. The difference between these structures is, as shown in figure 24 and in table 2, in the positions of water molecules and in the cell parameters.

lattice parameters	BCD03	BCD04	BCD05	BCD10
a (Å)	21.283	21.161	21.233	21.290
b (Å)	10.322	10.254	10.294	10.330
c (Å)	15.092	15.110	15.103	15.100
β (°)	112.41	111.91	112.22	112.30

Table 2: Comparison of lattice parameters for different β-CD structures

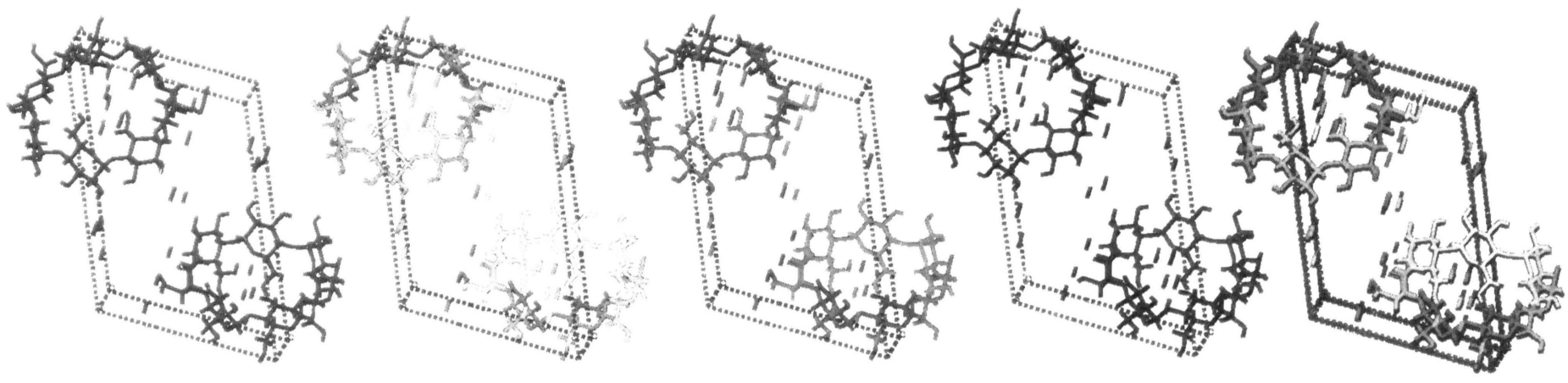

Figure 24: Picture of unit cells of BCD03, BCD04, BCD05, BCD10 and of all of them overleaping each other (in this order).

Diffraction patterns were calculated for all four structure models (see figure 25) and compared with the diffraction pattern measured for the β-CD sample used for experimental complexation.

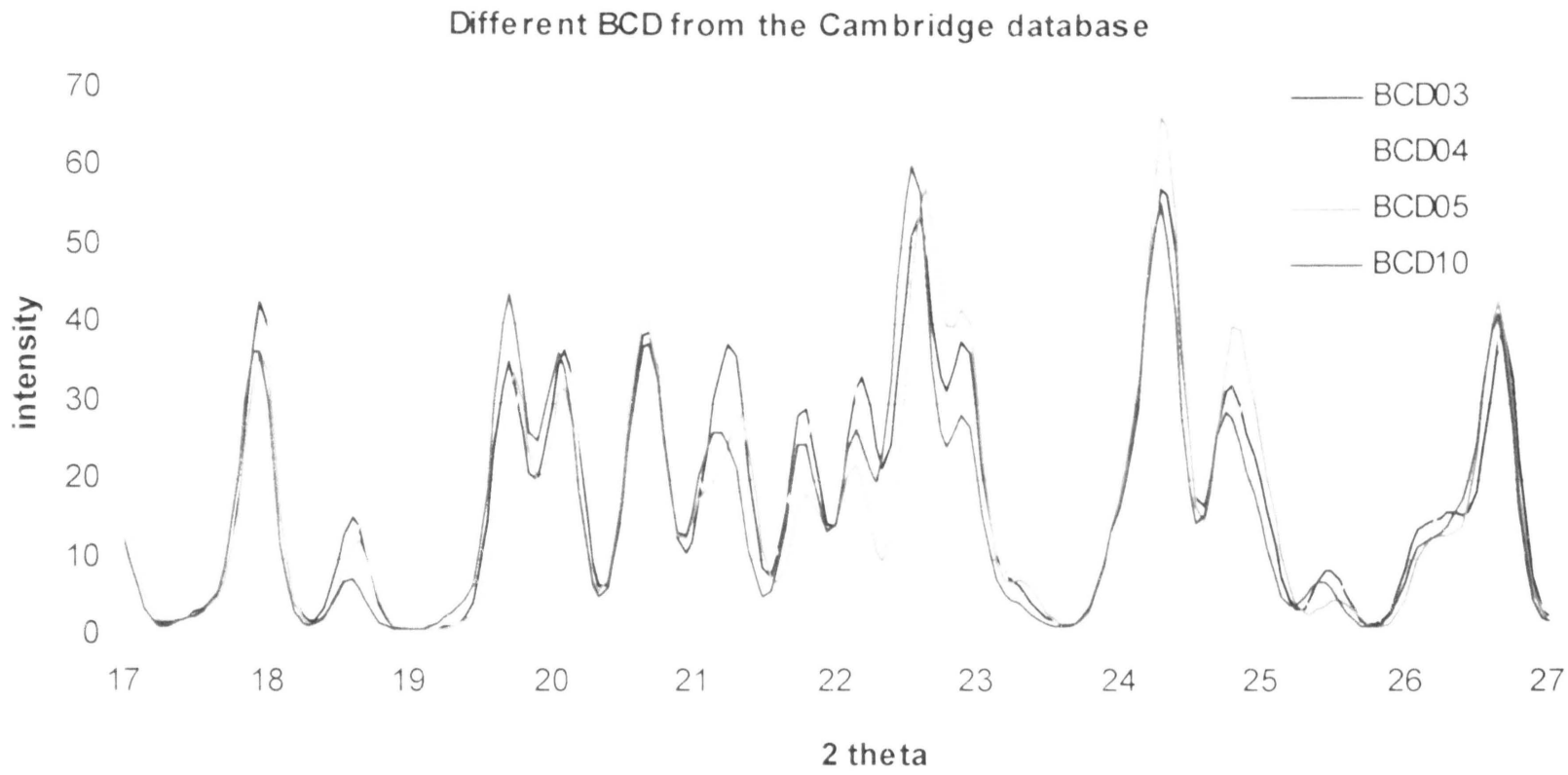

Figure 25: Diffraction pattern of four β-CDs from Cambridge database

The diffraction pattern obtained for the β-CD used in the pharmaceutical company was measured on Seifert 3000 XRD with graphite monochromator, radiation CoKa (λ = 1.790 Å) with the following settings parameters: range 4° - 40° 2 theta, step 0.06°, time 1s, speed 0.1.

The simulated diffraction pattern was done on Material Studio (Cerius2). The settings were adjusted (assimilated) to the real conditions and settings used in experimental measurements in order to get a diffraction pattern fulfilling (meeting) the majority positions of maxima and minima and intensities.

The best agreement between the measured and calculated diffraction pattern has been found for the structure BCD04 (see figure 26) and this structure was used for the building of tibolone-β-CD initial models.

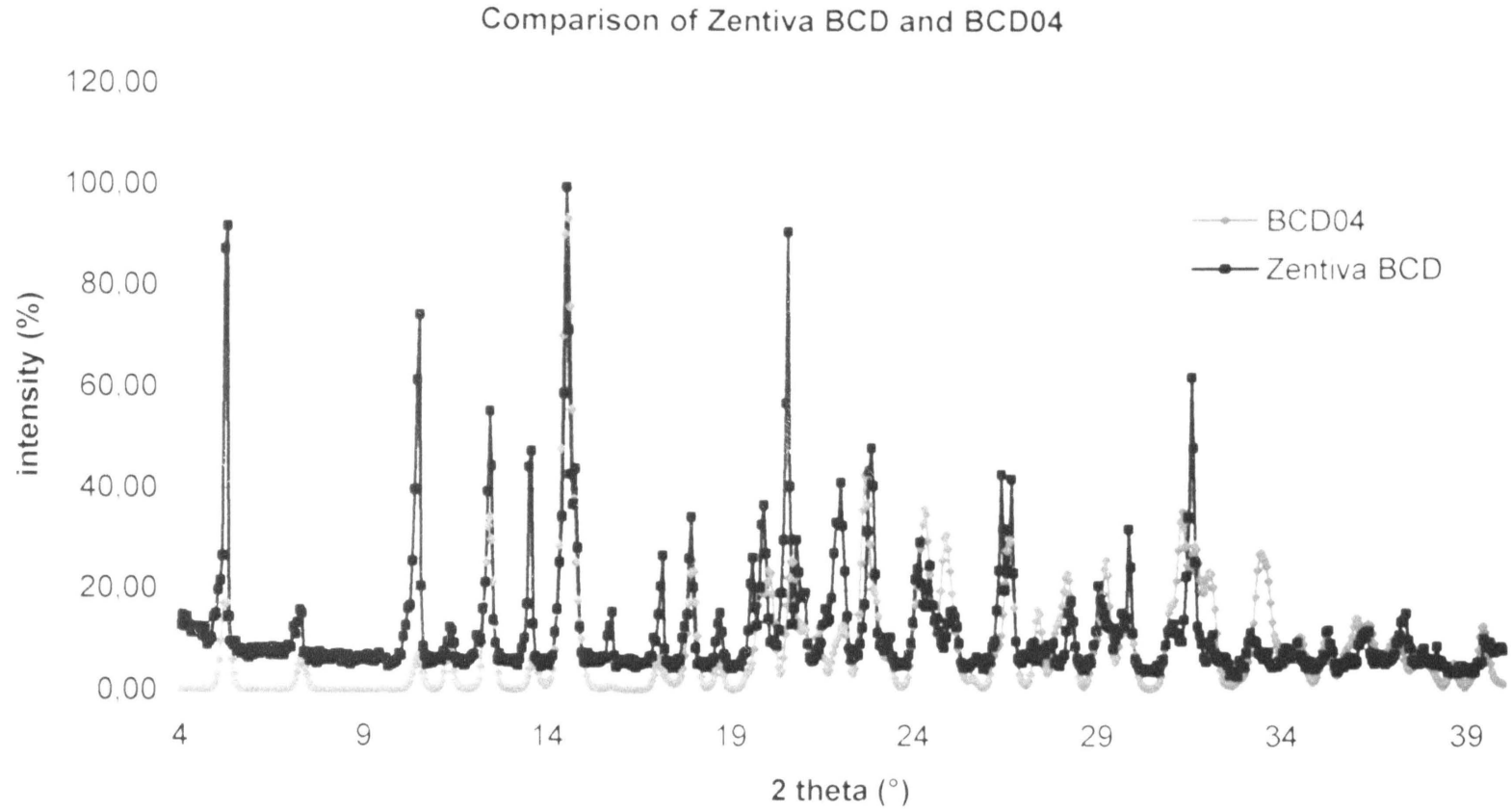

Figure 26: Diffraction patterns of BCD04 and β-CD used for experimentally made complex

2.1.3 Tibolone and the Initial Models

The search for the crystal structure provided us with no result. As we did not find any tibolone crystal structure in the accessible database we did not have the Cerius2 *.pdb* format input file. For molecular simulations it was necessary to build the tibolone molecule in Cerius2 (Material Studio) 3D builder. The molecule was build according to the structure found in the .... and on the internet (www.medscan.com), see figure 7.

Modeling of one guest molecule in β-CD basket is the first step in structure investigation, analyzing the host guest complementarity: i.e. geometrical factors like the mutual relationship between the size and shape of host and guest molecules and the host-guest interaction energy. The series of initial models were systematically generated to cover all the mutual positions and orientations of the guest molecule tibolone (TB) in the β-CD basket.

The preliminary energy minimization was carried out with the rigid β-CD basket (only OH groups were variable) and variable bonding geometry and positions and orientation of the TB molecule. This modeling gave us the first information about the

ability of guest molecule to form a complex. Two criteria were used for this purpose: (1) The guest molecule should have fitted into the CD basket cavity and (2) Van der Waals energy must have been negative.

In the case of TB-β-CD the result of the analysis is in the table 3, where we can see: A) the host-guest interaction including tibolone intramolecular energy, B) the host-guest interaction energy and its components (Van der Waals and electrostatic) for the two types of minimized models: (1) tibolone with the OH group on the top and (2) tibolone with the OH group in the bottom of the basket, as shown in figure 28. The lowest energy structures for both models are energetically nearly the same.

Energy calculated in[kcal/mol]	A) Energy calculated for β-CD as a rigid unit and variable tibolone molecule			B) Energy calculated for both β-CD and tibolone molecule as rigid units		
model	Total energy	Van Der Waals energy	Coulombic energy	Total energy	Van Der Waals energy	Coulombic energy
(1) OH top	-47.9	-9.9	-13.6	-35.3	-30.5	-5.0
(2) OH bottom	-48.3	-11.6	-12.7	-33.6	-30.1	-3.5

Table 3: Interaction energy and its components for two models of TB-β-CD complex, calculated using force field cff91

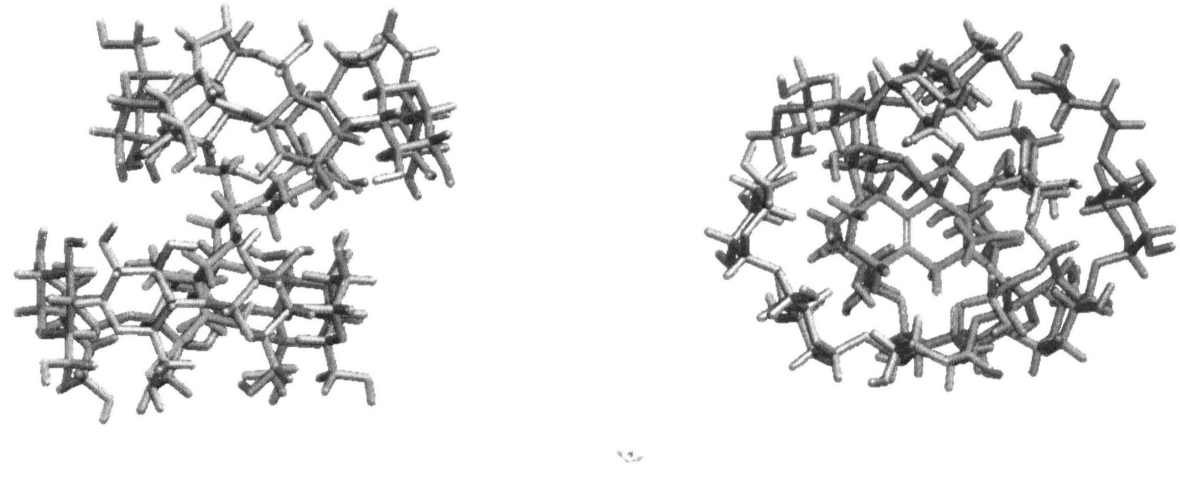

Figure 27: Picture of one tibolone molecule encapsuled by 2 β-CD baskets forming dimers.

The stoichiometry 1:2 was also studied. One tibolone molecule was encapsuled by 2 β-CD baskets ending up in dimer creation, as shown in figure 27. Again many initial models were created and minimized and the energy calculated. However as the

experimentally prepared complex was made approximately in the ratio of 1 tibolone molecule to 20 β-CD baskets and in this ratio it is not very likely that the dimers will be formed. we did not continue in modeling using these models.

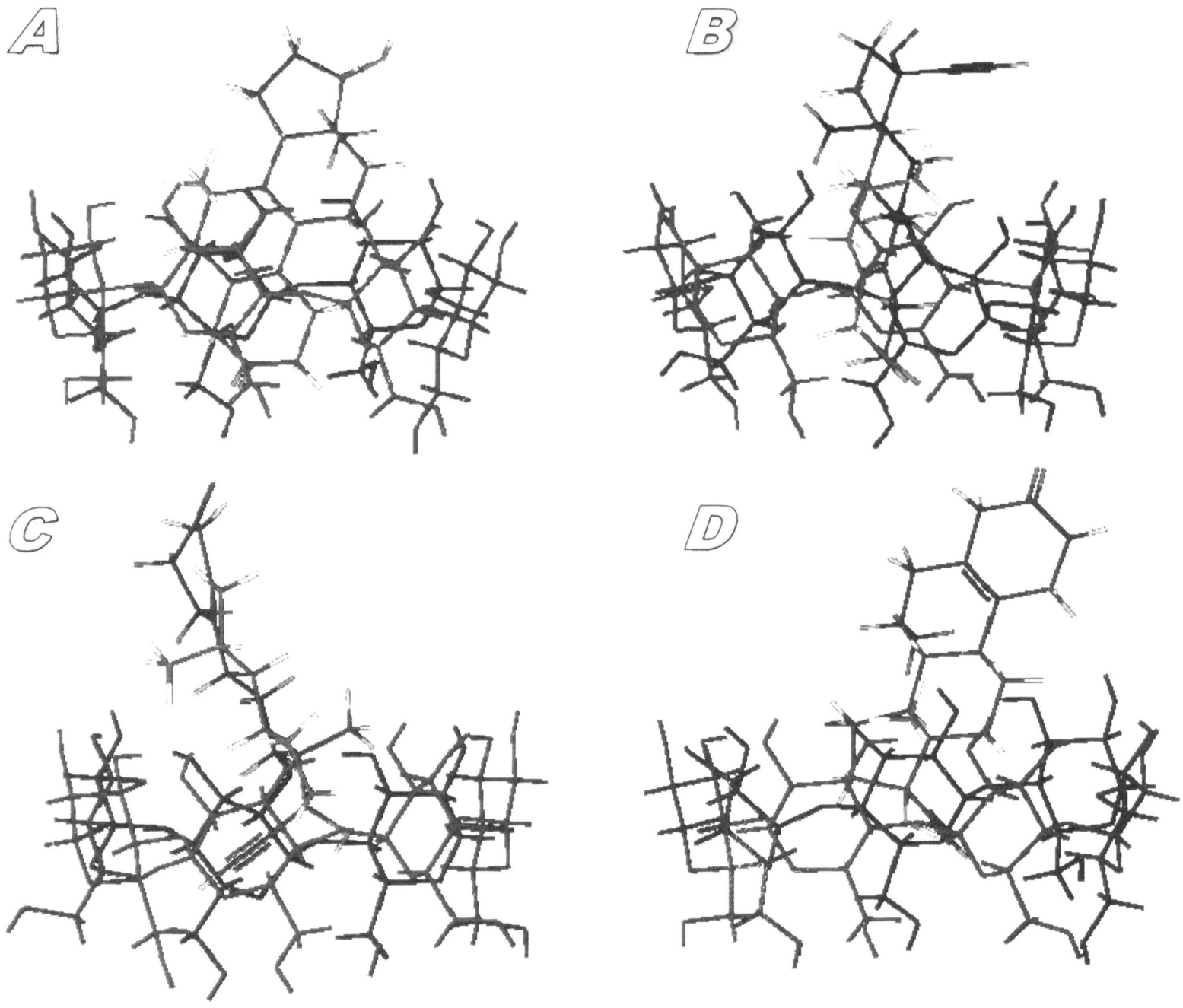

Figure 28: Picture of tibolone immersed into the β-CD basket, made in Cerius2. A, B- tibolone with OH group on the top, above the basket; C, D – tibolone with OH group in the bottom of the basket

2.1.4 Force Field Test

Every force field (FF) is described with simple energy expressions with a set of unique parameters. Different force fields are created for different groups of atoms. In order to get a valuable result in molecular modeling it is important to find the right force field for each set of molecules (atoms).

Some types of force fields expect charges to be calculated before the actual use of the force field. If this is the case there are two available methods for charge calculations

in Cerius2 (charge equilibration (Qeq) and Gasteiger). Force fields developed for modeling the biological set of atoms are designed so to include the charges calculations in their design.

Force fields from Cerius^2 library were tested using β-CD structure from the database BCD04. Energy minimization of BCD04 structure was carried out under following conditions: variable all lattice parameters a, b, c, β (i.e. in space group P21) for various force fields and various set of atomic charges.We tested both universal and biological sets of force fields, namely Universal force field with charges calculated by both Qeq and Gasteiger and two biological force fields cff 91 and cvff 950. The results are shown in table 4.

cell parameters	BCD04 database	FF type charges	cff 91 included in FF	cvff 950	Universal Qeq	Universal Gasteiger
a (Å)	21.16		21.13	21.07	21.07	24.39
b (Å)	10.25		10.75	10.58	10.54	10.39
c (Å)	15.11		15.83	16.57	16.60	16.02
β (°)	111.91		106.04	113.52	104.89	111.39
Energy (kcal/mol)			-1063	-547*	-472*	+317

Table 4: Comparison of lattice parameters of BCD04 crystal strucutre taken from the database before minimalization and after minimalization in different force fields and using different methods for charge calculations.

The best agreement between calculated and experimental structure parameters has been found for the force field cff91. Before the correct concentration (ratio) of experimentally prepared inclusion complex was known we verified this force field on a model of inclusion complex, containing β-CD, from the database (fiure 29). The results are shown in table 5.

benzyl alcohol-β-CD complex, from database	cell parameters	a (Å)	b (Å)	c (Å)	γ (°)
	database	15,36	10,1	21,29	112,8
	cff 91	15,67	10,38	21,26	112,7

Table 5: Comparison of lattice parameters of benzyl alcohol-β-CD crystal structure taken from the database before and after minimalization in cff 91 force field.

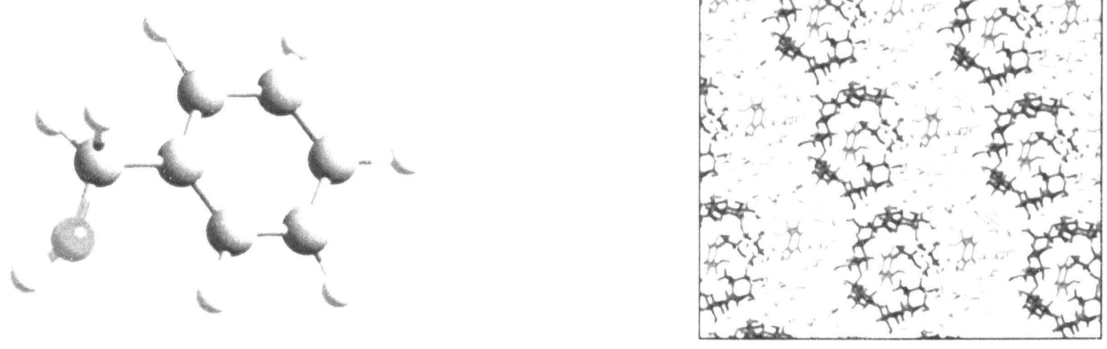

Figure 29: Benzyl alcohol on the left and the benzyl alcohol-β-CD crystal structure on the right, taken from the database, [5]

Once we got to know the correct concentration we verified the cff 91 force field by minimizing the supercell with 40 β-CD baskets (20 cells built from original cell in ratio 2x5x2). Energy minimization of BCD04 supercell structure was carried out under following conditions: variable all lattice parameters a, b, c, α, β, γ (i.e. in space group P1) and no constrains. The result is shown in table 6.

Supercell 2x5x2 created from BCD04 from database, measured and minimized	cell parameters	a (Å)	b (Å)	c (Å)	β (°)	α (°)	γ (°)	Energy (kcal/mol)
	database	42.32	51.27	30.22	111.91	90	90	NA
	cff 91	40.83	53.85	31.16	111.96	90	90	-21065

Table 6: Comparison of lattice parameters of BCD04 super cell built from the crystal structure of BCD04 taken from database (cell parameters, apart the angles, are just multiples of unit cell parameters) before and after minimalization.

This force field, cff 91, has been chosen for modeling of tibolone-β-CD structure. The important result of this test was that in the force field cff91 the structure preserves the space group $P2_1$ (angles α and γ remain 90°) and the differences between experimental and calculated parameters are acceptable within the empirical force field accuracy.

2.1.5 Tibolone-β-CD Crystal Structure; Supercell **2a × 5b × 2c**

Initial models of supercell were built according to the real guest concentration. The mass ratio tibolone : β-CD in experimentally prepared complex was 2.5 mg : 200 mg. The corresponding molar ratio is 1 molecule of tibolone (TB) per 22 molecules of β-CD. To create the host structure supercell of reasonable size and 3D arrangement for calculation with realistic guest distribution we built the supercell 2a x 5b x 2c (figure 30). Two molecules of tibolone were placed into this supercell ensuring the ratio of one tibolone molecule per 20 molecules of β-CD.

Around 580 water molecules were inserted into the supercell corresponding to the experimentally estimated water content in real samples. Positions of water molecules were overtaken from the database. Tibolone molecules were placed into the CD baskets in crystal into the same positions, which have been found by energy minimization with one complex molecule in the vacuum. Water molecules in the baskets where tibolone molecules were placed were deleted so that the tibolone molecules could easily fit in.

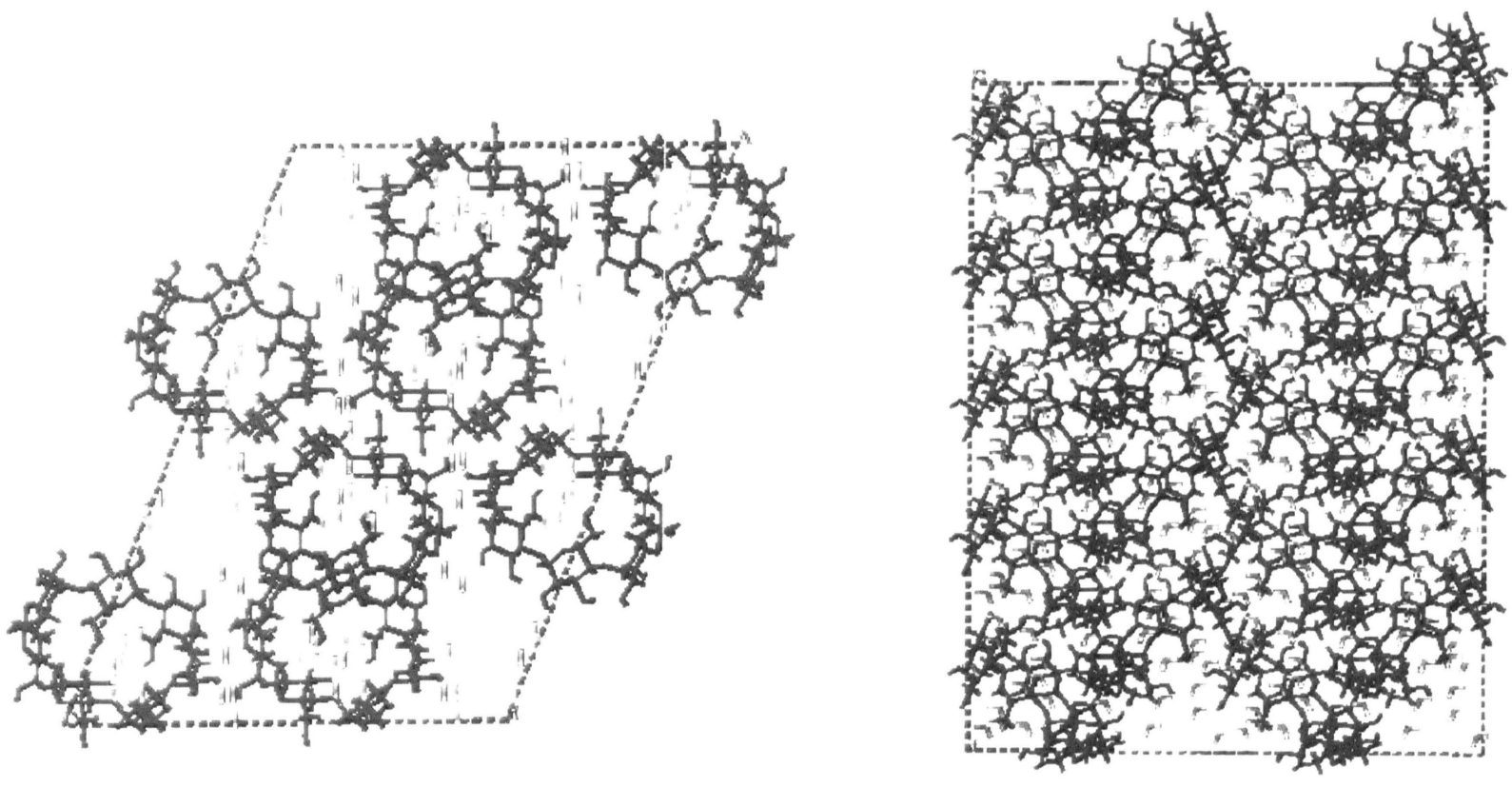

Figure 30: Two views on supercell built from unit cell in ratio 2x5x2. CD baskets are in blue and green, water molecules in red and white.

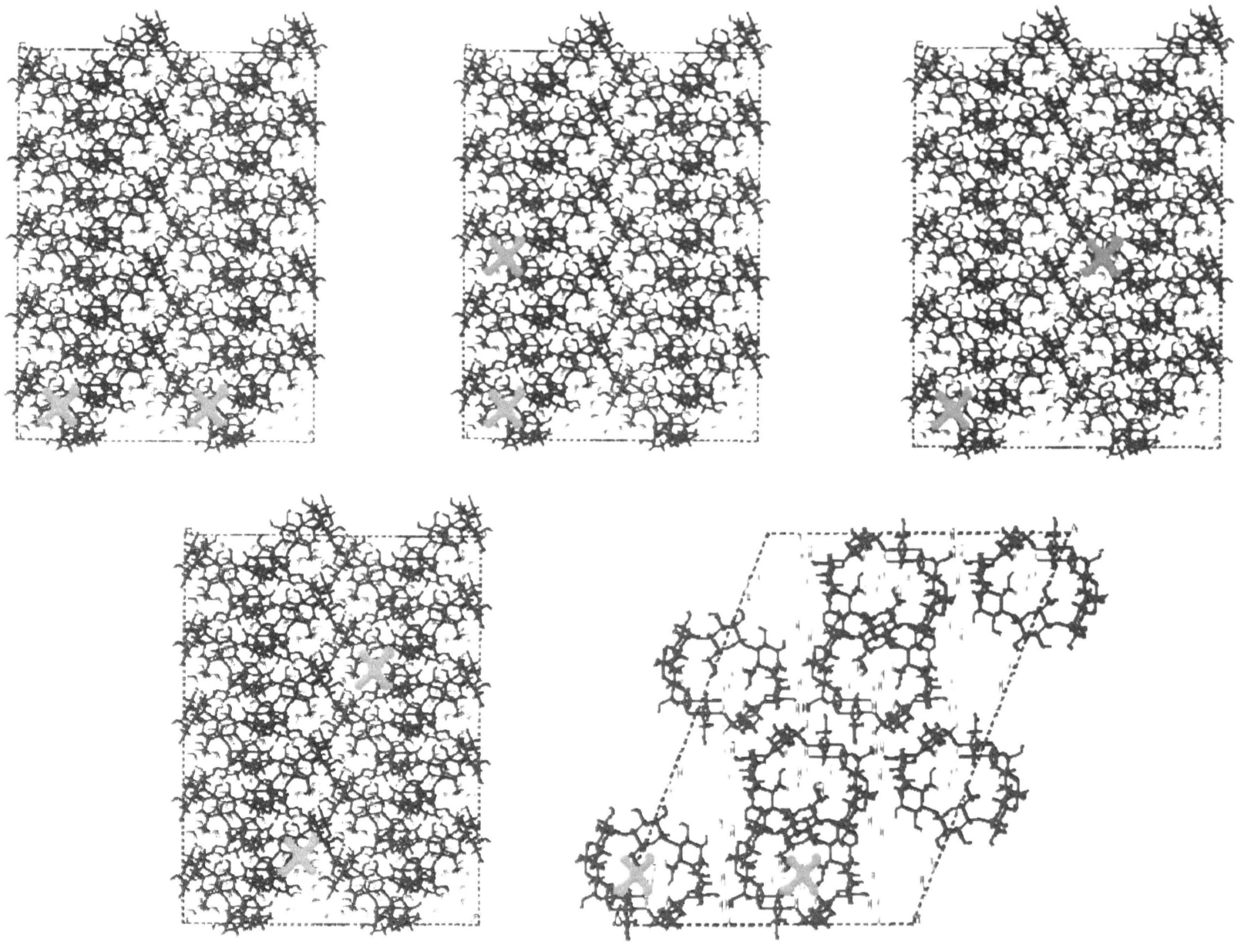

Figure 31: Five models with various arrangement of tibolone molecules. Red cross signifies in which basket the tibolone molecule was immersed.

As figure 28 shows, there are two ways of immersing tibolone molecule into the β-CD basket and both of them seem to be energetically equal. We used both of these structures in further modeling. Ten different models, five models with various arrangements of tibolone molecule in supercell (figure 31) for each structure, were built keeping the guests evenly distributed. The results as to the total sublimation energy and lattice parameters were nearly the same, therefore we present only one example of TB-β-CD supercell crystal structure in the figure 32 and fragment of this structure in figure 33.

The strategy of energy minimization was based on the diffraction data. Comparing the diffraction patterns for β-CD host structure and TB-β-CD complex measured in Zentiva (figure 34) we can see that the reflections common for both samples did not change their positions after complexation. That means in real samples the crystal lattice was not significantly expanded due to the insertion of the TB molecules into the

structure. Therefore in the first step we minimized the energy with fixed lattice parameters. CD baskets and water molecules were movable rigid bodies. TB bonding geometry was set variable and molecules of tibolone were not set as rigid units in order to move freely to obtain the lowest energy possible.

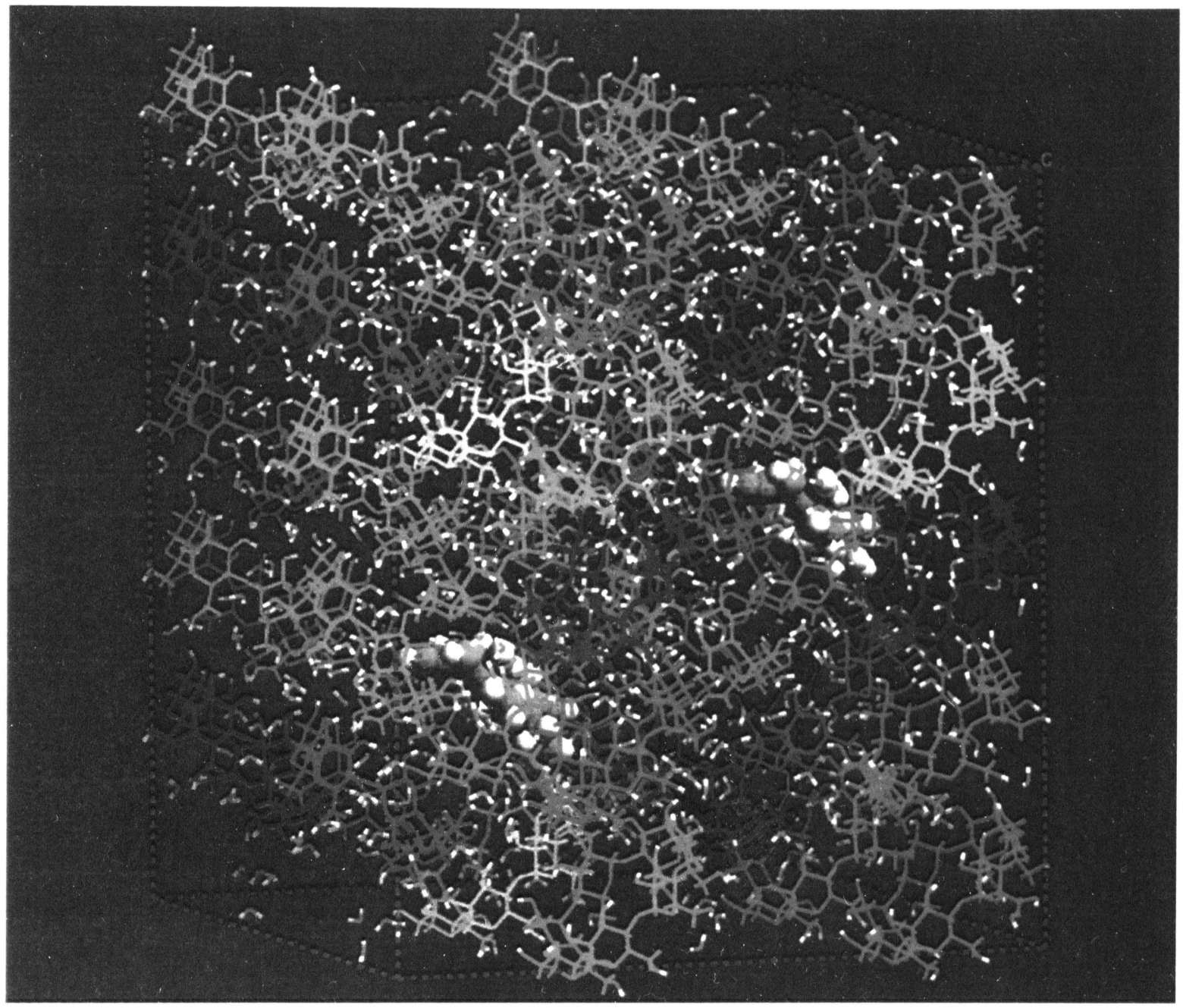

Figure 32: Picture of one of the supercells with two tibolone molecules placed inside two of the 40 β-CD baskets

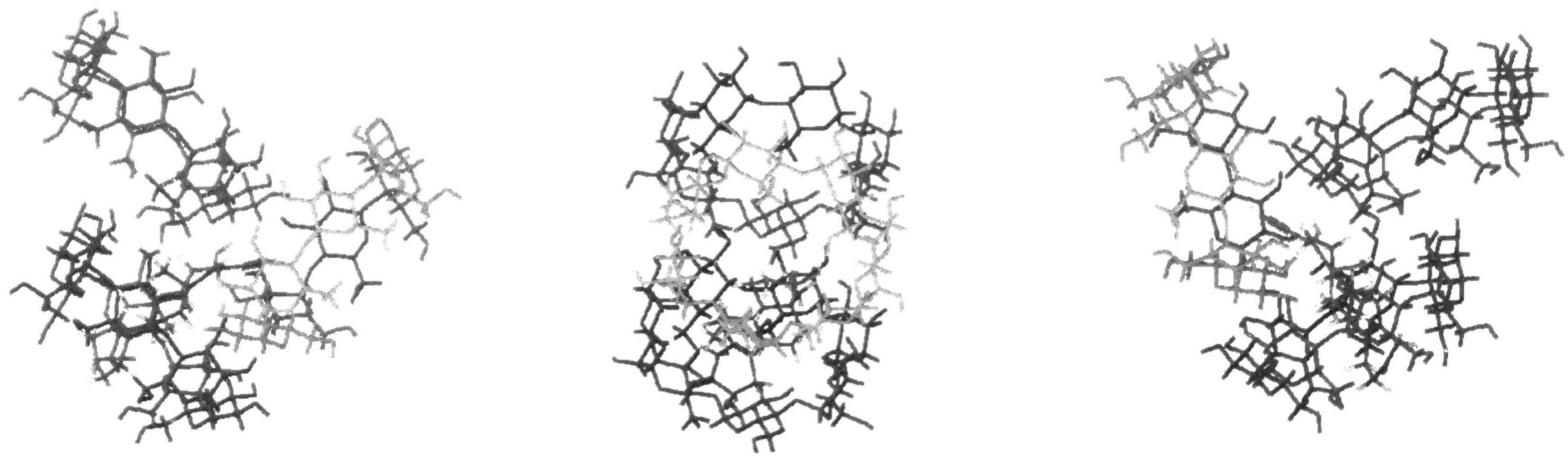

Figure 33: Fragment of the structure shown in figure 32 showing in detail the arrangement of TB in β-CD crystal structure; 3 views

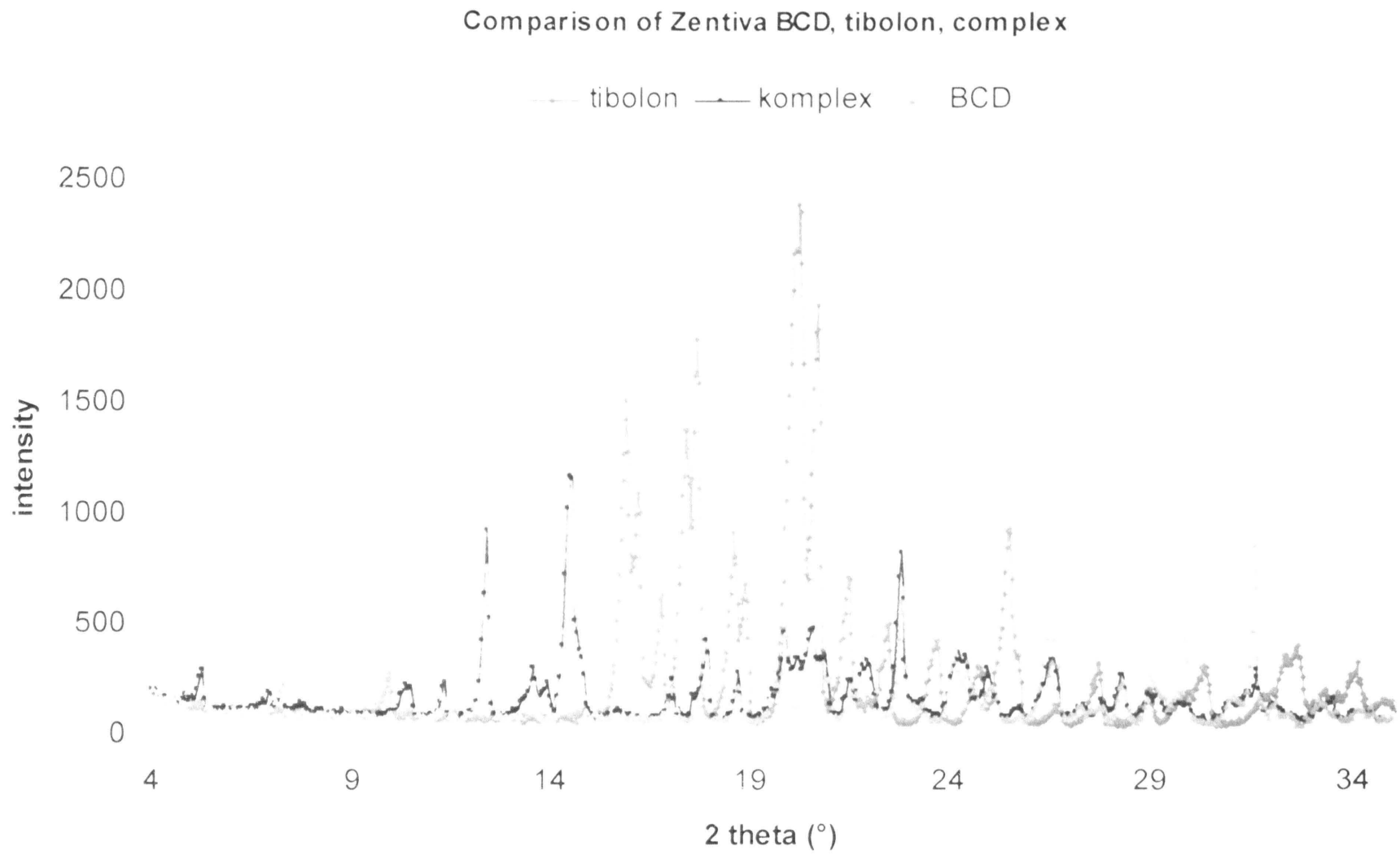

Figure 34: Comparison of diffraction patterns measured in Zentiva for the host structure β-CD and the TB-β-CD complex. The main reflections common for both samples have the same positions in both diffraction patterns indicating that the insertion of TB does not change the lattice parameters. The rearrangement of CD baskets in the vicinity of guest molecules and the variable water content caused the changes in intensities.

To make the simulations as realistic as possible the OH groups on all β-CD baskets were set to be free to move. As there exists no model for such settings in Cerius2 all 21 OH groups on all 40 BCD baskets had to be set to move freely manually by unmarking them when setting baskets as rigid units (cca 1000 hits).

Lattice parameters	a (Å)	b (Å)	c (Å)	α(°)	β(°)	γ(°)
Original β-CD supercell	42.322	51.270	30.220	90	111.91	90
TB-β-CD complex after energy minimization	42.61	52.665	31.186	90.01	113.54	90

Table 7: Comparison of lattice parameters for the supercell $2a \times 5b \times 2c$ for the host structure β-CD (from database) and for the calculated model of TB-β-CD complex.

In the second step the energy was minimized with fixed lattice parameters and all atomic positions in supercell were variable. The diffraction pattern remained nearly the same as in the first step. In the third step energy minimization was carried out with variable lattice parameters and variable all atomic positions in the supercell. Table 7 shows only slight changes in lattice parameters after insertion of tibolone into the β-CD host structure. No rearrangement of the host β-CD structure has been observed after complexation.

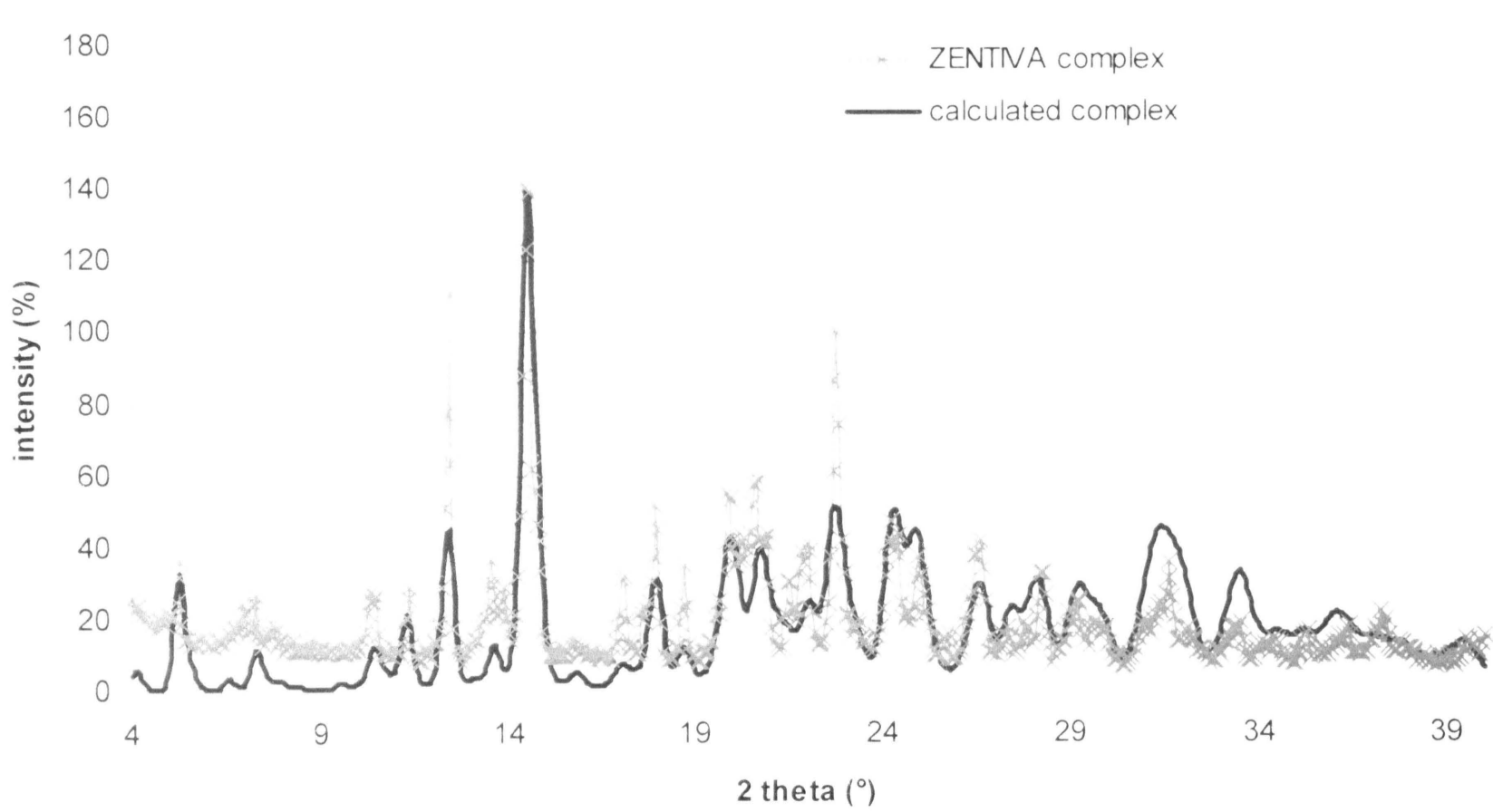

Figure 35: Comparison of the calculated diffraction pattern for the model structure from the figure 31 (blue) and measured diffraction pattern for TB-β-CD Zentiva (red).

Figure 35 shows the comparison of measured and calculated diffraction pattern of TB-β-CD complex. As we can see the calculated diffraction line positions fit reasonably well the corresponding experimental lines. The intensities ratio is slightly modified. There can be several reasons for this change:

- Intensities are very sensitive to water content and to arrangement of water molecules in the supercell.
- Local disorder in the vicinity of the guest molecule TB.

- Sample effects like preferred orientation of crystallites in powder sample, crystallite size (coherent domain size) and surface absorption (surface roughness effect).
- Instrumental effects: like divergency of X-ray beam, too large angle step and too short time step and consequently bad counting statistics.

2.1.6 Acetone in the Tibolone-β-CD Crystal Structure

Looking carefully at the tibolone-β-CD complex preparation technique we can see that there are some residues of acetone in the final complex. Allowed acetone presence is only around 0.5%. There are couple of techniques for determining the acetone presence in complexes however the objective was to find out whether it is possible to detect the acetone presence in tibolone-β-CD complex by X-ray diffraction.

We have done couple of calculations for determining the number of acetone molecules corresponding to presence of 1%. We chose this amount as the reference. If the presence of this amount would have been visible on the diffraction pattern we would have lower it to 0.5%.

The amount of 1% corresponds to about 6 molecules of acetone per supercell. We implemented these molecules randomly into the tibolone-β-CD complex. Some into the β-CD baskets, some into the space between them (figure 36).

The diffraction pattern of tibolone-β-CD complex structure with 1% acetone seem to be identical with the diffraction pattern of crystal structure without acetone. As figure 37 shows, neither this amount of acetone, and therefore nor the amount of 0.5% acetone, is determinable by X-ray diffraction. Other methods have to be used to prove the presence of acetone in such a small amount.

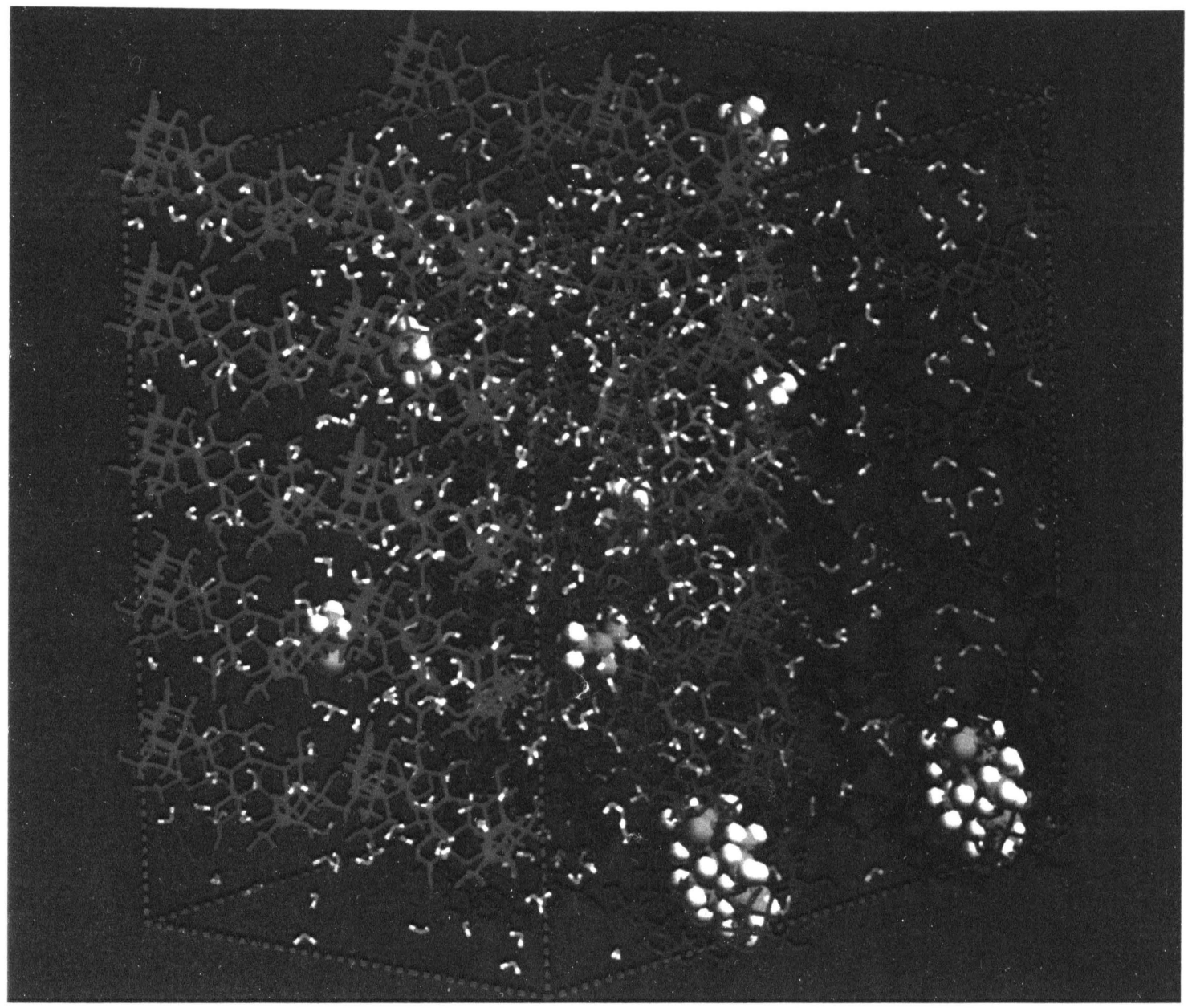

Figure 36: Tibolone –β-CD complex supercell with 1% acetone; CDs in blue and green, water molecules displayed as small red-and-white sticks, 2 tibolone molecules in the right bottom corner displayed in van der Waals mode and 6 acetone molecules displayed in the same mode scattered in the supercell.

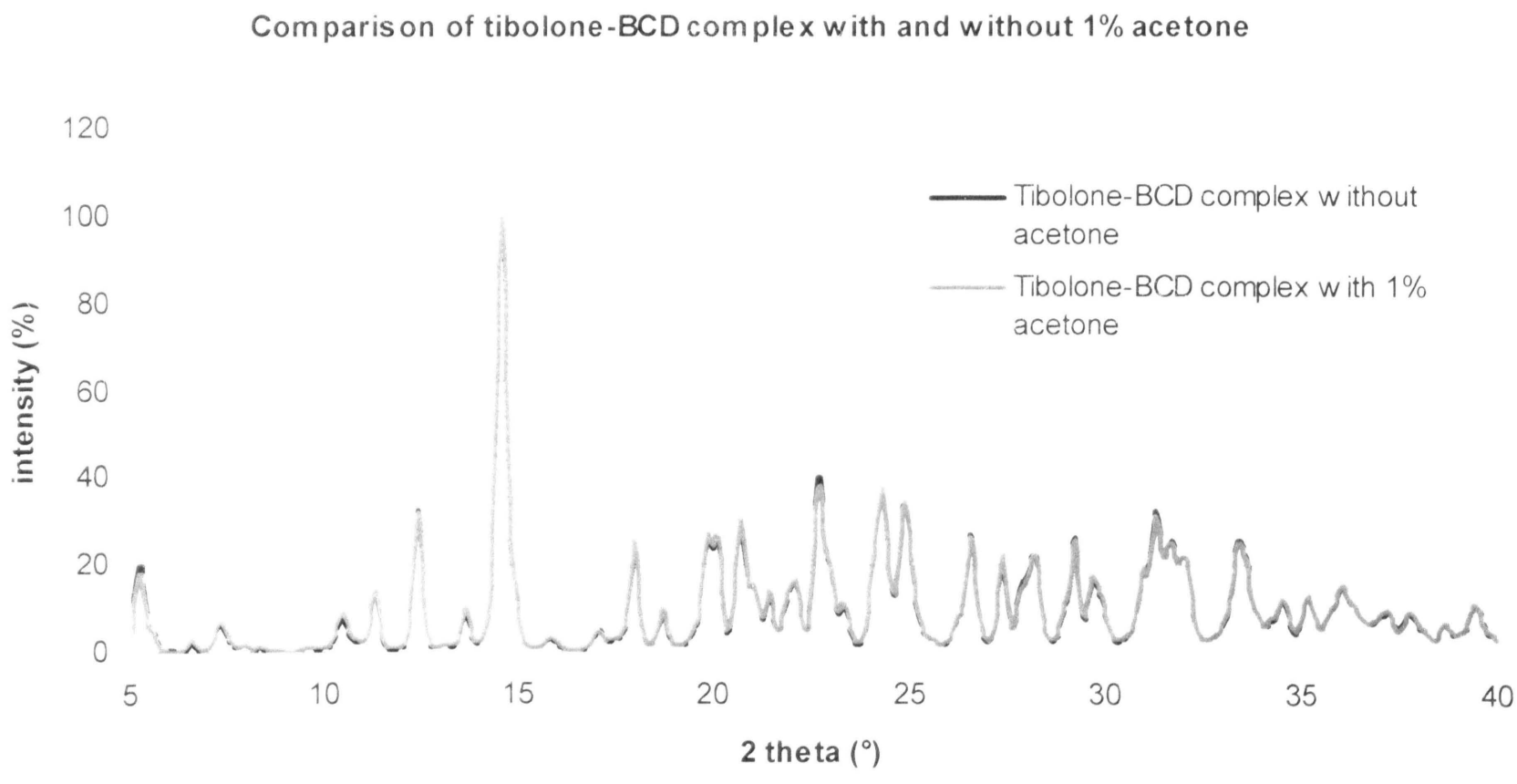

Figure 37: Comparison of calculated diffraction patterns of tibolone-β-CD complex with and without 1% acetone.

2.1.7 "Water problem" Encountered in Modeling Tibolone-β-CD Crystal Structure

During the initiation part of this study it was found out that water molecules strongly affect the intensity and peaks appearance in diffraction patterns. Not only the amount of water molecules is important but also their positions with respect to β-cyclodextrine baskets. It is proved by the calculated diffraction patterns that some peaks can even disappear and some new appear as a result of this "water problem" (figure 38).

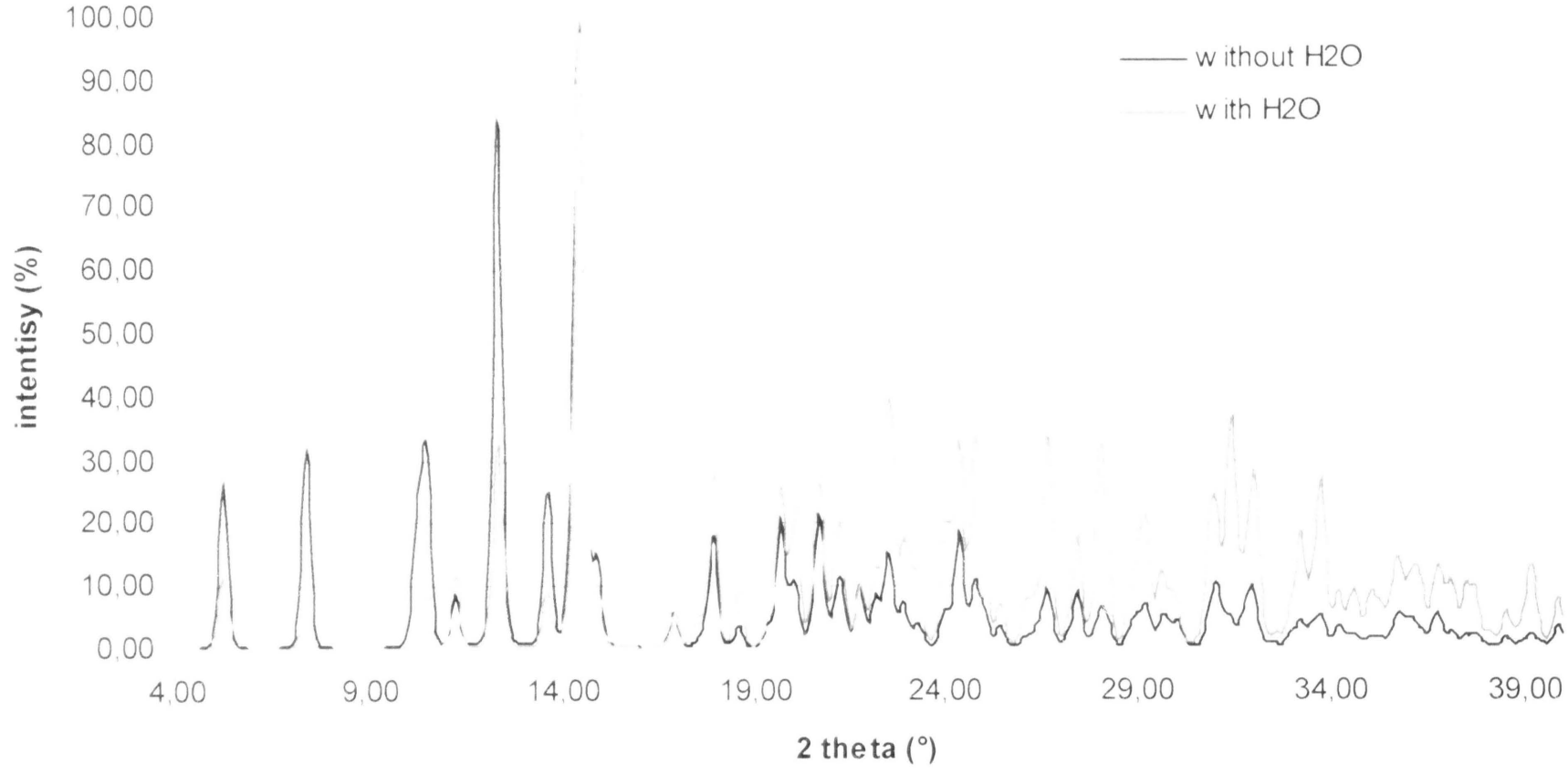

Figure 38: Comparison of calculated diffraction patterns of BCD crystal structure with and without water molecules.

Due to the above stated facts it was very important to be careful while implementing the water molecules into the supercell. The amount of implemented water molecules had to be very similar to the amount of water molecules in the experimentally prepared complex. Only the percentage of water content was known so the number of water molecules per supercell had to be calculated. Positions of water molecules in the experimentally prepared complex are not known so they were overtaken from the database structures, as already stated in paragraph *2.1.5 Tibolone-β-CD crystal structure; supercell 2a x 5b x 2c.*

2.2 CONFORMATIONAL BEHAVIOUR OF TIBOLONE

2.2.1 Stability of Tibolone Versus Δ^4 isomer (Isotibolone)

The stability of both tibolone and isotibolone were studied using the molecular dynamics. The NVT ensemble was used for this purpose as it is the most competent ensemble for determining the conformational behaviour of molecules.

Dynamic simulations were done under the following conditions: time step of 1fs, duration of dynamic trajectory 100 000 steps (100 fs), quench dynamics with 200 minimization steps after each 200 steps of dynamics, thermostat – Berendsen. Quench dynamics means that the structure is in between the dynamic calculations minimized by selected number of minimization steps. The frequency of minimization is also optional.

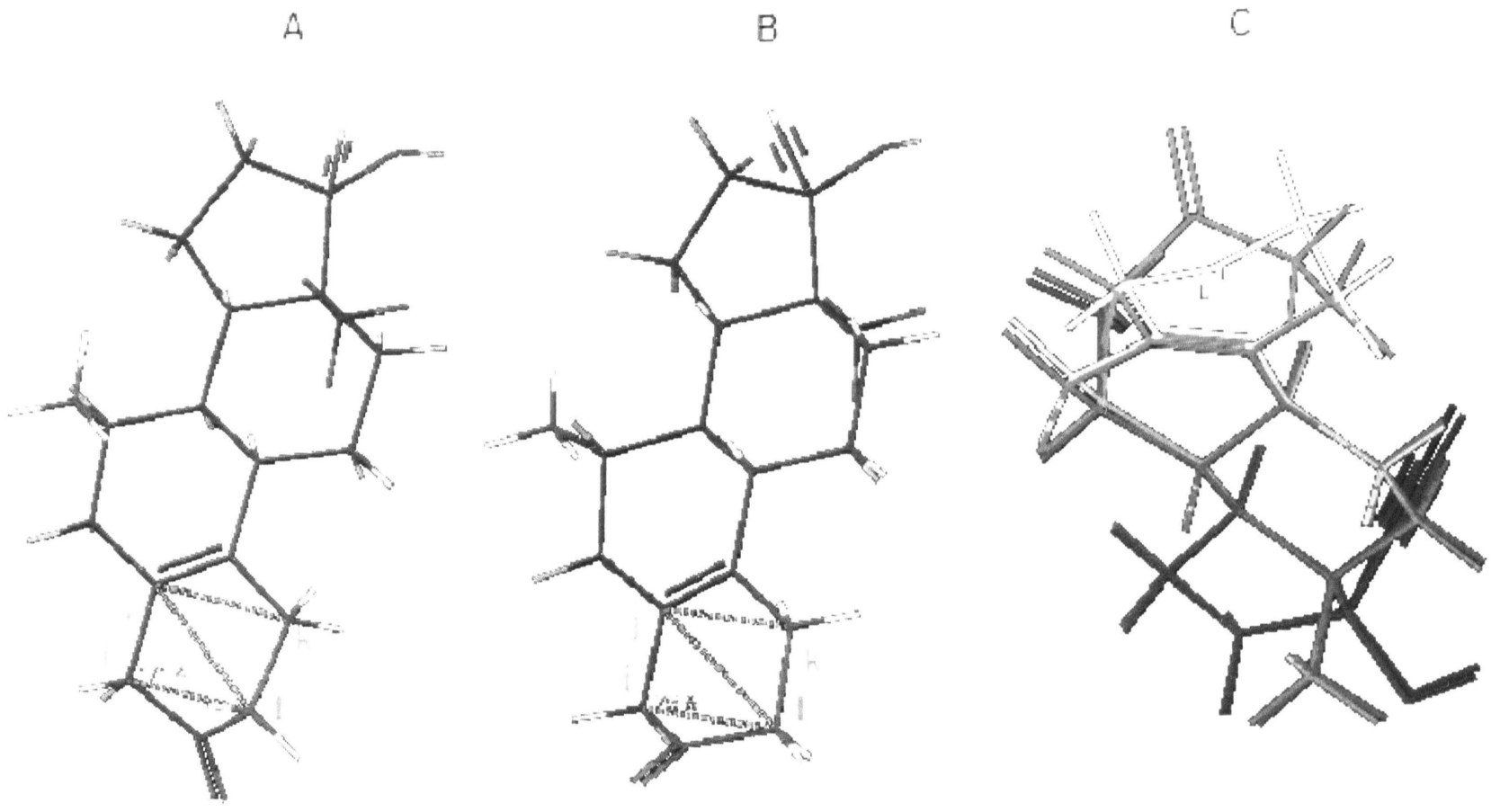

Figure 39: Schematic illustration of tibolone molecule with positive (A) and negative (B) inversion angle between the bond *il* (C_2-C_4) and the plane defined by atoms *ijk* (C_2, C_1, C_5)and comparison of these two conformations (C).

The first dynamic simulation of the tibolone molecule at room temperature was done in order to get the overview of the molecule behaviour and to identify which factors are changing and should be measured and monitored. It was found out that the two most changing parameters in tibolone conformation are: 1) rotation of the O-H bond around the C-O bond and 2) the inversion angle shown in figure 39.

1) The rotation of O-H bond was expected and the appearance of this conformational change only confirmed the general assumption. The torsion angle C-C-O-H (see figure 40) was measured during the dynamic trajectory and the statistical distribution of the measured torsion angle for both tibolone and isotibolone is shown in figures 41 and 42.

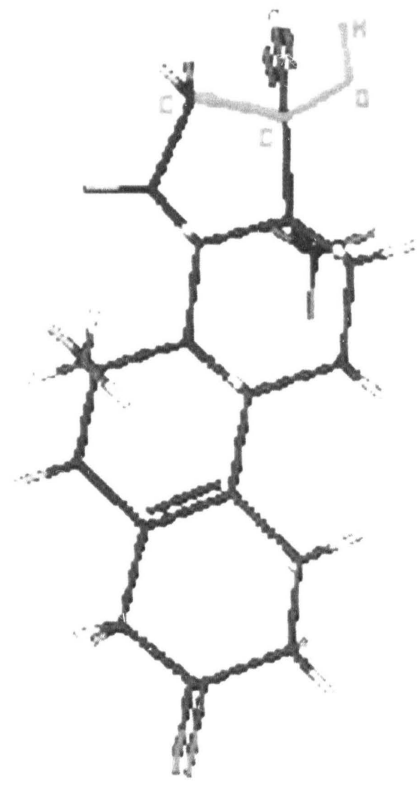

Figure 40: Schematic illustration of torsion angle C-C-O-H, shown in red

It can be seen that there is one main region (in graphical illustration this region is divided into two regions: 50° to 180° and -130° to -180°) and one minor region (around -50°) where the torsion angle for most of the conformations lies. This minor region is in case of tibolone seen mainly at higher temperature (340K) what is probably due to the higher thermal energy available. The interesting fact is that isotibolone seems to behave exactly the opposite way to tibolone; at room temperature the minor region is represented more than at higher temperature therefore the assumption of higher thermal energy fails. Further and more detailed studies are needed to discover the justification of this conformational behaviour however they are not part of this present work.

Conformational changes of torsion angle C-C-O-H were studied also for tibolone immersed into the β-CD cavity. While in the case of tibolone immersed into the β-CD with O-H bond inside the cavity no major deviations from behaviour of torsion angle of free tibolone were observed (figure 43), in case of tibolone immersed into the β-CD with O-H bond outside the cavity the conformational behaviour of torsion angle seems to be the same for both the room temperature and the temperature of 340K (figure 44) so it can be assumed that this kind of encapsulation stabilizes the conformational behaviour of tibolone.

2) As the conformational behaviour and change of the inversion angle might have something to do with the non-stability of tibolone and creation of its metabolite isotibolone by overleaping the double bond we have made two initial models of both tibolone and isotibolone, one with negative angle and one with positive angle (as shown in figure 39).

All four models were studied both at room temperature (RT) and at the temperature of 340K. The graphs representing the conformational behaviour of the inversion angle of tibolone and isotibolone are extracted from the dynamics trajectory and are shown in figure 45 and 47 respectively, where the course of inversion angle along the dynamic trajectory can be seen.

It was found out that, as shown in table 8, the isotibolone molecule has in both conformations lower total bond energy and consequently higher stability than the tibolone molecule. The difference in energies for negative and positive inversion angle is very small in case of isotibolone, however in case of tibolone this difference is bigger. It can be concluded that the tibolone molecule is less stable than its metabolite isotibolone.

Analysis of the dynamics trajectory shows that at room temperature as well as at the temperature of 340K the tibolone molecule prefers the conformation with negative inversion angle as can be seen also at the histograms (figure 46) showing statistical distribution inversion angle. This result is in agreement with the calculation of total bond energy, see table 8, where the conformation with negative inversion angle exhibits

lower total bond energy and therefore higher stability than the conformation with positive inversion angle.

In case of isotibolone, higher conformational stability in comparison to tibolone can be observed at both room temperature and the temperature of 340K. Isotibolone is stable in both conformations and even at higher temperatures the frequency of conformational changes of inversion angle is very low. This is probably due to very high potential barrier between energetical stages corresponding to positive and negative inversion angle conformation.

Total bond energy in kcal/mol		
	positive angle	negative angle
isotibolone	-26,6	-26,8
tibolone	-15,4	-16,3

Table 8: Total bond energy calculated in cff 91 force field for tibolone and isotibolone; both conformations of inversion angle were taken into account.

2.2.2 Stability of Tibolone Immersed into the β-CD

As cyclodextrines serves also as stabilizers the stability of tibolone immersed into the β-CD cavity was studied. Conformational changes of inversion angle were studied as it was found out that apart this angle only the position of OH group changes, what was expected. Two initial models for each conformation (figure 39) were built, tibolone with the OH group both inside and outside the cavity. Minimized models from molecular mechanics studies were used.

All of the above mentioned four models were studied at room temperature and at temperature of 340K, again the NVT ensemble was used and the same settings as in the previous dynamics simulations. The graphs representing the conformational behaviour of the inversion angle of tibolon being immersed into the β-CD cavity with OH group upwards (angle of interest being inside the cavity) and tibolon being immersed into the

β-CD cavity with the OH group downwards (inversion angle being outside the cavity) are shown in figure 48 and 50 respectively.

It was discovered that tibolone immersed into the β-CD cavity with the OH group being upwards and the inversion angle being inside the cavity statistically prefers the conformation set in the initial models (see figure 49) what indicates that tibolone conformation is in some way stabilised by immersion into the β-CD cavity. Higher stability of tibolone inside the β-CD basket is supported by comparison of histograms showing inversion angle distribution for free tibolone and tibolone inside the β-CD cavity (figures 46 and 49 respectively). For free tibolone the distribution of inversion angle depends on temperature (300K and 340K), whereas the distribution of inversion angle for tibolone being immersed into the β-CD cavity with OH group upwards is the same for both temperatures.

Tibolone being immersed into the β-CD cavity the other way, OH group inside the cavity and inversion angle outside, is neither less nor more stable than tibolone alone and it can be seen that the preferred conformation of tibolone with OH group inside the β-CD cavity is that one with negative inversion angle (figure 51) as for free tibolone.

As in the real crystal structure the molecules of tibolone can be immersed into the cavities of β-cyclodextrine randomly, as none of the two possibilities (OH group outside and OH group inside the β-CD basket) is more favoured, it can be concluded that the complexation of tibolone with β-CD does contribute to the conformational stability of tibolone to a certain extent. It should be noticed that there can be also certain effect of neighbouring CD molecules on the conformational behaviour of tibolone immersed into the CD basket with, anyway this effect was not studied in present work.

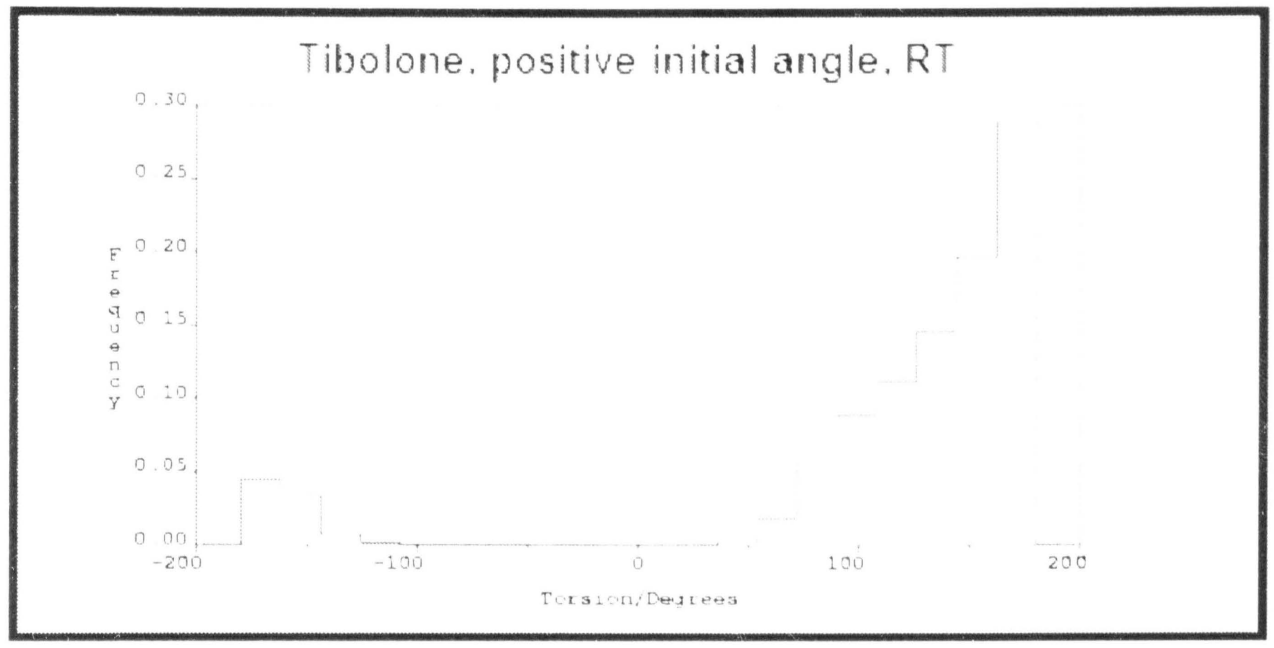

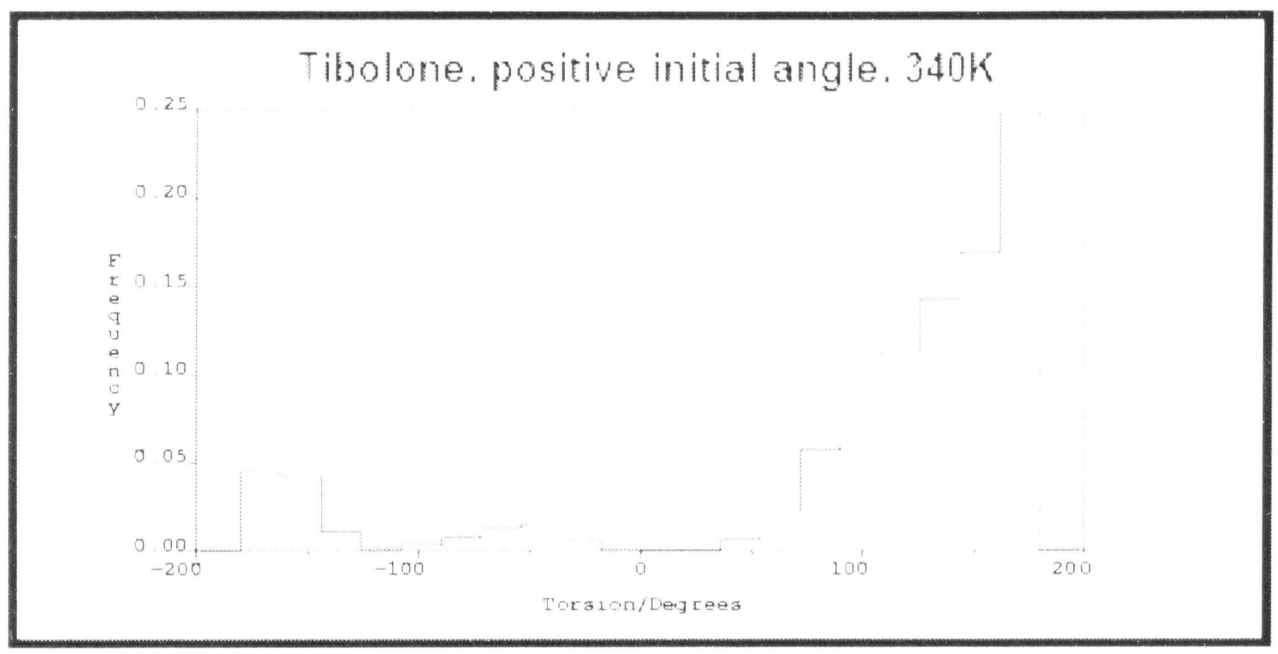

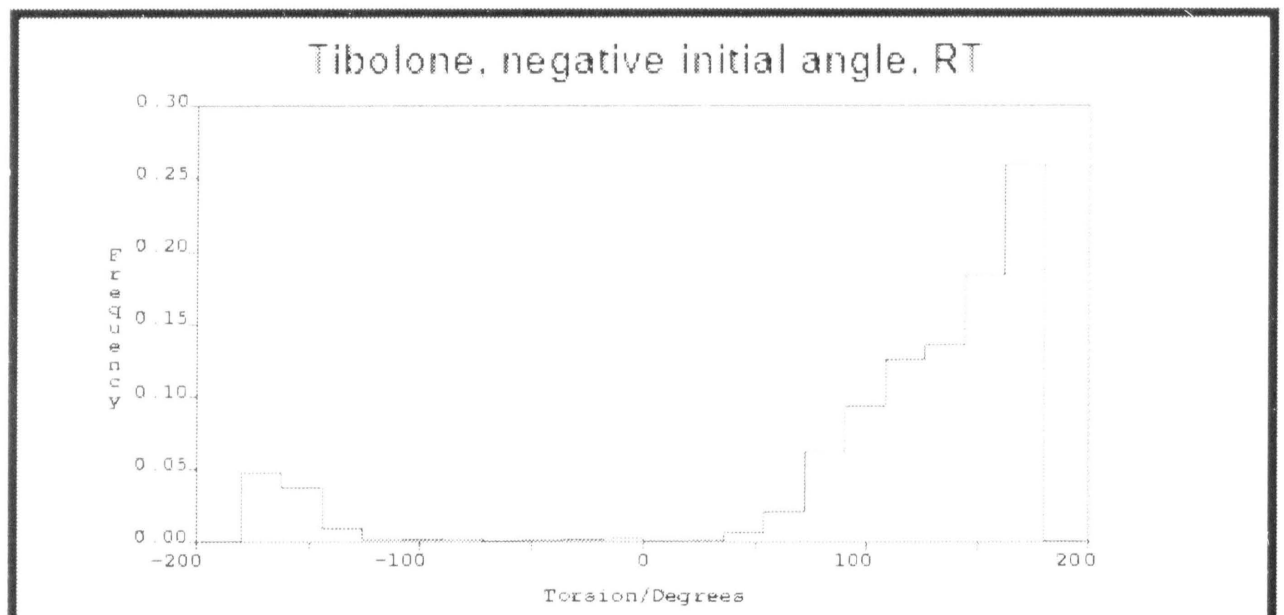

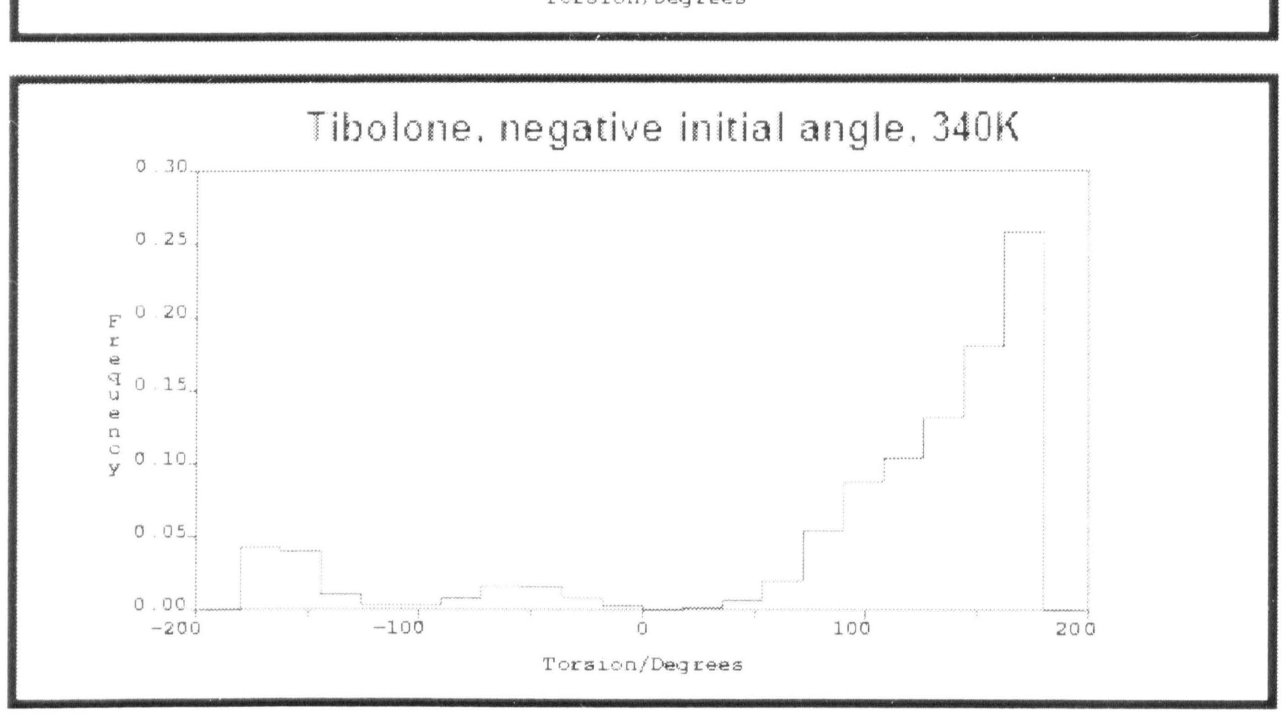

Figure 41: Statistical distribution of torsion angle *C-C-O-H,* extracted from the dynamics trajectories of two tibolone models (positive and negative initial inversion angle) at room temperature (RT) and at temperature of 340K, made in Cerius[2]

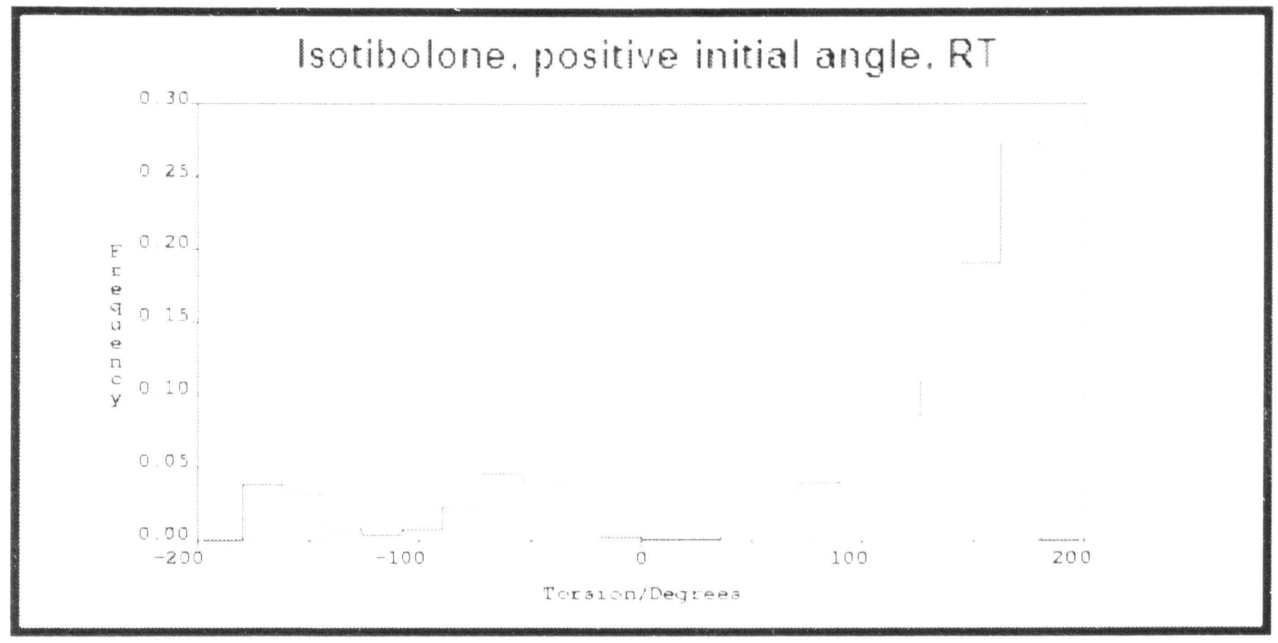

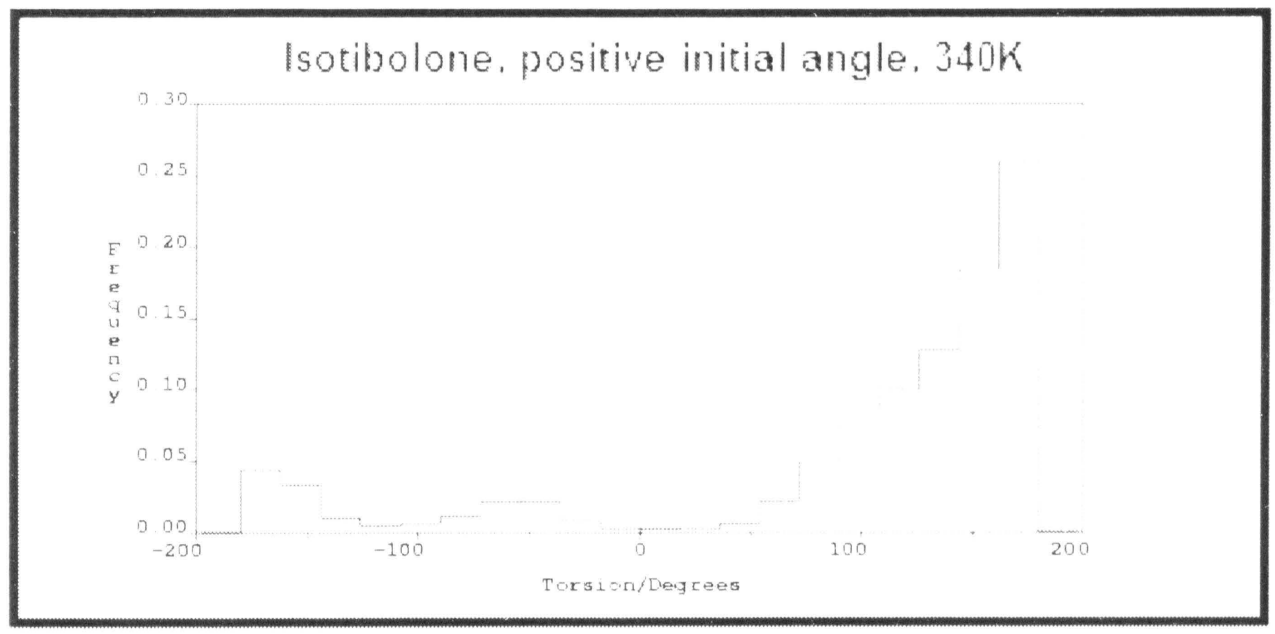

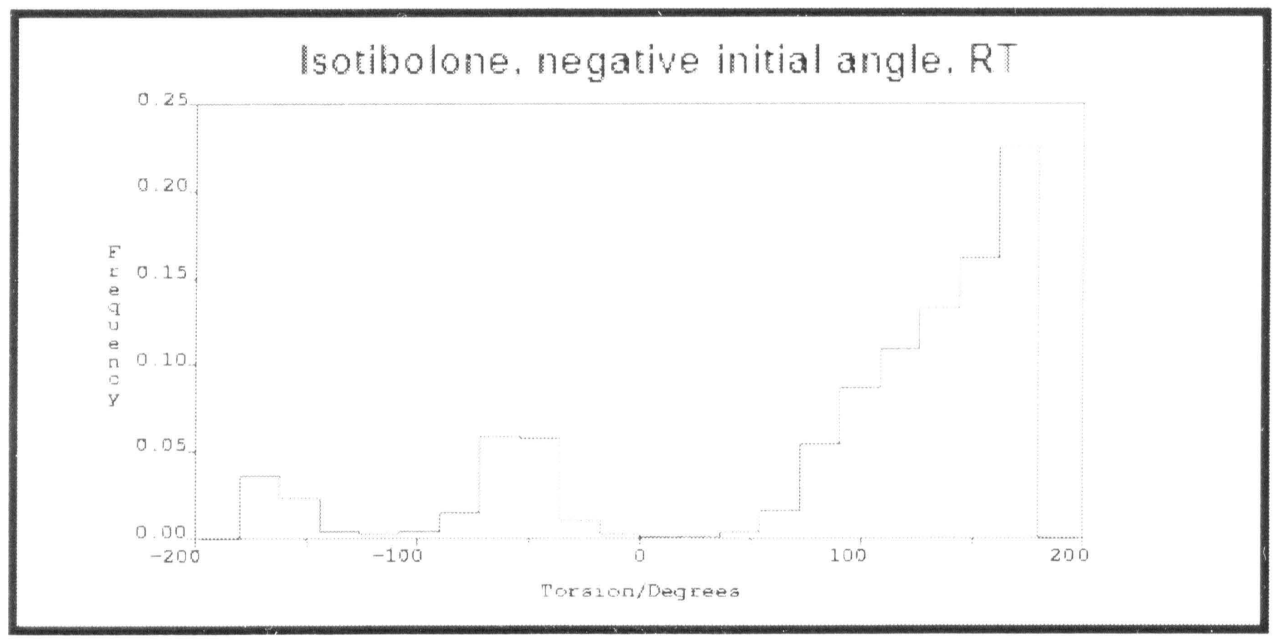

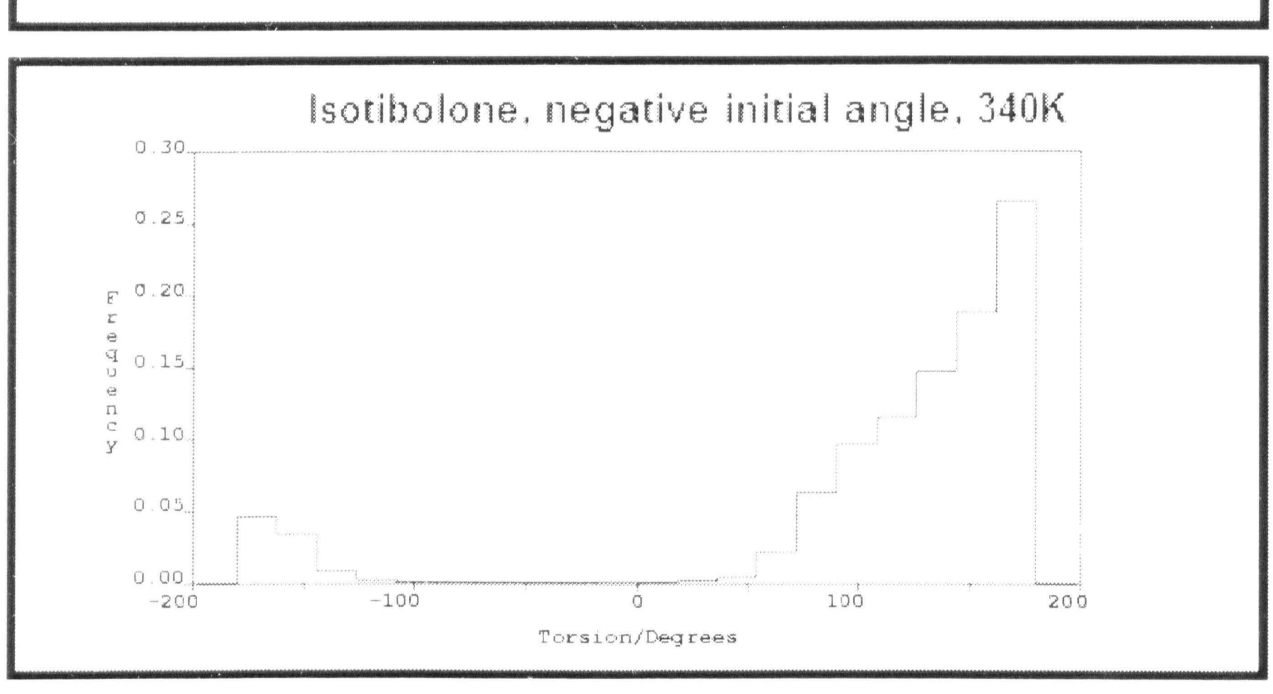

Figure 42: Statistical distribution of torsion angle *C-C-O-H,* extracted from the dynamics trajectories of two isotibolone models (positive and negative initial inversion angle) at room temperature (RT) and at temperature of 340K, made in Cerius[2]

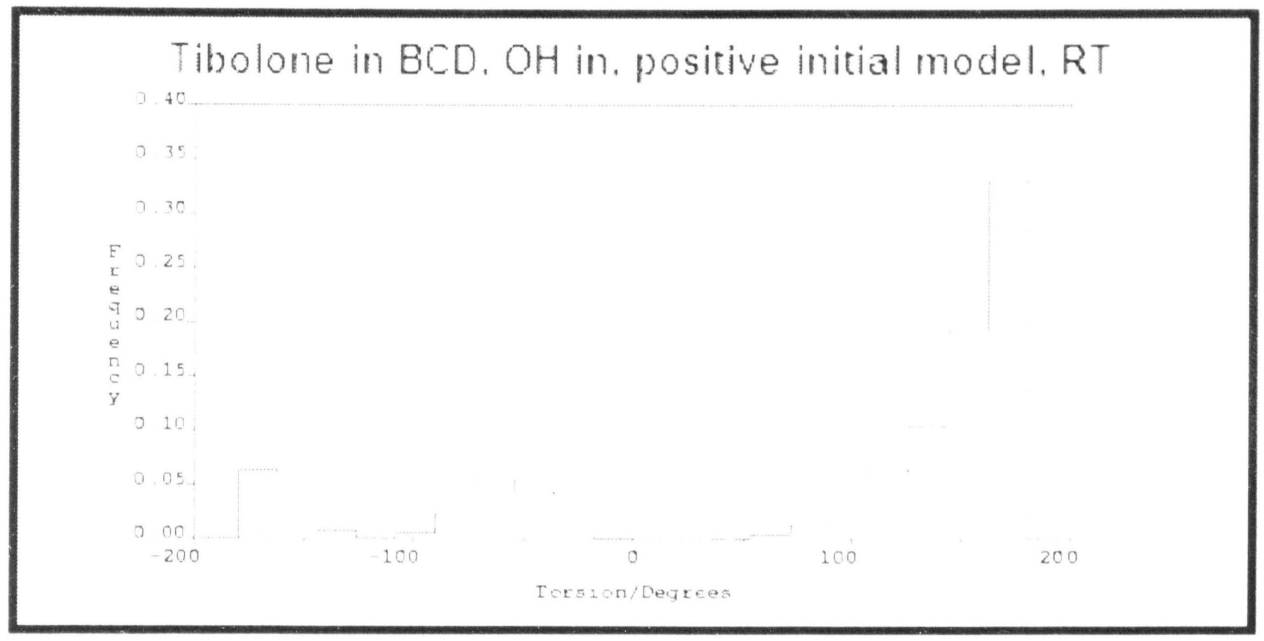

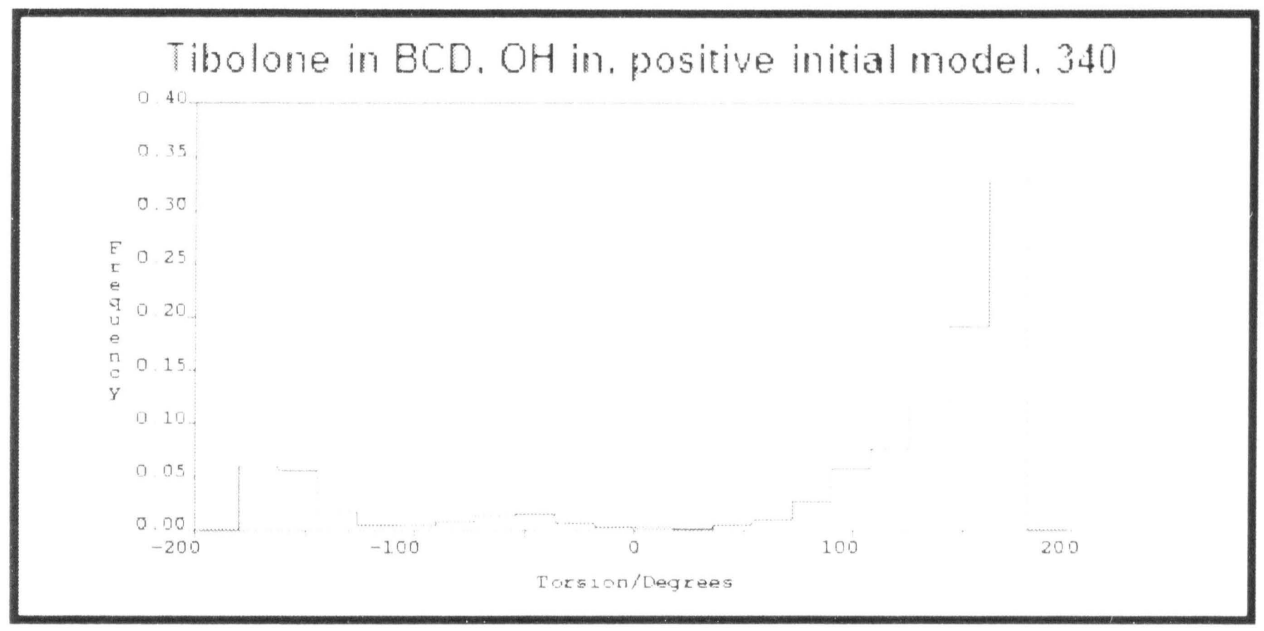

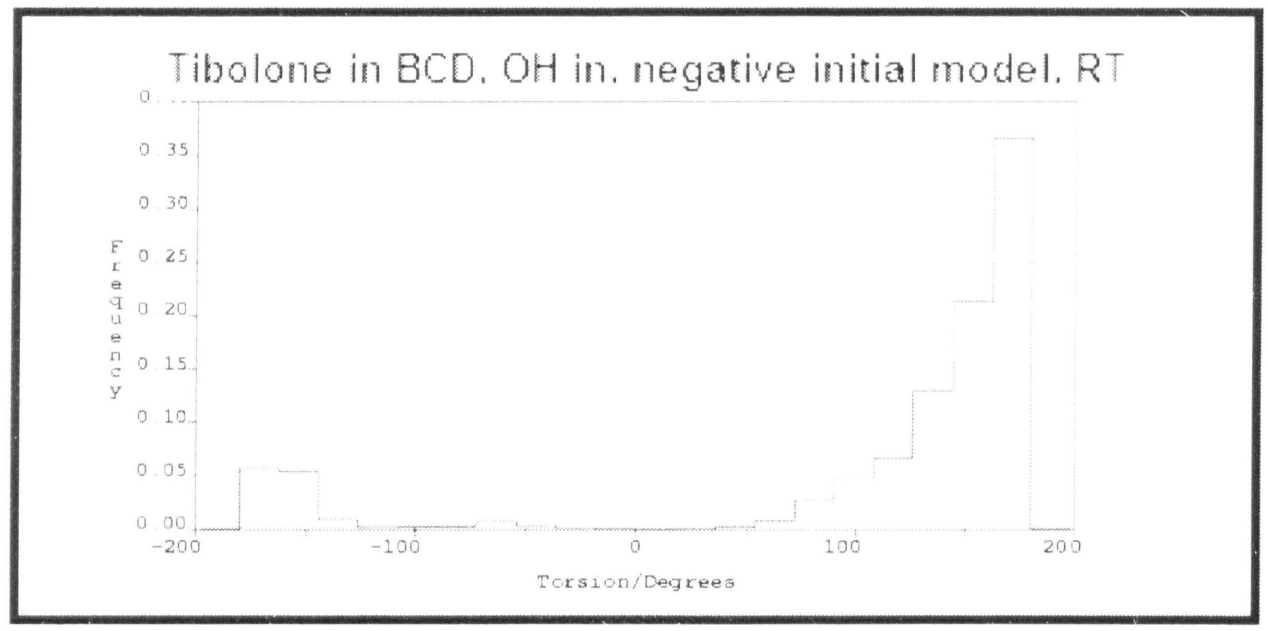

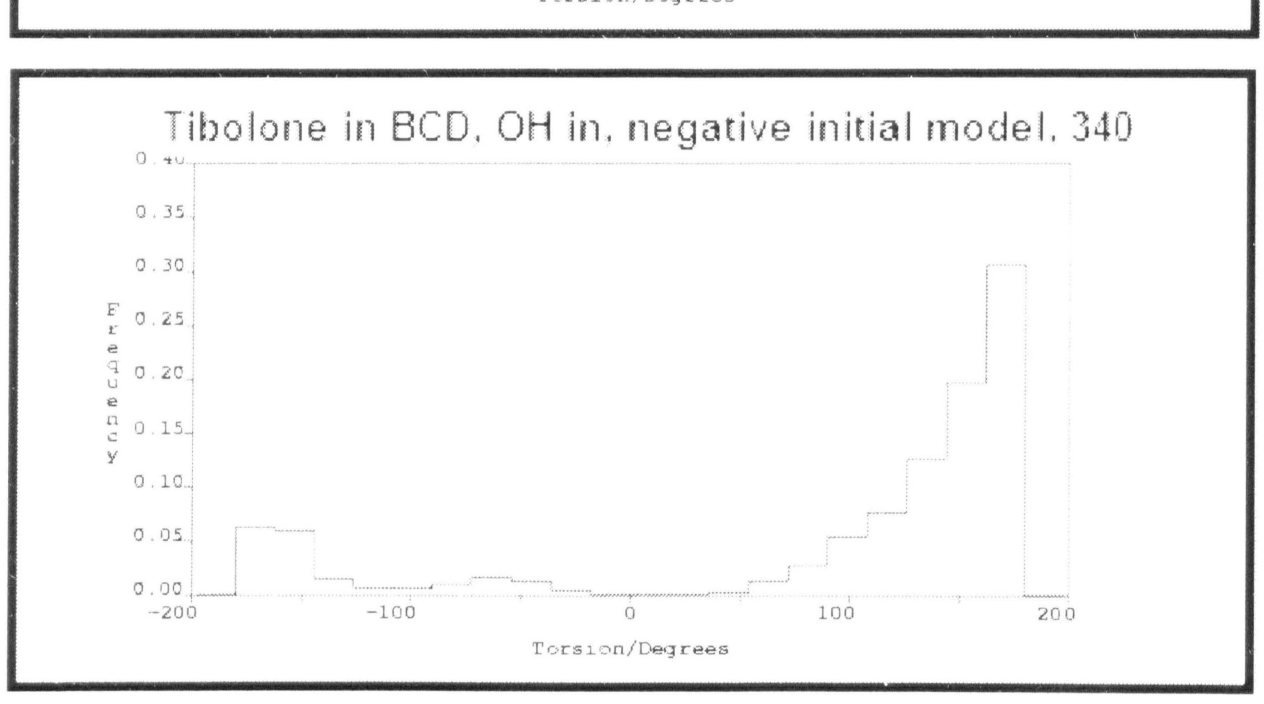

Figure 43: Statistical distribution of torsion angle C-C-O-H in two tibolone models (positive and negative initial inversion angle) at room temperature (RT) and at temperature of 340K immersed into the β-CD cavity with OH group being inside the cavity and inversion angle being outside, made in Cerius[2]

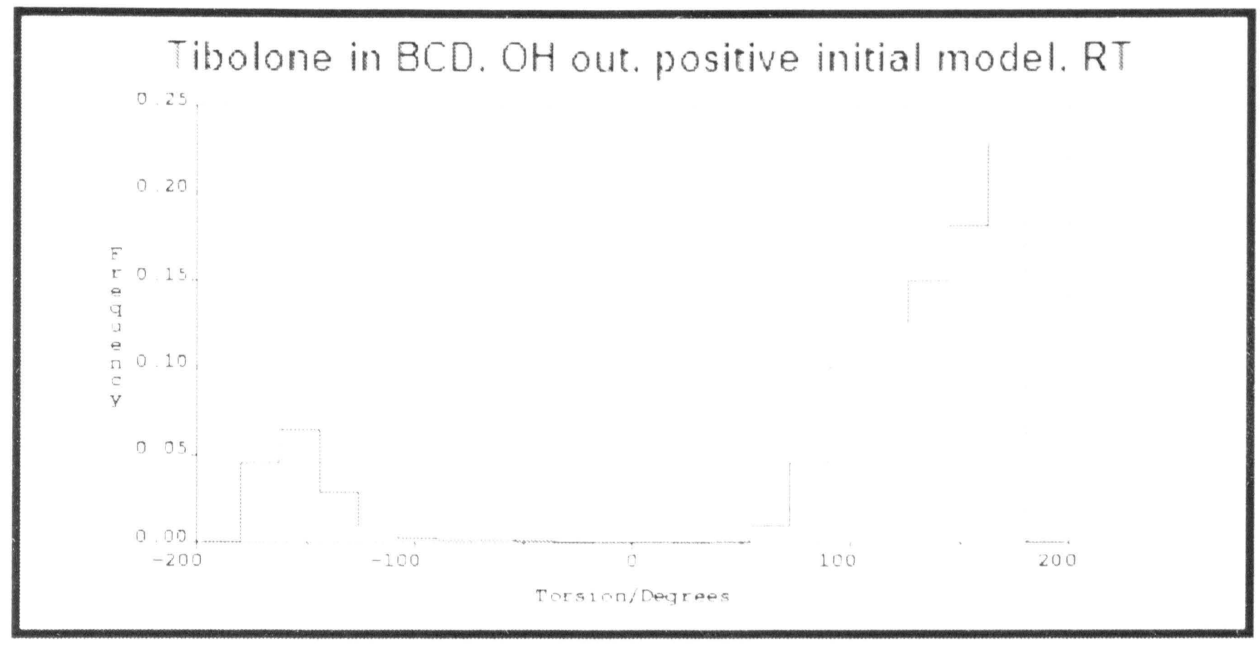

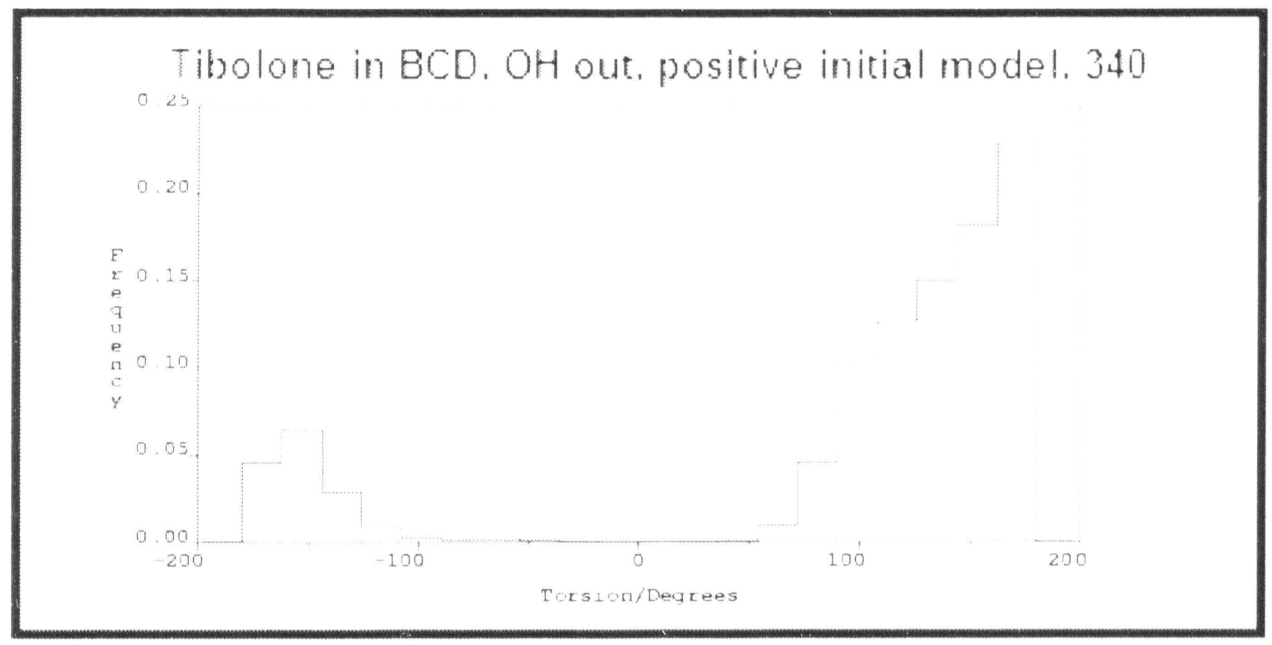

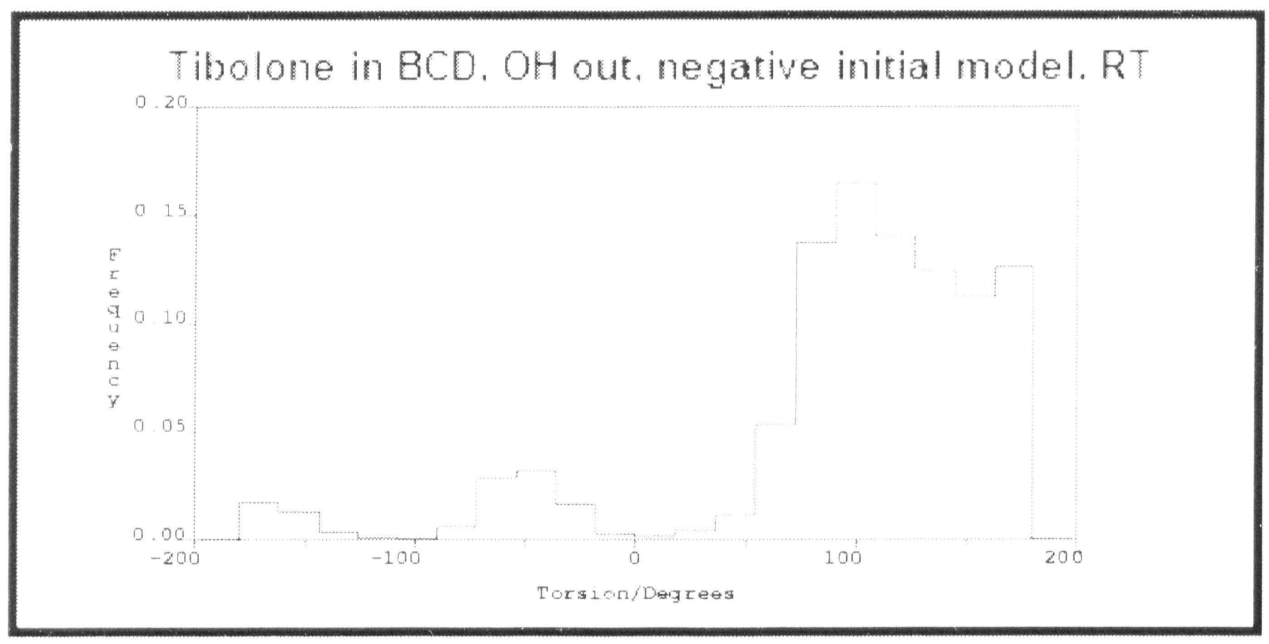

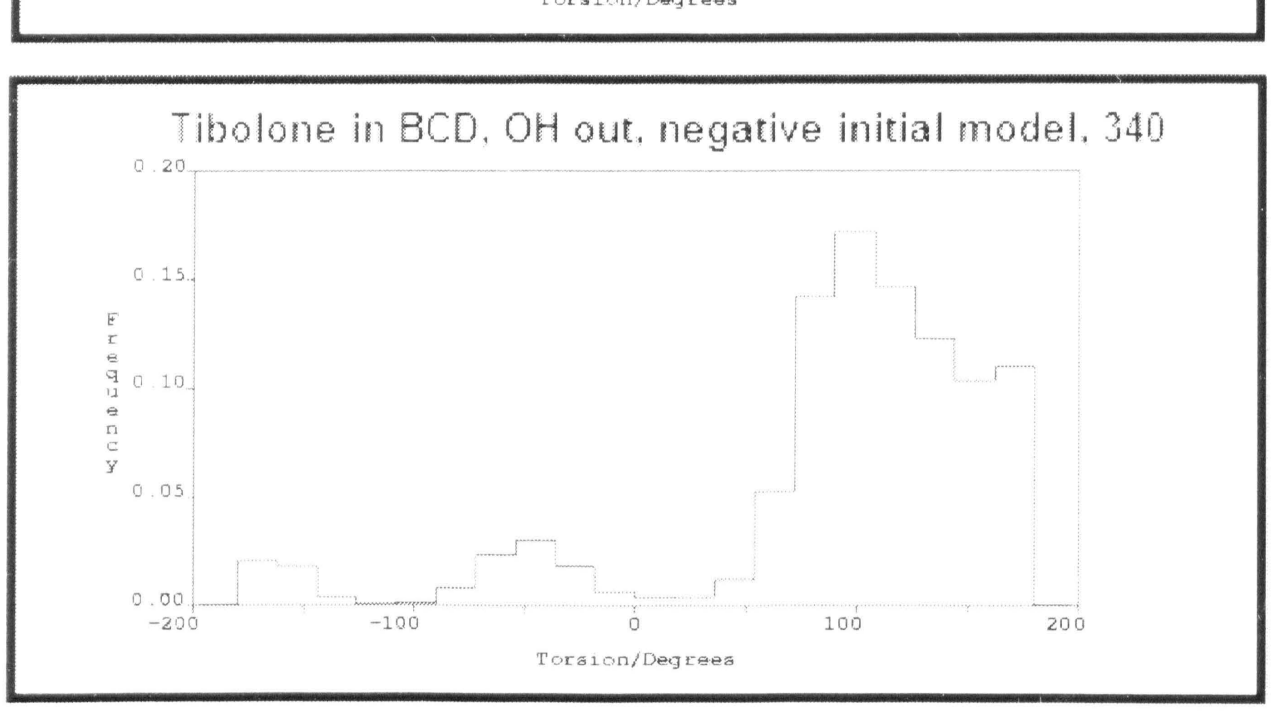

Figure 44: Statistical distribution of torsion angle C-C-O-H in two tibolone models (positive and negative initial inversion angle) at room temperature (RT) and at temperature of 340K immersed into the β-CD cavity with OH group being outside the cavity and inversion angle being outside, made in Cerius[2]

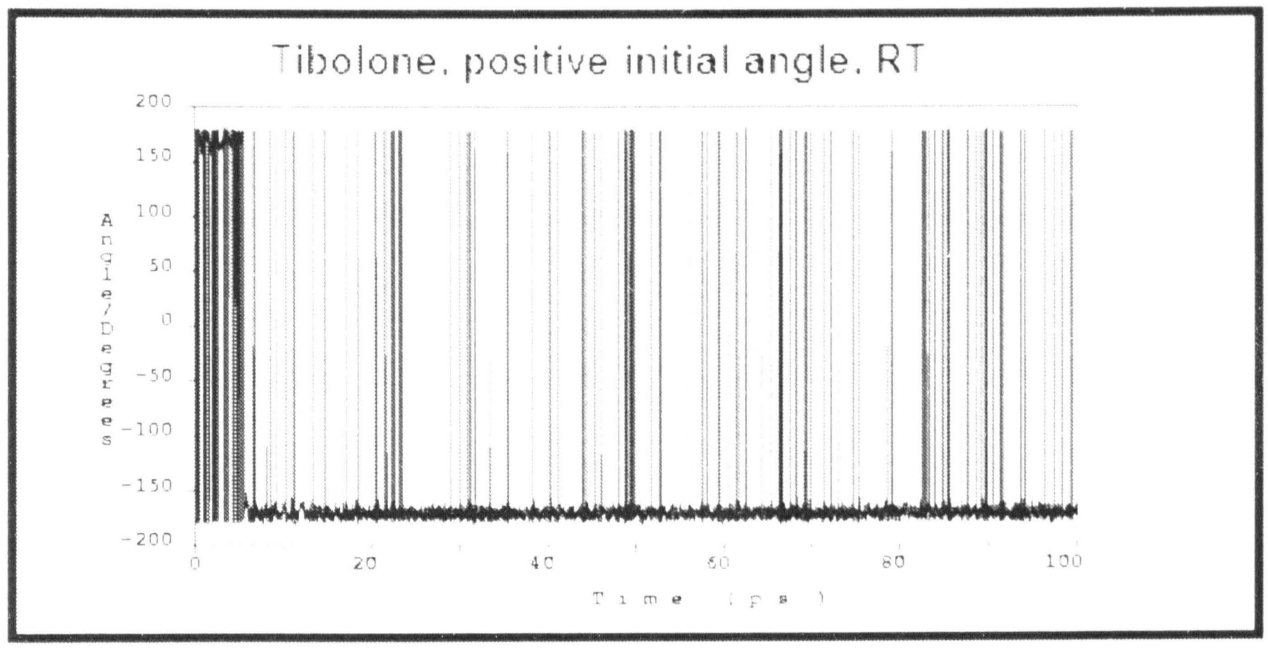

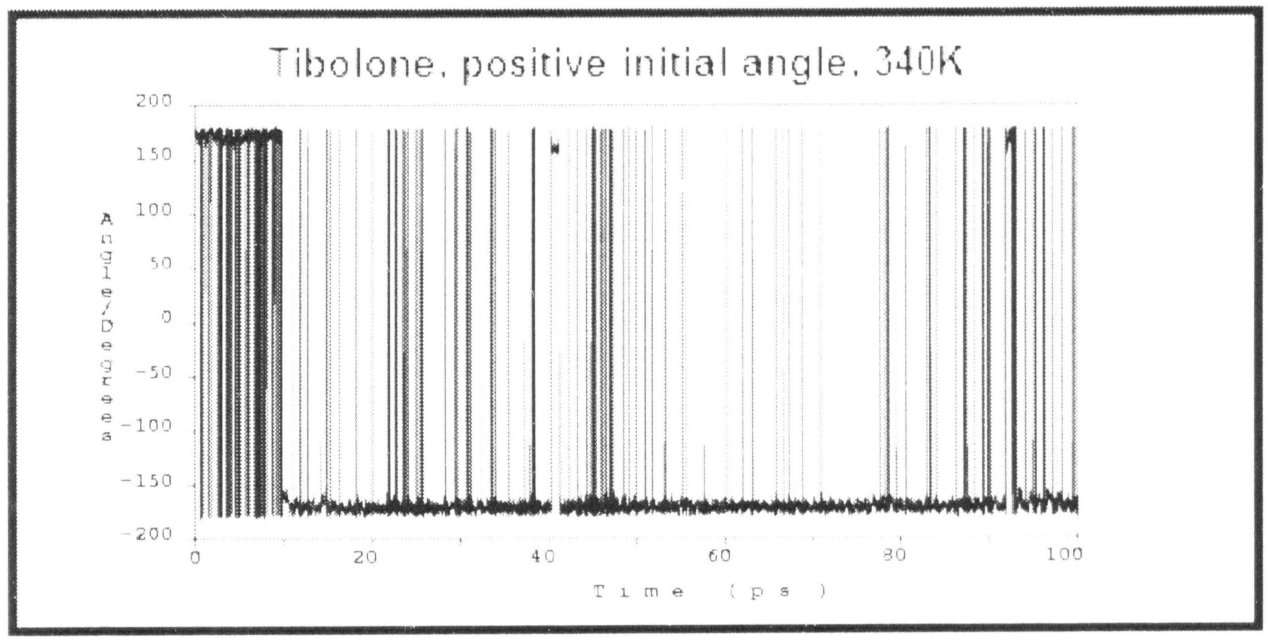

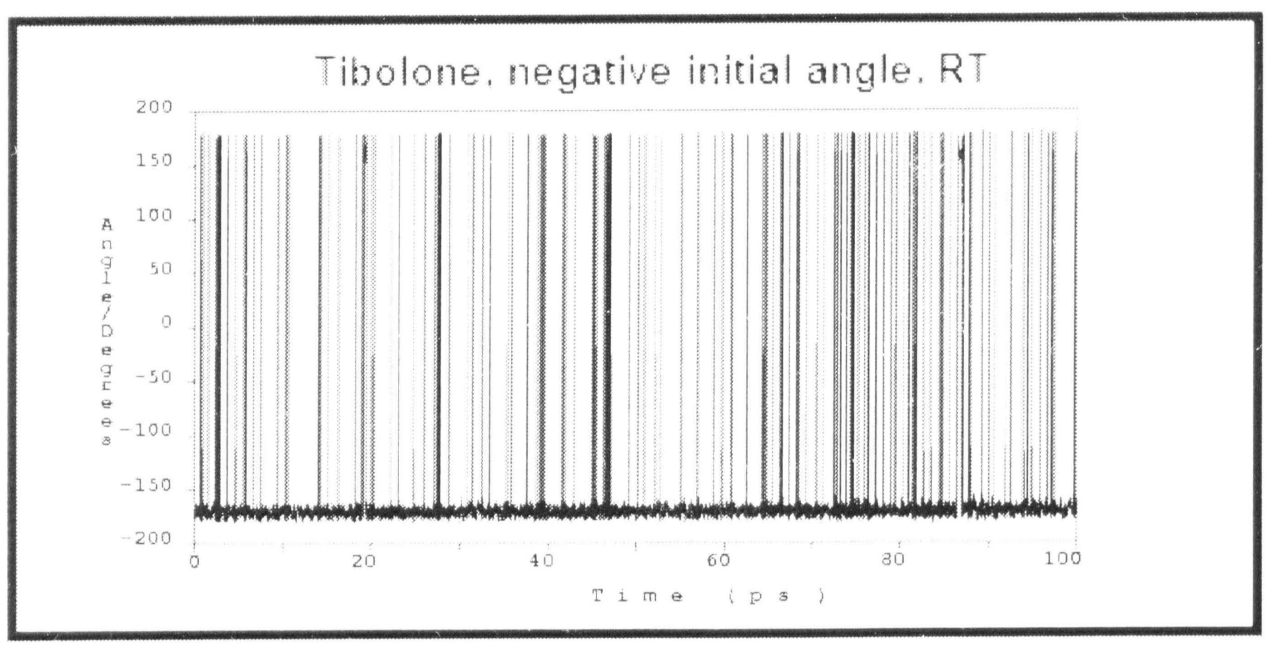

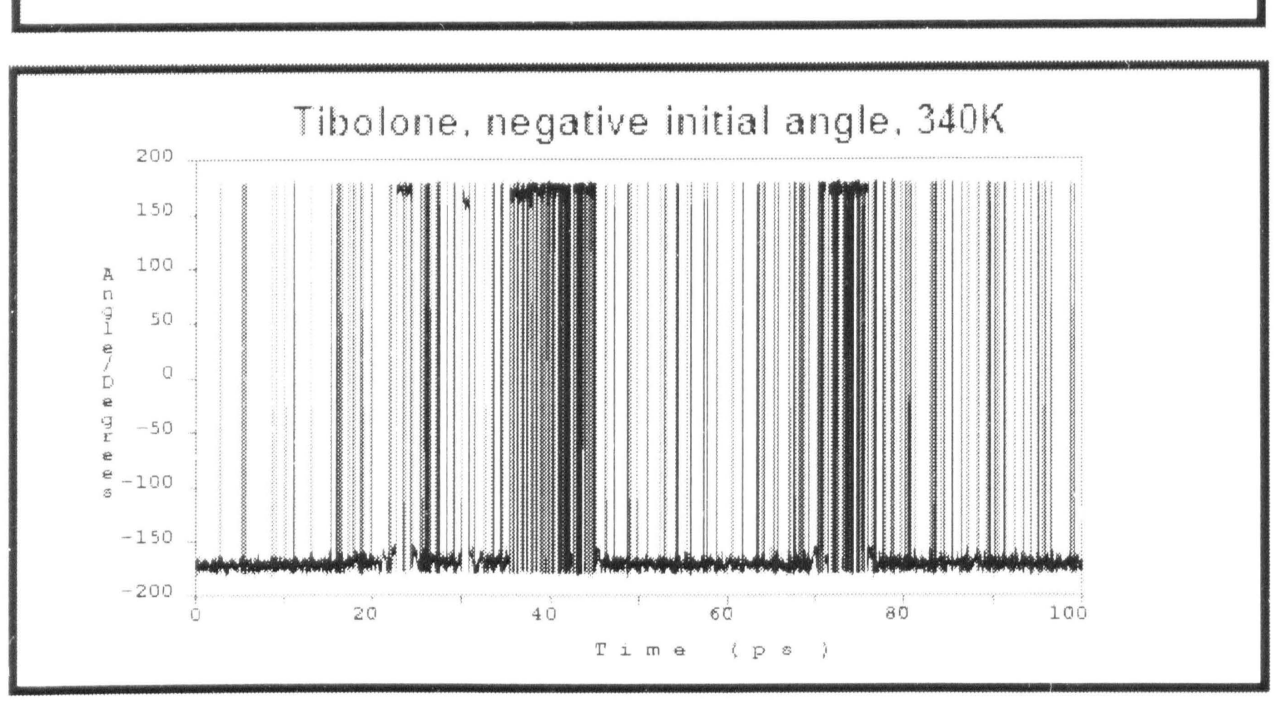

Figure 45: Conformational changes of inversion angle in two tibolone models (positive and negative initial inversion angle) at room temperature (RT) and at temperature of 340K, made in Cerius[2]

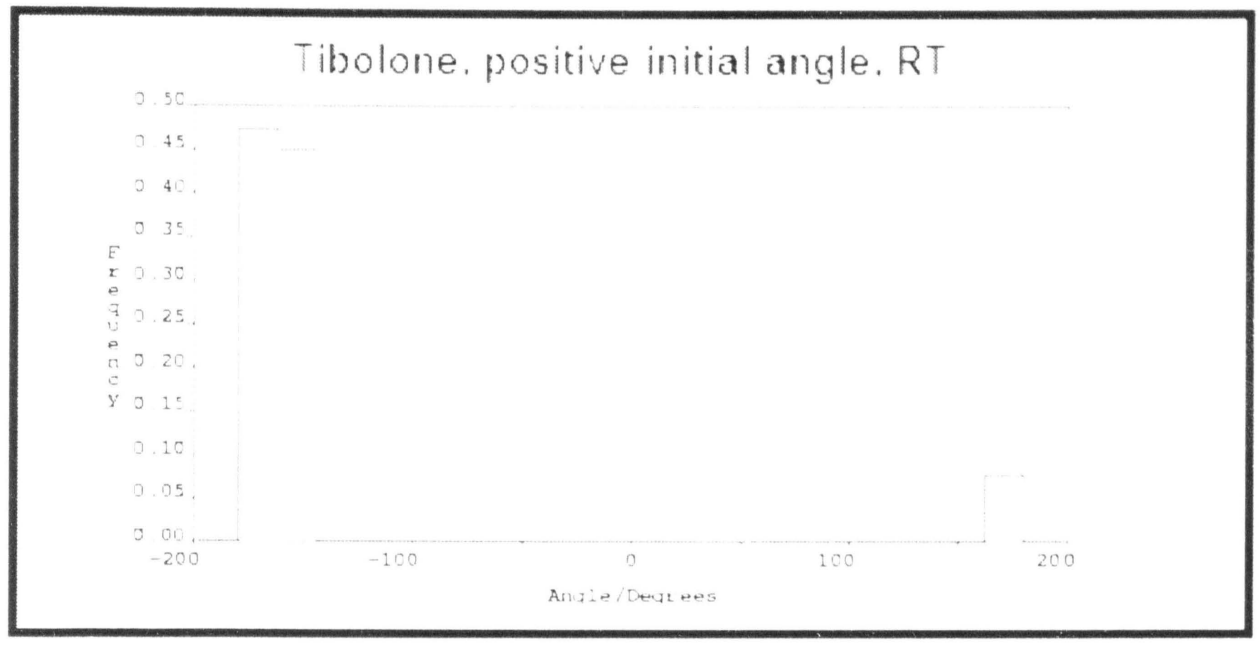

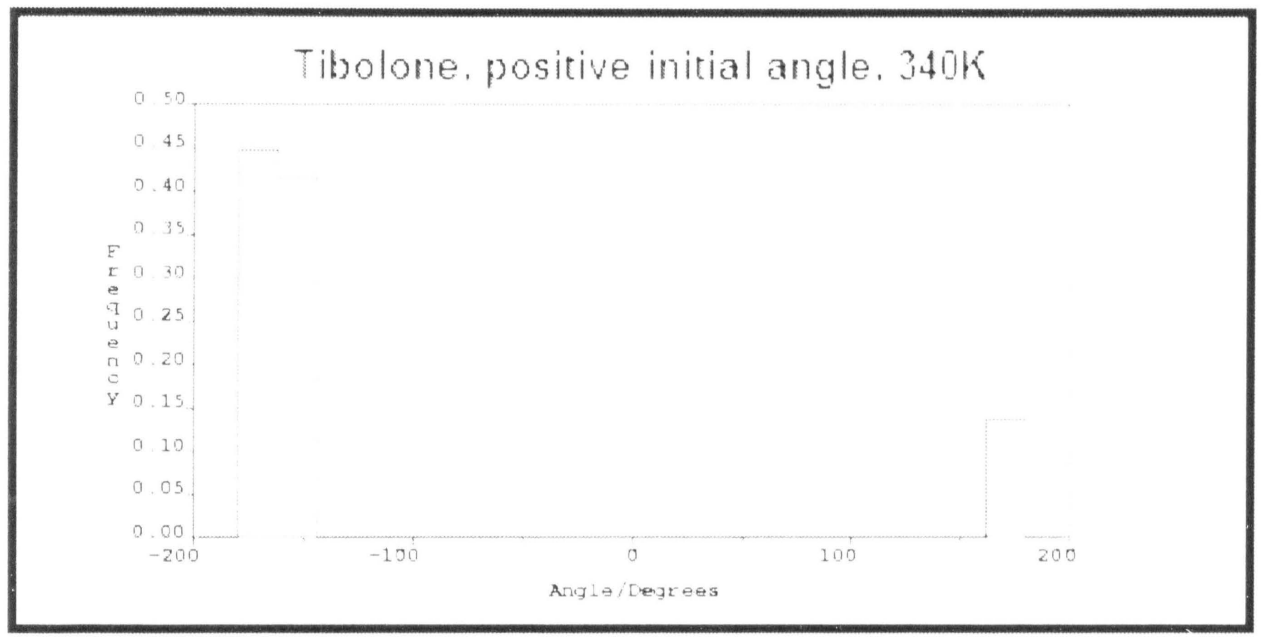

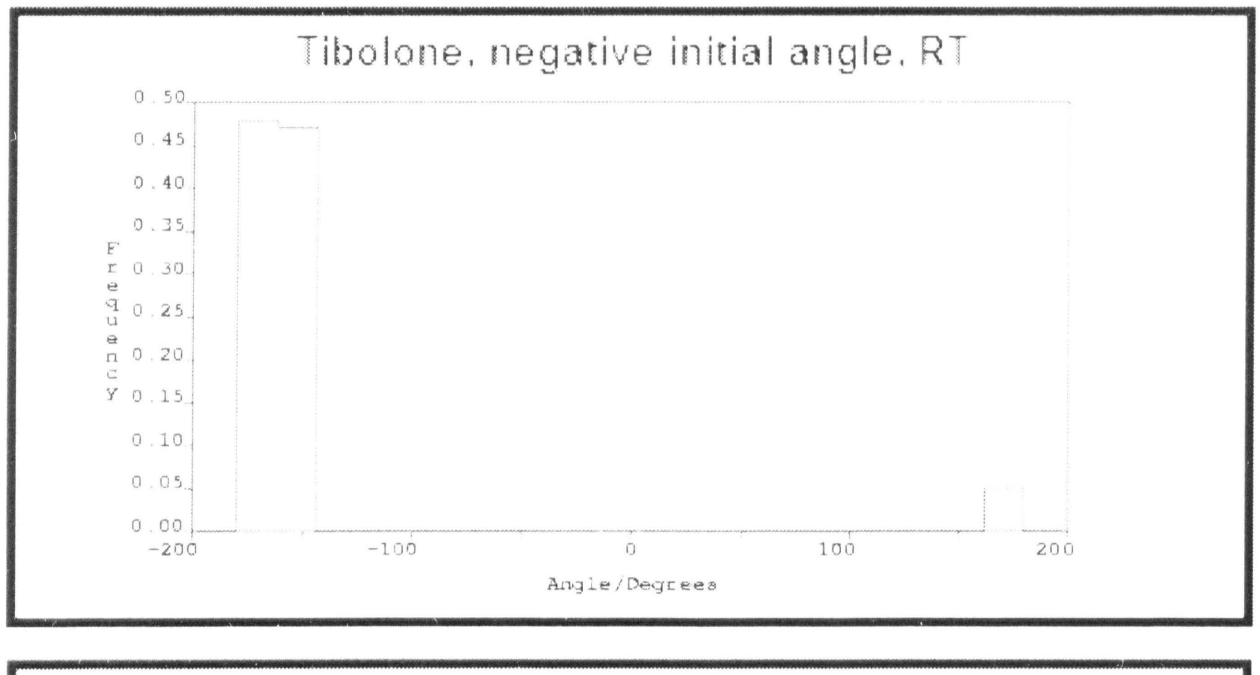

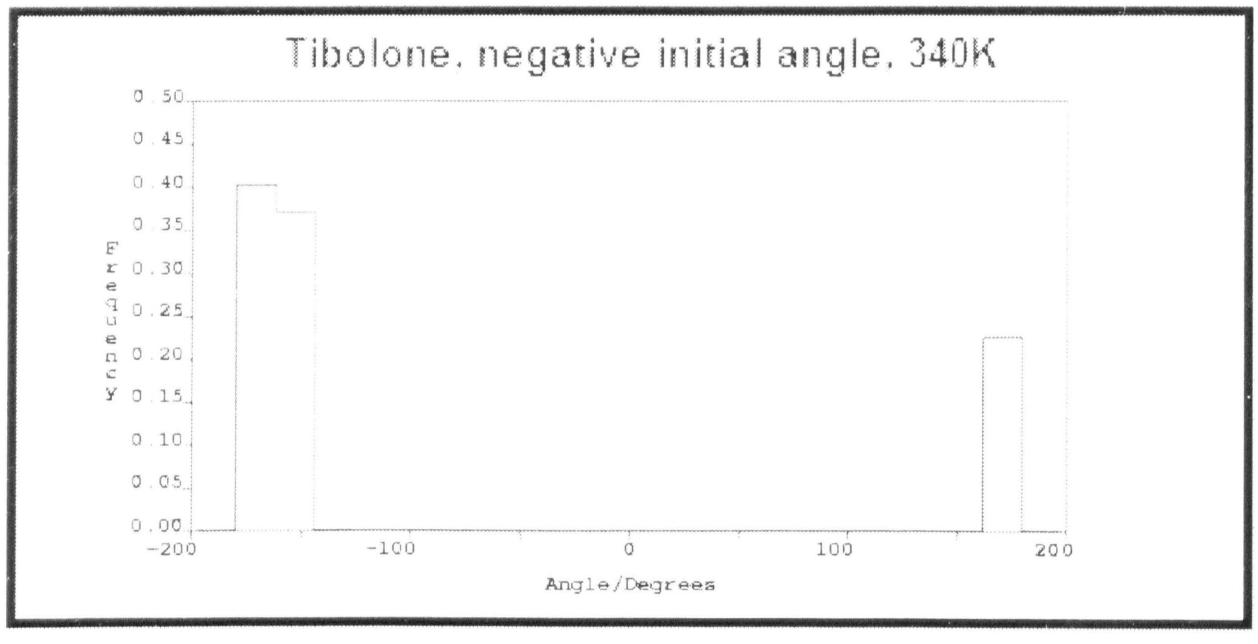

Figure 46: Statistical distribution of inversion angle, extracted from the dynamics trajectories of two tibolone models (positive and negative initial inversion angle) at room temperature (RT) and at temperature of 340K, made in Cerius[2]

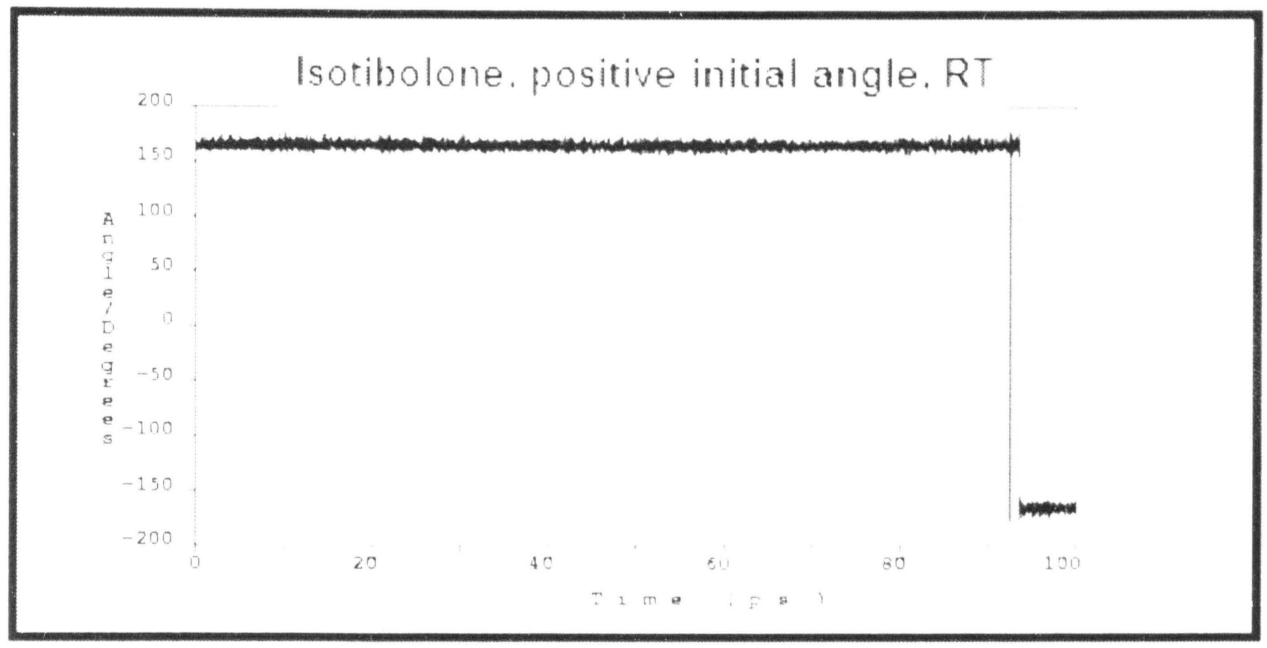

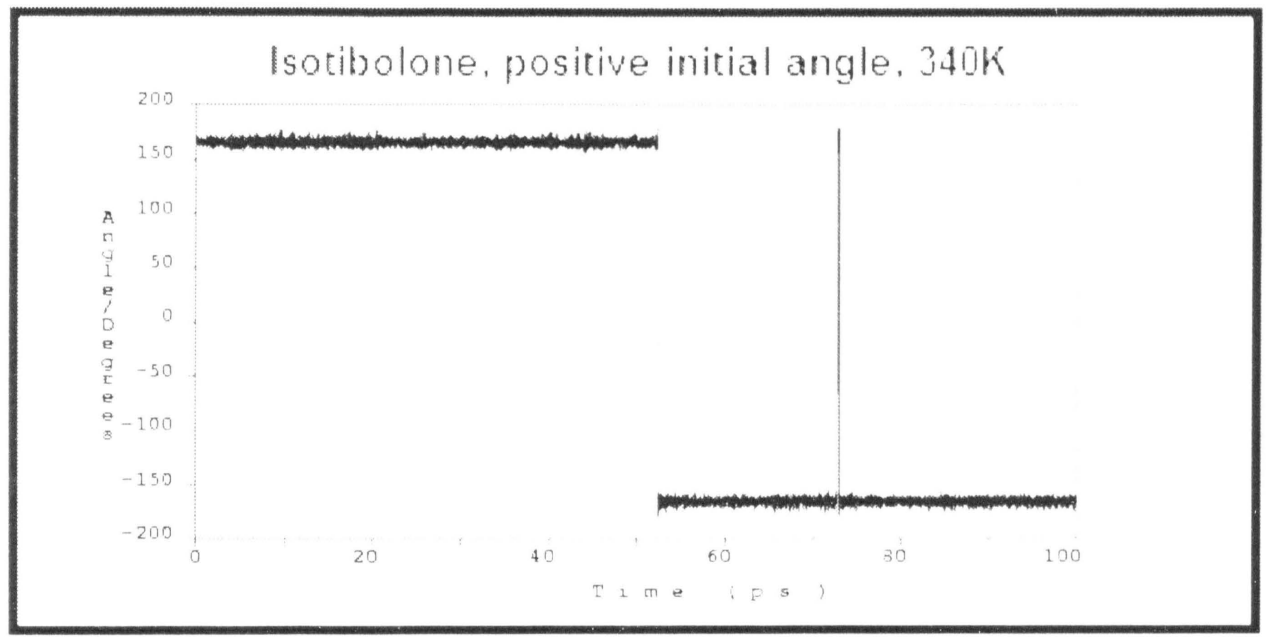

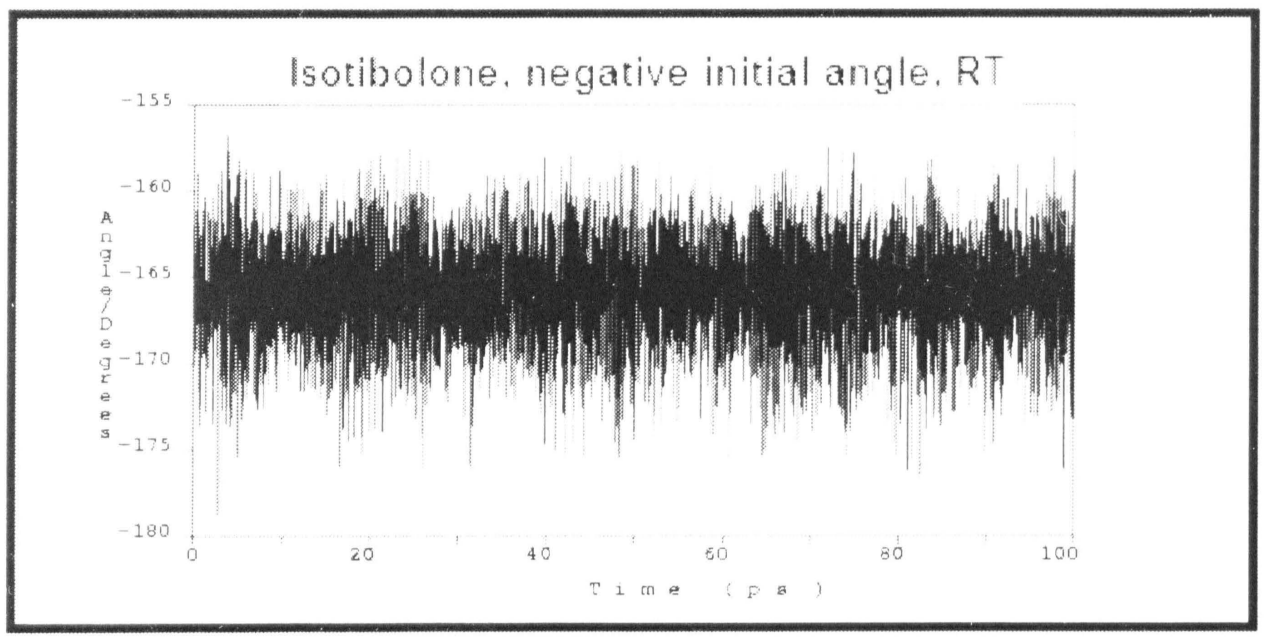

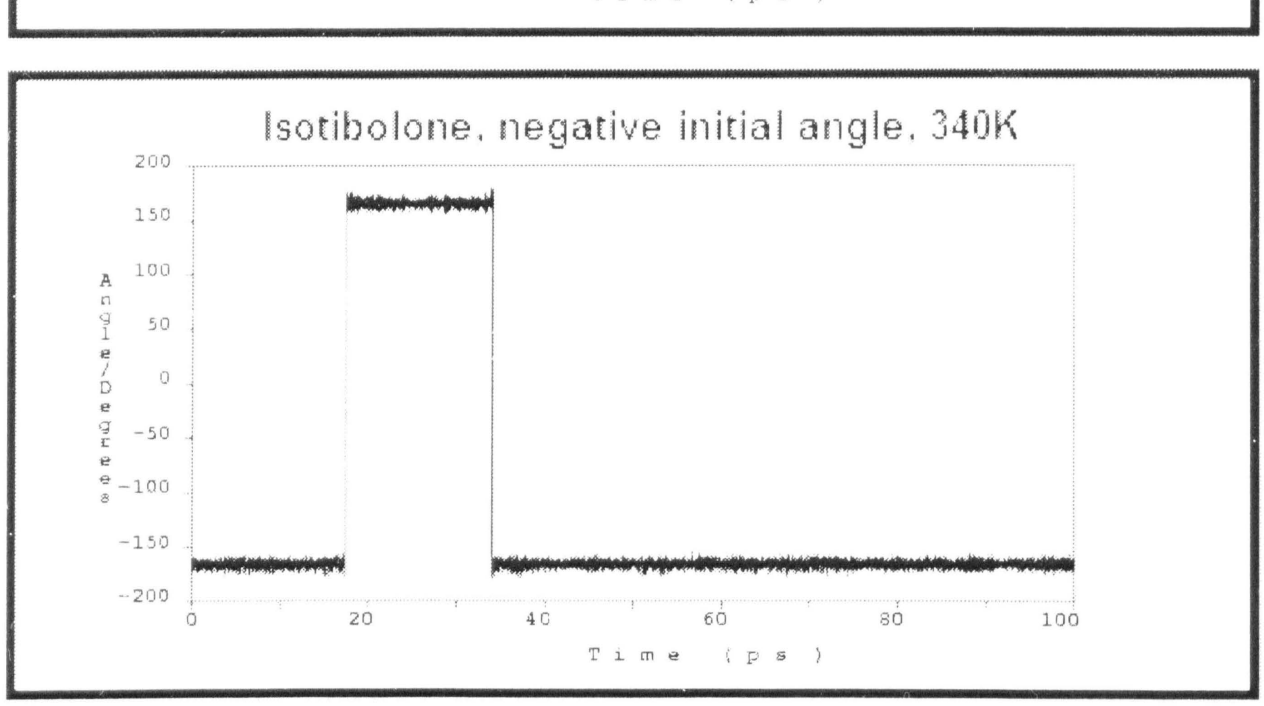

Figure 47: Conformational changes of inversion angle in two isotibolone models (positive and negative initial inversion angle) at room temperature (RT) and at temperature of 340K, made in Cerius[2]

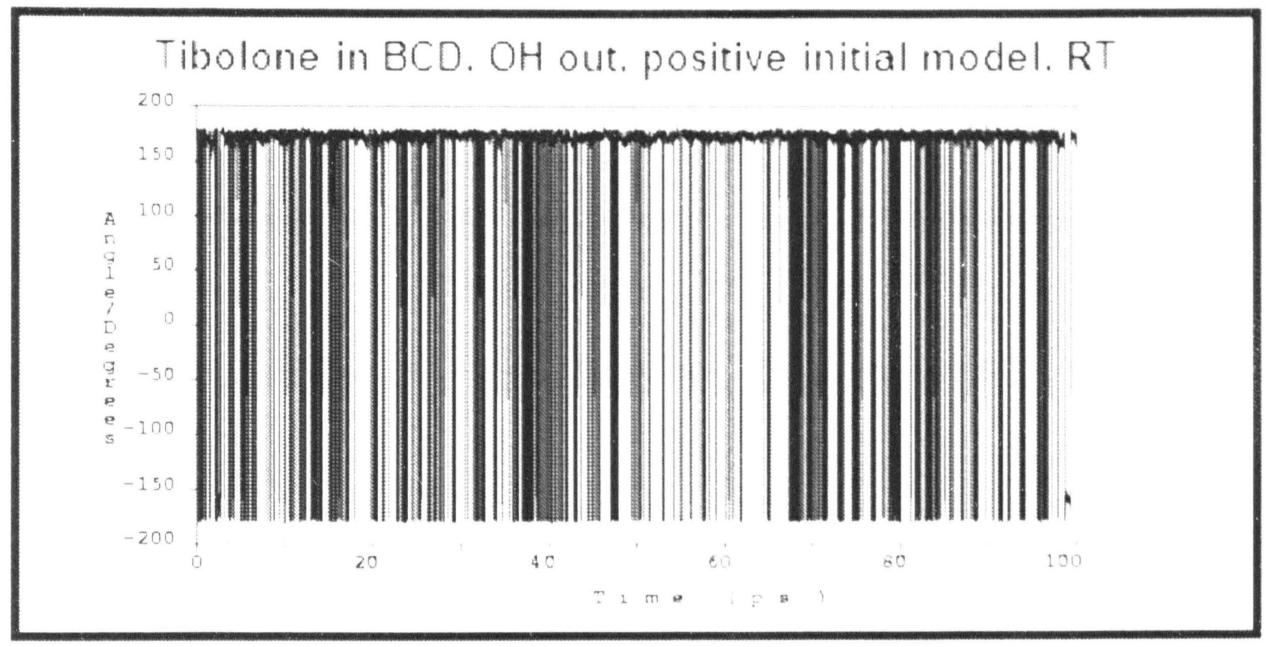

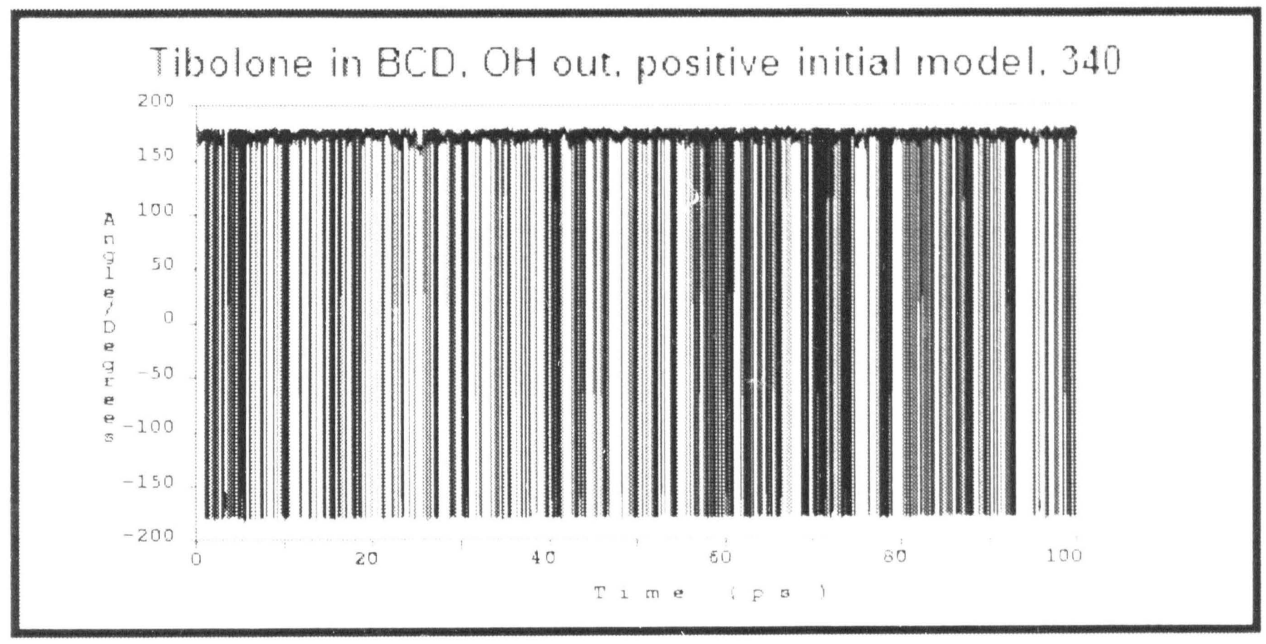

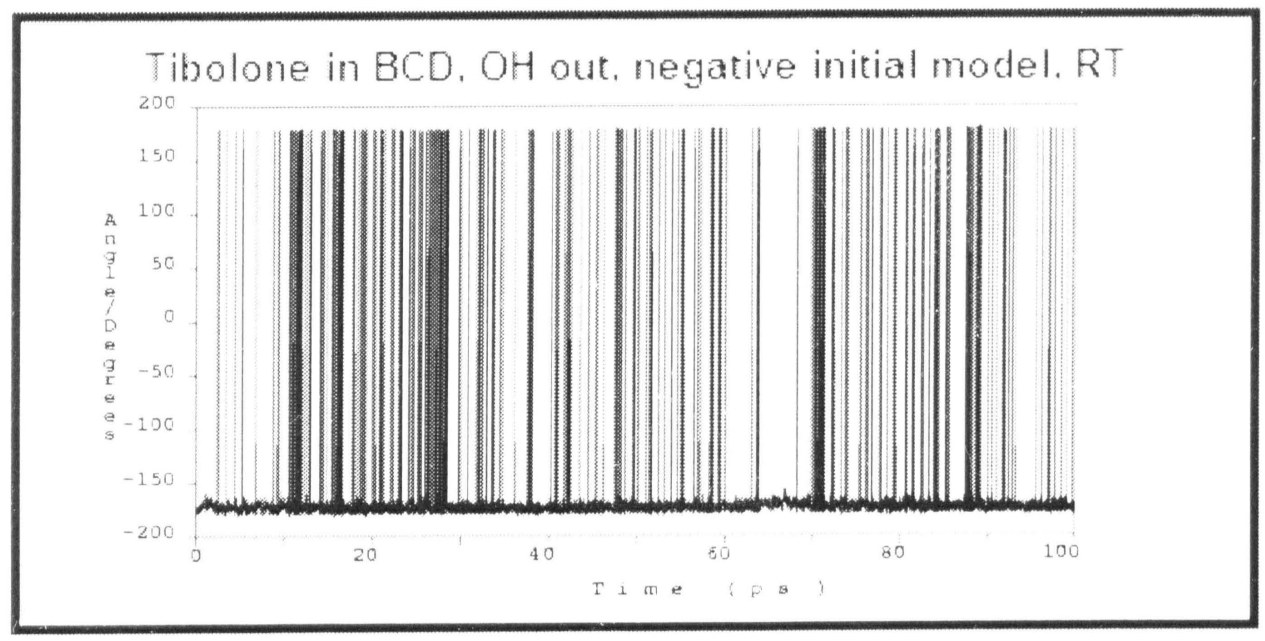

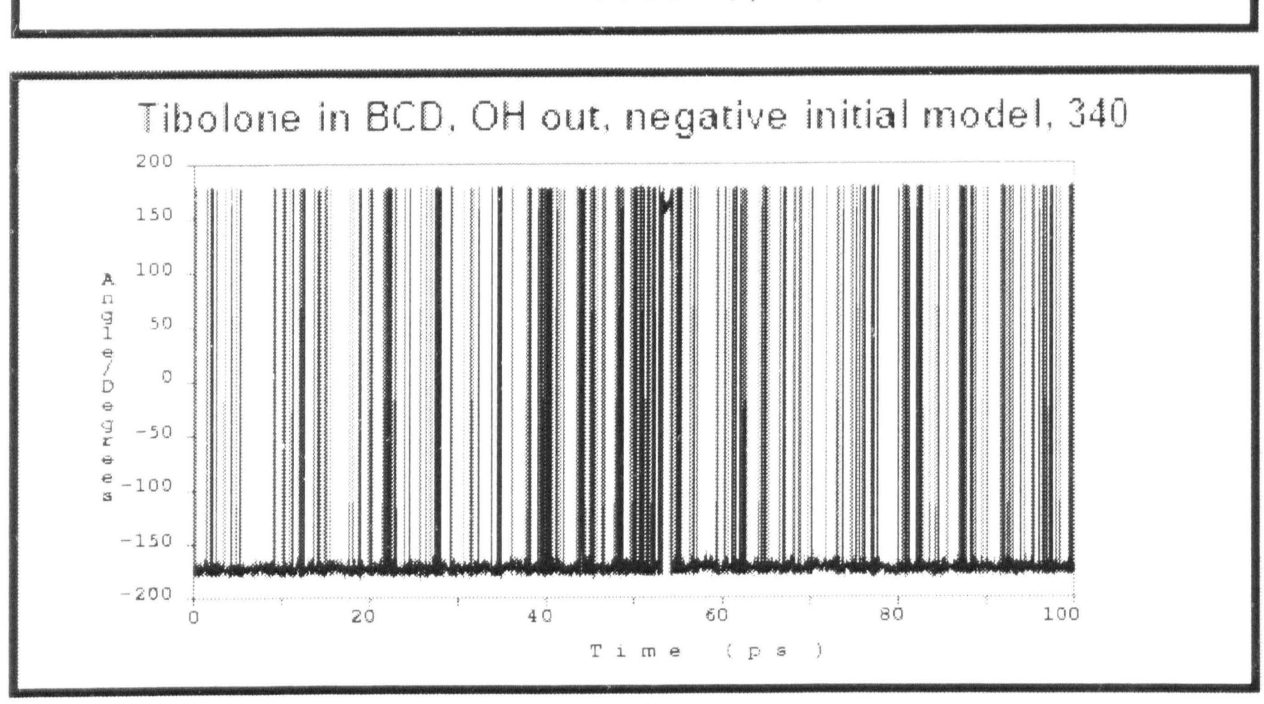

Figure 48: Conformational changes of inversion angle in two tibolone models (positive and negative initial inversion angle) at room temperature (RT) and at temperature of 340K immersed into the β-CD cavity with OH group being outside the cavity and inversion angle being inside, made in Cerius[2]

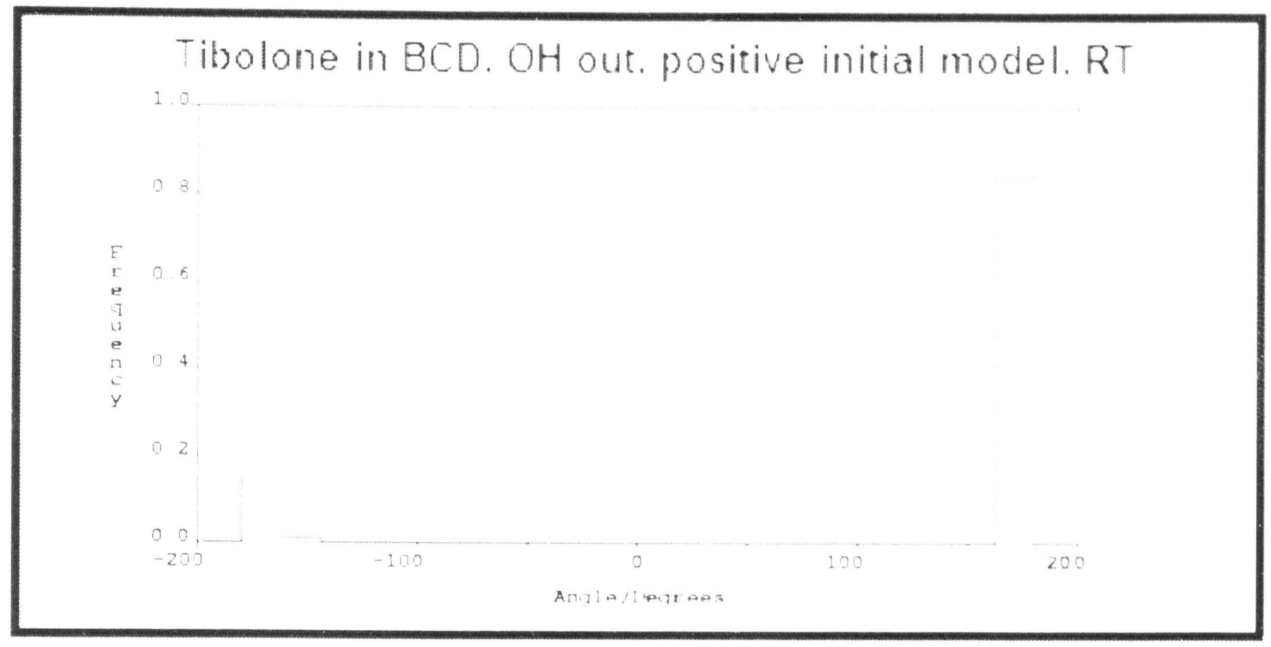

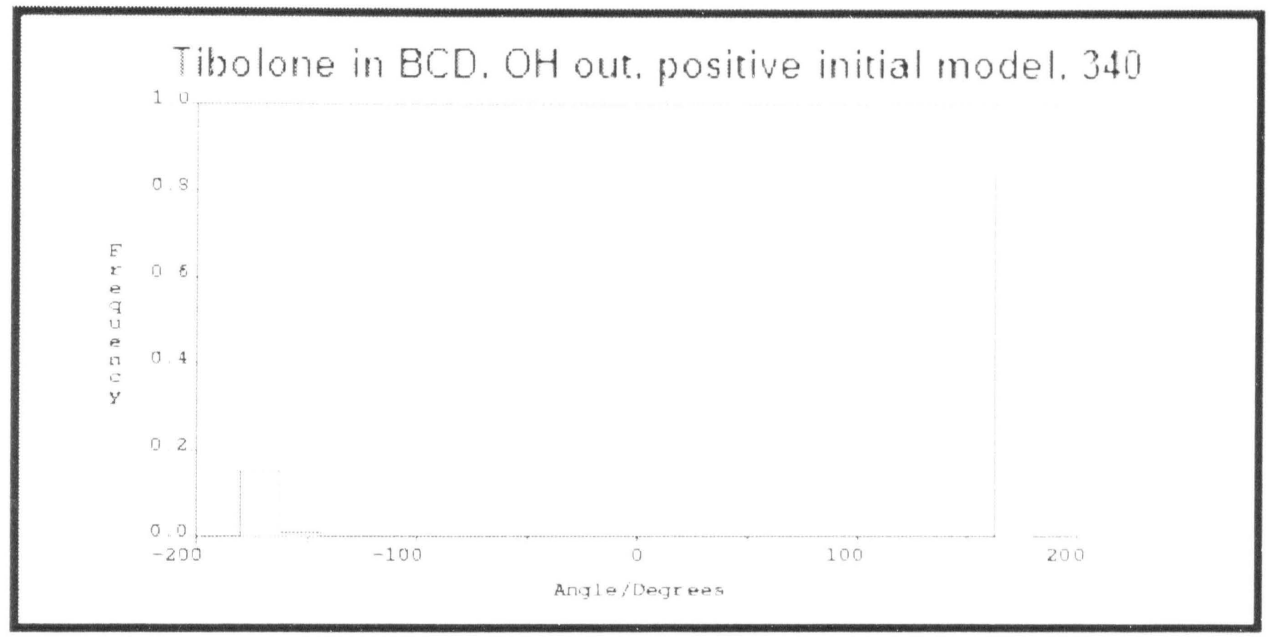

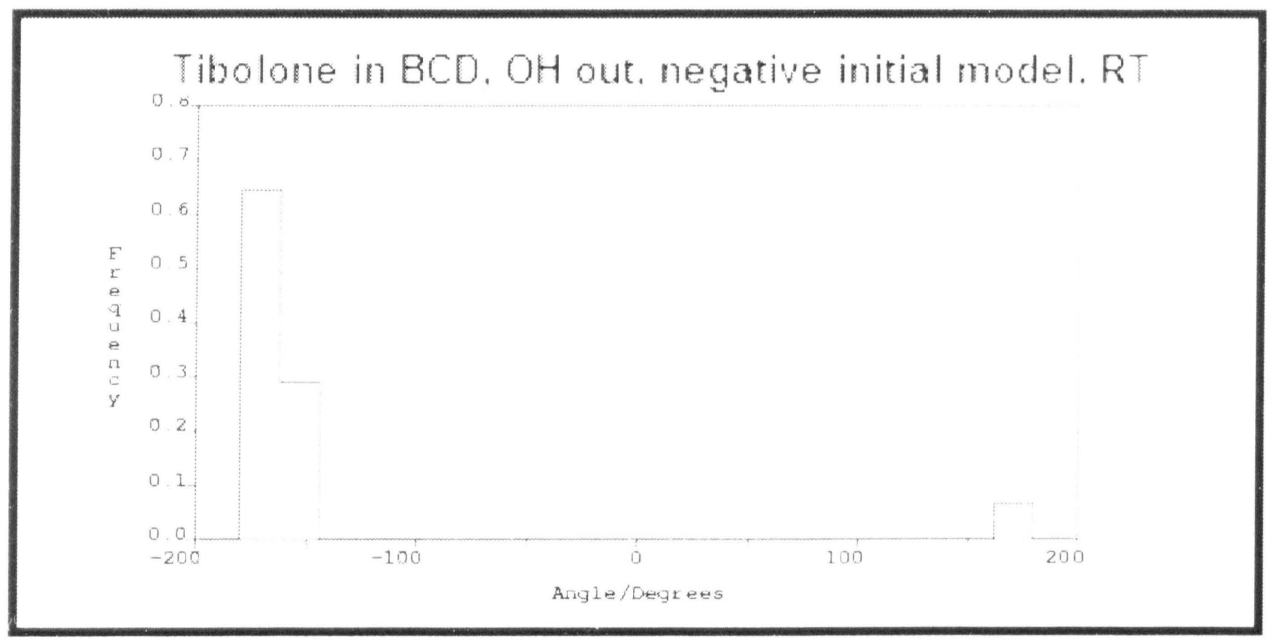

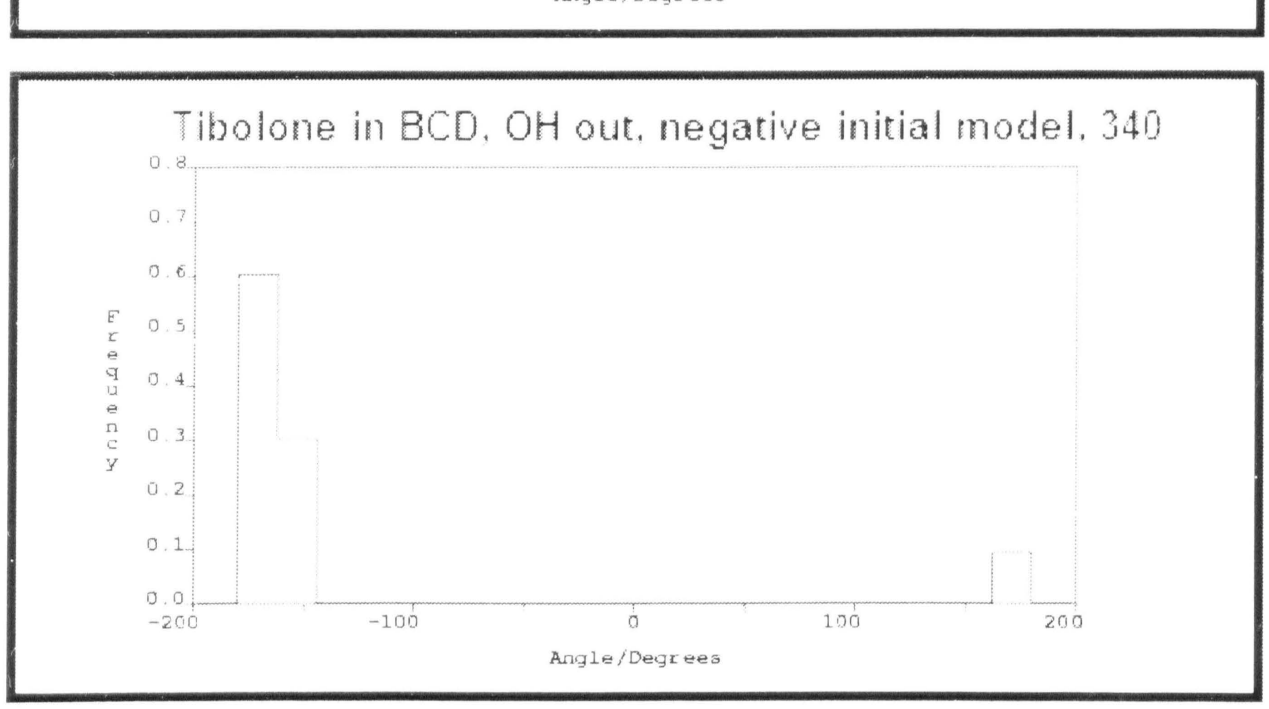

Figure 49: Statistical distribution of inversion angle in two tibolone models (positive and negative initial inversion angle) at room temperature (RT) and at temperature of 340K immersed into the β-CD cavity with OH group being outside the cavity and inversion angle being inside, made in Cerius[2]

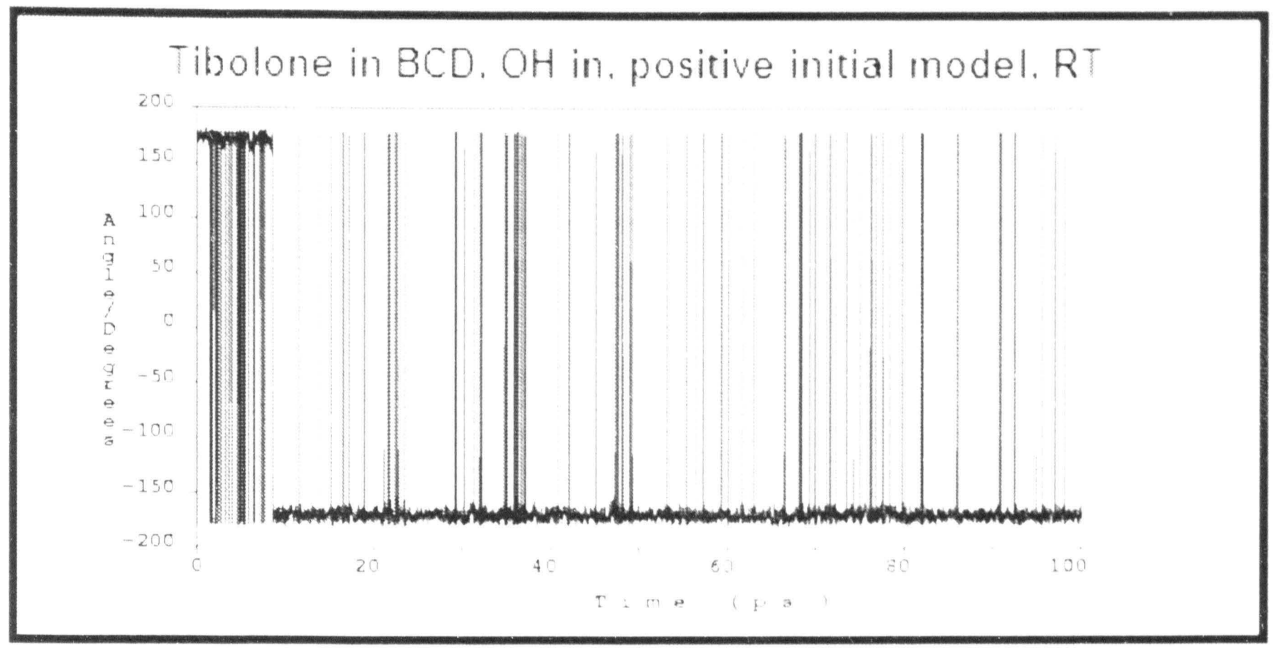

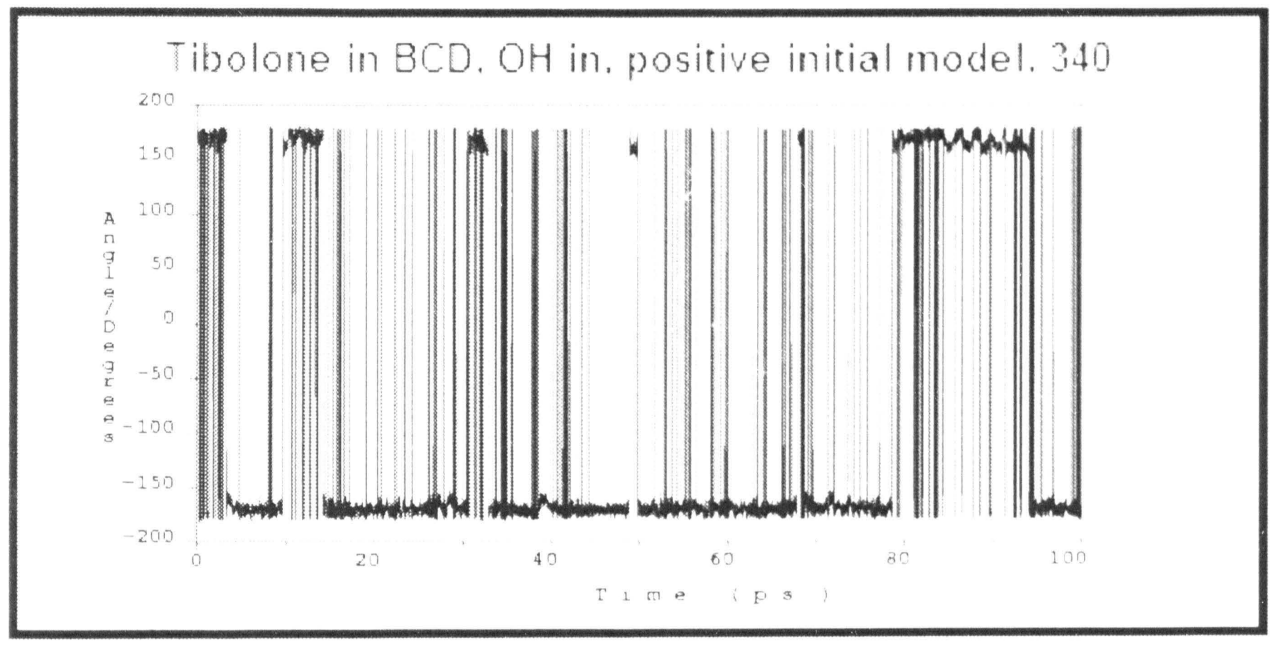

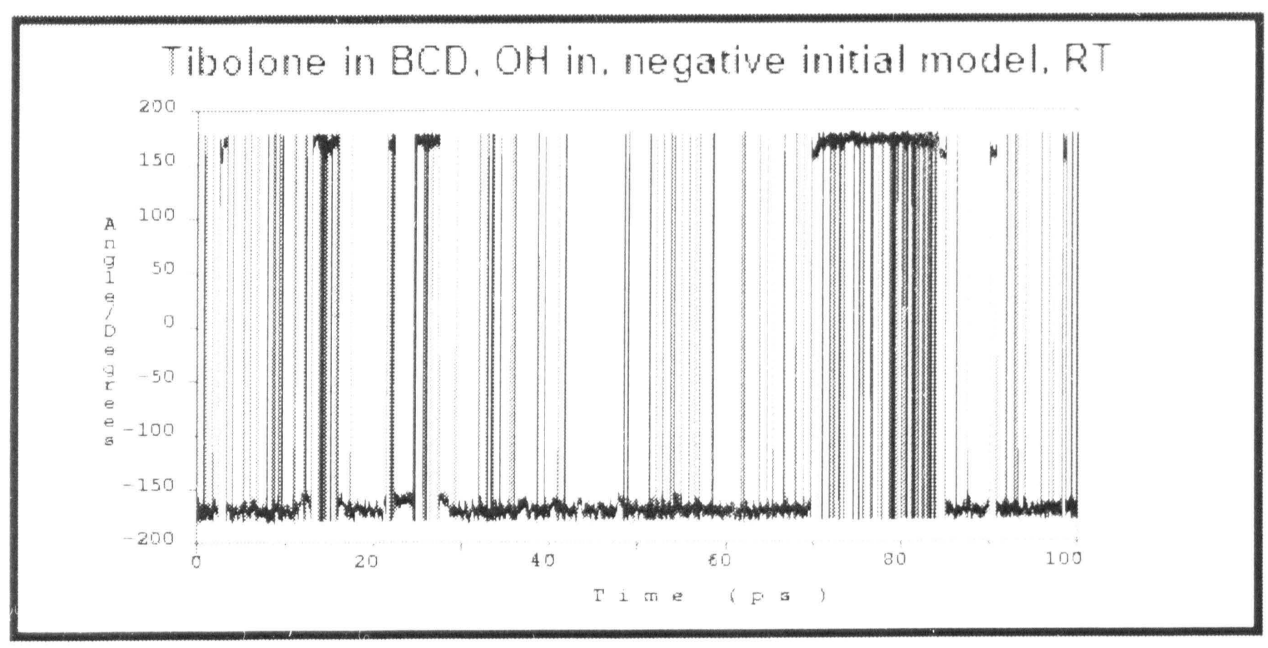

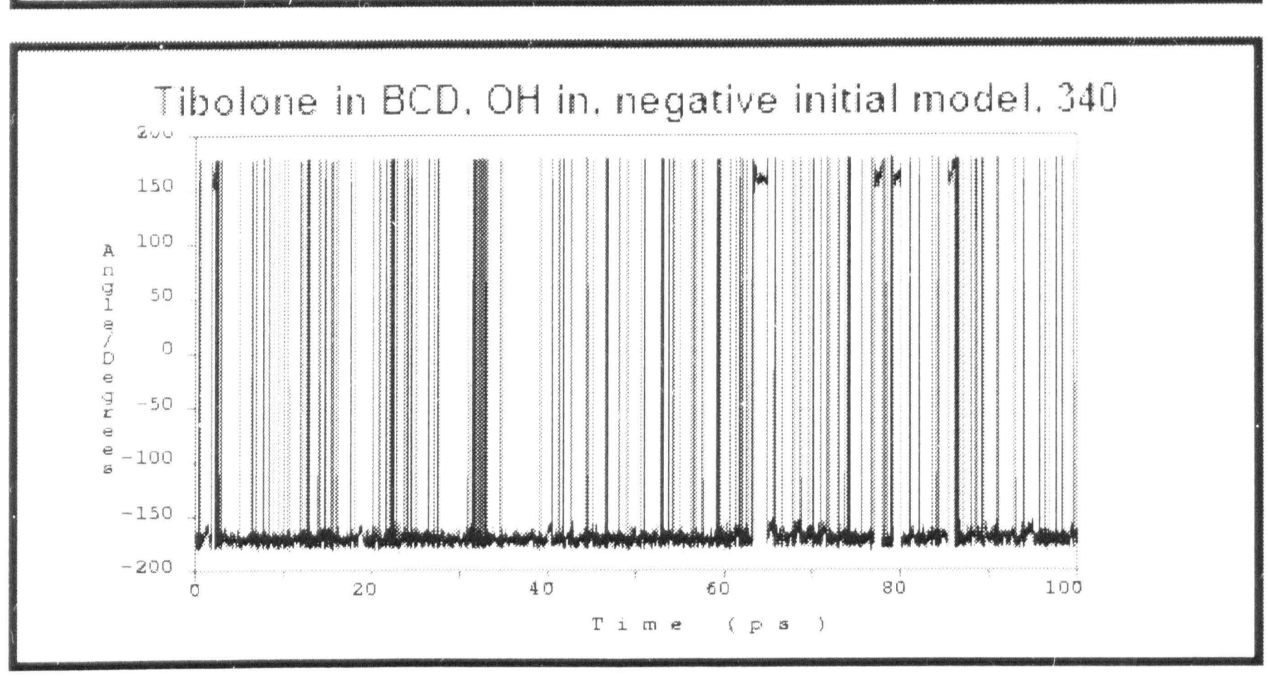

Figure 50: Conformational changes of inversion angle in two tibolone models (positive and negative initial inversion angle) at room temperature (RT) and at temperature of 340K immersed into the β-CD cavity with OH group being inside the cavity and inversion angle being outside, made in Cerius[2]

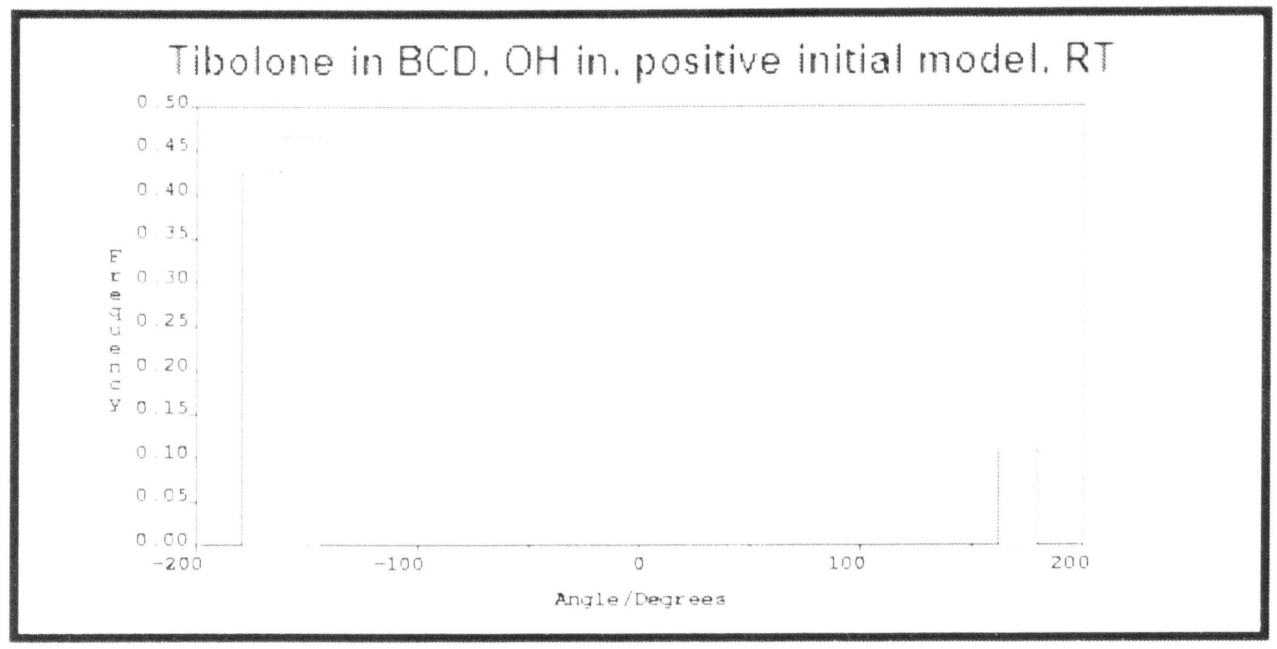

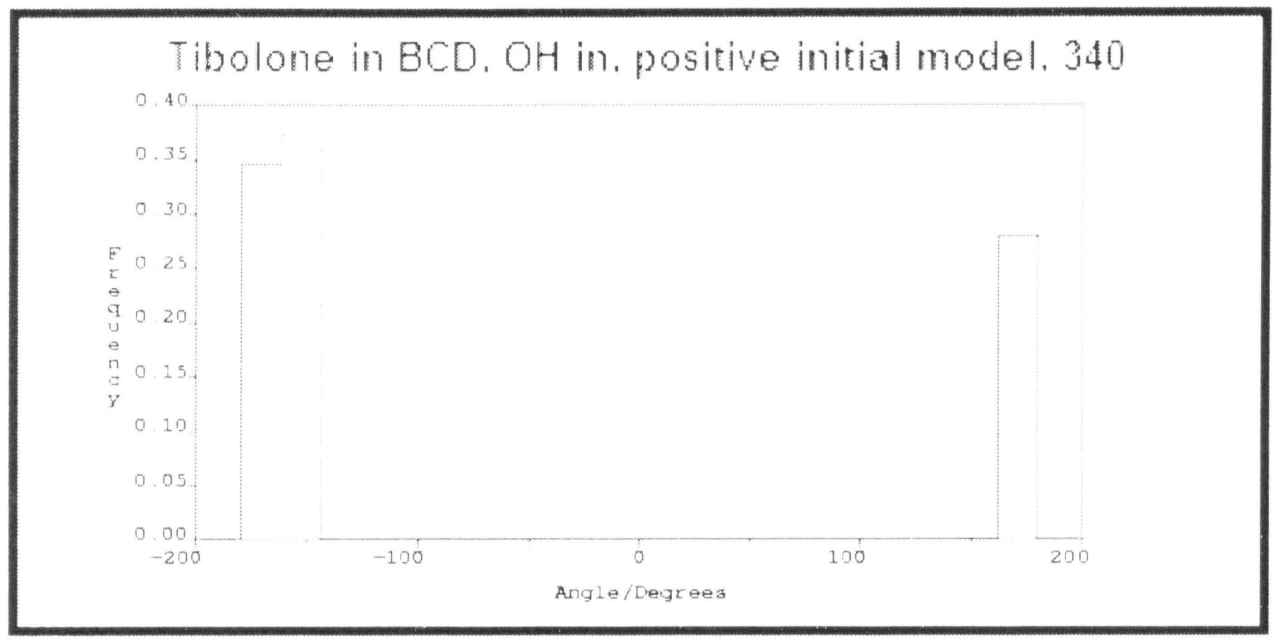

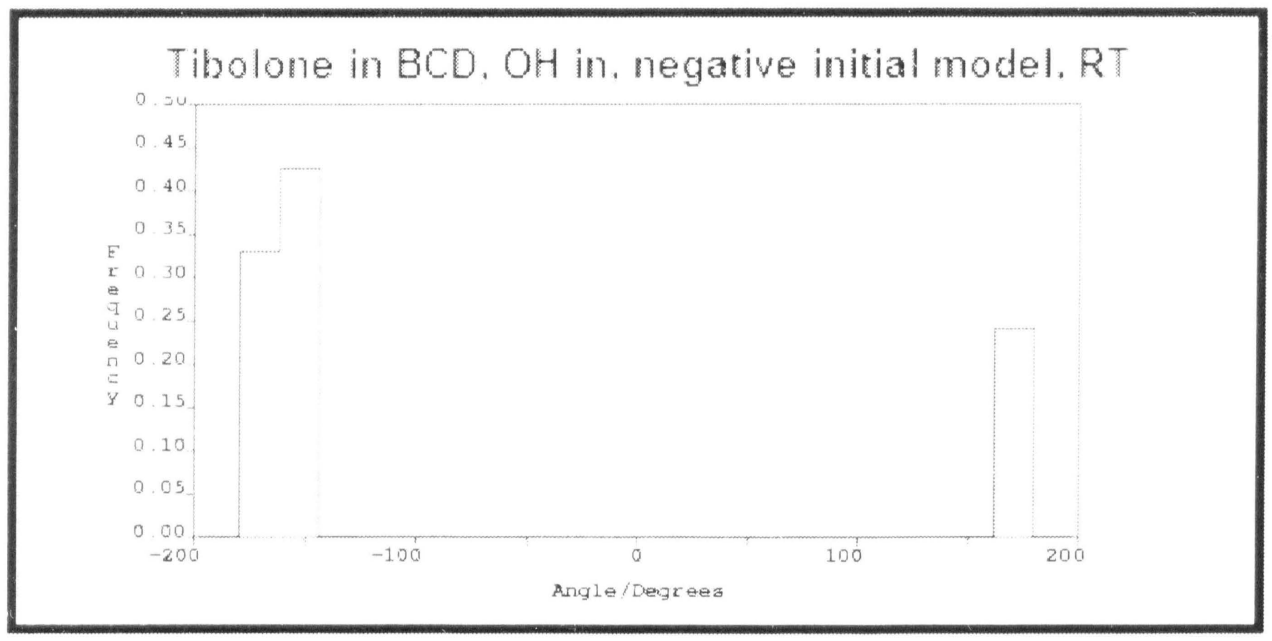

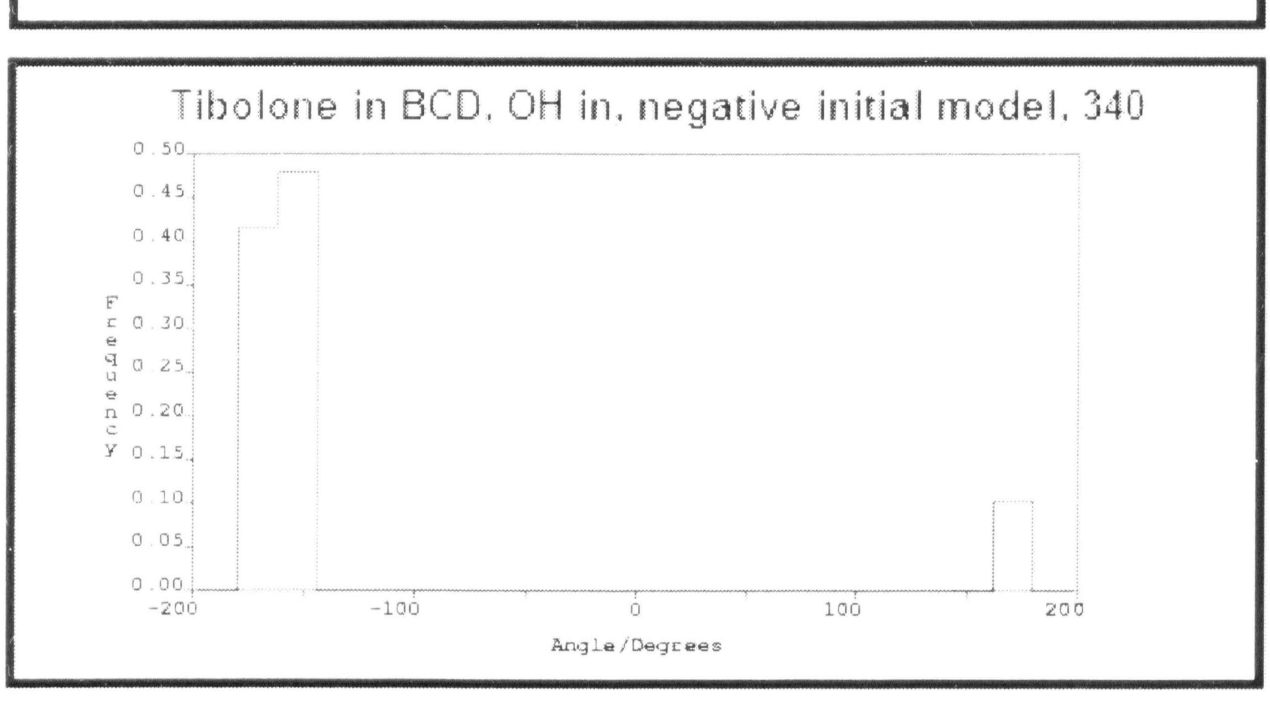

Figure 51: Statistical distribution of inversion angle in two tibolone models (positive and negative initial inversion angle) at room temperature (RT) and at temperature of 340K immersed into the β-CD cavity with OH group being inside the cavity and inversion angle being outside, made in Cerius[2]

3 CONCLUSION

The aim of the present work was to solve two main problems linked to the drug design based on the inclusion of pharmacologically active molecule tibolone into the β-cyclodextrine: (1) The ability of tibolone to form the complex and (2) the conformational stability of tibolone. Both problems have been solved using combination of modelling with available experimental data. The results are briefly summarized in following two paragraphs.

3.1 TIBOLONE-β-CD COMPLEX

Ability of tibolone to form complex with β-CD was confirmed by present study. Initial models in 1:1 ratio were created and minimum energy was found. These minimized models were then used for the concentration 1:20 (tibolone:CD). Results of modeling show that tibolone molecule is able to be inserted into the β-CD basket and to form the energetically favored tibolone-β-CD complex. For the given host-guest concentration ratio tibolone molecules do not cause any expansion of the host crystal structure, only local distortions in basket arrangement in the vicinity of the guest molecule. Results of modeling are in good agreement with the powder diffraction data.

3.2 CONFORMATIONAL BEHAVIOUR OF TIBOLONE

Using molecular dynamic simulations the conformational behaviour of tibolone and isotibolone was studied and the results of this study can be summarised as follows:

1) Isotibolone is more stable than tibolone

2) Both molecules tibolone and isotibolone exhibit certain common features in conformational behaviour. For both molecules we can observe conformational changes in inversion angle describing the departure from planarity of the terminal ring (see figure 39) and in orientation of the OH group.

3) There is difference between tibolone and isotibolone is in the frequency of conformational changes (jumps between two inversion angles)

4) Tibolone prefers the negative inversion angle conformation

5) Isotibolone can exist in both conformations with approximately the same probability

6) Complexation of tibolone with β-CD results in higher conformational stability of tibolone

Present work confirmed the complexation ability of tibolone with β-CD and stabilizing effect of complexation on the conformation of tibolone.

REFERENCES

[1] http://www.netsci.org/Science/Compchem/feature01.html

[2] www.ees.hokudai.ac.jp/.../ cyclodextrine.html

[3] http://www.hi.is/nam/lyfjafr/chem/abstracts/c8.html

[4] http://www.ispcorp.com/products/pharma/content/forwhatsnew/cyclodex/

[5] Pavla Čapková, Miroslava Fraňová: Modeling of cycldoextrine-drug complexes, *Rational Modifications of Original Drugs*, 32-37, 2004

[6] Fromming, K.-H. and J. Szejtli: Cyclodextrins in pharmacy, Kluwer Academic Publishers, 1993

[7] Wolfram Saenger and Thomas Steiner: Cyclodextrine Inclusion Complexes: Host-Guest Interactions and Hydrogen-Bonding Networks, *Acta Cryst.* A**54**, 798-805, 1998

[8] www1.elsevier.com/.../ eccc3/paper60/welcome.html

[9] http://www.medscape.com/content/1999/00/41/79/417974/art-pharm1905.stev.fig1.gif

[10] http://www.aisonschem.com/beta-cyclodextrine.htm

[11] Kloosterboer HJ: Die Rolle der Sulfatasehemmung und andere Wirkungen von Tibolon auf die Brust, Journal für Menopause 2003; 10 (Sonderheft 3): 2-8 (Ausgabe fürÖsterreich)

[12] Martin Negwer: Organic-chemical drugs and their synonyms, Akademie Verlag, 1994

[13] http://www.nos.org.uk/InfoSheets/TIBOLONE.pdf

[14] Peter Comba, Trevor W. Hambley: Molecular Modeling of Inorganic Compounds, Wiley-VCH Verlag GmbH, 1995

[15] Cerius2: User Guide. Forcefield – based Simulations. Molecular Simulations Inc., San Diego, 1997

[16] Peter Entel et al.:Molecular Dynamics Simulations, *Lect. Notes Phys.* **642**, 177–206, 2004 (http://www.thp.uni-duisburg.de/Paper/entel/entel-heraeus-springer-2004.pdf)

[17] Rappé, Goddard: Charge equilibration for molecular dynamics simulations, *J. Phys. Chem*, 95, 3358-3363, 1991

[18] Jana Čurdová: Diplomová práce Studium struktury a interakce lipidové membrány s fluorescenční sondou s využitím molekulárně dynamických simulací, Praha, 2004

[19] http://materials.binghamton.edu/labs/xray/xray.html

[20] http://www.mrl.ucsb.edu/mrl/centralfacilities/xray/xray-basics/Xray-basics.html

[21] http://www.geosci.ipfw.edu/xrd/techniqueinformation.html

[22] http://www-structure.llnl.gov/xray/101index.html

[23] http://www.psc.edu/science/Hauptman/Hauptman-phase.html

[24] http://www.ilpi.com/inorganic/glassware/xrd.html

[25] http://epswww.unm.edu/xrd/xrdclass/06-Diffraction-II.pdf

[26] RNDr. Václav Valvoda: Rentgenové difrakční metody, Univerzita Karlova, Praha, 1983

[27] The Cambridge Structural Database: a quarter of a million crystal structures and rising, *Acta Cryst.*, **B58**, 380-388, 2002

PUBLICATIONS

Appendix 1:

Pavla Čapková, Miroslava Fraňová: Modeling of cycldoextrine-drug complexes, *Rational Modifications of Original Drugs*, 32-37, 2004

Appendix 2:

Miroslava Fraňová: Determining the crystal structure and conformational behaviour of tibolone, its metabolites and tibolone-β-cyclodextrin (TB-b-CD) complex using molecular simulations, Pharmaceutical Sciences Fair & Exhibition, 2005

APPENDIX 1

Pavla Čapková, Miroslava Fraňová: Modeling of cycldoextrine-drug complexes, *Rational Modifications of Original Drugs*, 32-37, 2004

MODELING OF CYCLODEXTRINE-DRUG COMPLEXES

Pavla Čapková[a], Miroslava Fraňová[a], Jiří Dohnal[b] and Miroslav Kuchař[c]

[a]Faculty of Mathematics and Physics, Charles University Prague, Ke Karlovu 3, 12116 Prague 2, Czech Republic, e-mail: capkova@karlov.mff.cuni.cz,
[b]Zentiva, a.s., U kabelovny 130, 10237 Praha 10,
[c]Zentiva VUFB, a.s., U kabelovny 130, 10201 Praha 10

The preparation of inclusive complexes of bioactive compounds including drugs with cyclodextrines is one of the important tools for the modification of their pharmacokinetic profile. These complexes are very promising for the specifically targeted pharmaceutical forms influencing dramatically the lipophilicity of compounds under consideration, determining their bioavailability. The effect of mentioned complexes on the biotransformation velocity of drugs and their stability in pharmaceutical forms is also of high importance. The cyclodextrine-drug complex formation is a result of interplay of many factors like size and geometry of guest molecules, the charge distribution on the host and guest molecules, the host-guest interaction energy and the mutual relations between the host-guest and guest-guest interaction energy etc... Molecular modeling using empirical force field represents very efficient tool in design of new cyclodextrine-drug complexes, as it enables to analyze all these factors affecting the complexability, to predict the structure and to characterize the disordered crystal structures when the conventional diffraction analysis fails.

Structure of cyclodextrine inclusion complexes

Cyclodextrine (CD, Fig.1) inclusion complexes may crystallize in three different forms, depending on the nature and size of guest molecules [1,2]: (i) Herringbone-type cage (Fig.2a); (ii) Brick-type cage (Fig.2b) and (iii) Channel-type with head-to-head or head-to-tail arrangement of CD molecules (Fig.2c). In the cage-type crystal structure the cavity of each CD molecule is blocked on both sides by adjacent CD molecules. In this type of arrangement the CD molecules can be packed crosswise in a herringbone fashion (Fig.2a) or in a brick-wall fashion (Fig.2b). In the channel-type crystal structures the CD baskets are stacked in a roll so that the cavities form infinite channels [3,4]. The guest molecules are embedded into endless channels, formed by aligned cavities. This alignment can be either head-to-head or head-to-tail. In some cases, guest molecules are also found co crystallized between the CD molecules, that means guest molecules are not included, but bound by hydrogen bonding to CD hydroxyl, forming a non-inclusion „outer sphere complex". The complex formation, structure type, stability and solubility are the result of geometrical and chemical factors, which determine the host-guest complementarity. Geometry and size of the guest molecule in relation to the size of CD basket is naturally the crucial factor in the

complex formation. The α-, β- and γ-CDs with different internal cavity diameter are able to accommodate molecules of different size, (α-, β- and γ-CD has 6-, 7- and 8-membered ring). For example naphtalen is too bulky for α-CD and anthracene fits only into γ-CD. The included molecules are normally oriented in the CD basket in such a position as to achieve the maximum contact between the hydrophobic part of the guest and the apolar CD cavity. The hydrophilic part of the guest remains as far as possible at the outer face of the complex. Too small guest molecules can be statistically disordered in the cavity volume, so that it is sometimes impossible to locate them properly.

Chemical factors include the character of the host-guest interaction and mutual relation between the host-guest and guest-guest interaction energy. The inclusion of guest molecule in a CD cavity is energetically favored process, as the water molecules originally included in hydrophobic CD cavity are replaced by a less polar guest. The complex formation depends on the polarity of the guest molecule. Strongly hydrophilic molecules, strongly hydrated and ionized groups are not, or only very weakly complex able [2]. That means only molecules, which are less polar than water, can be complexed by CD.

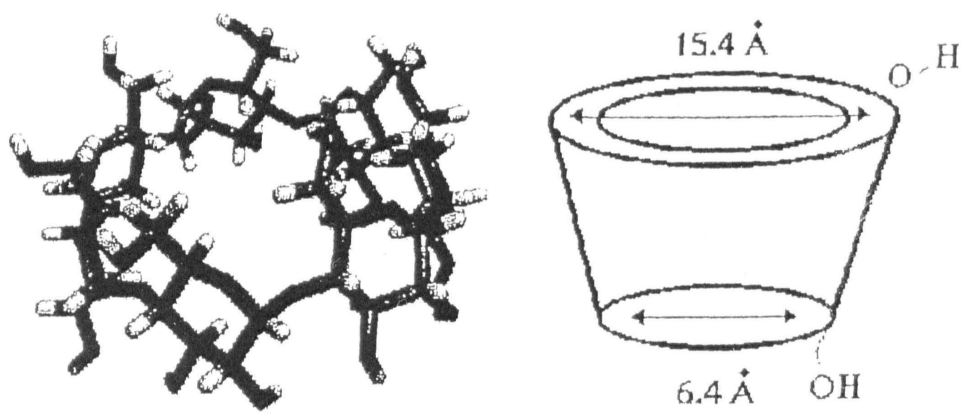

Figure 1: *One molecule of β-CD, basket shaped seven members ring.*

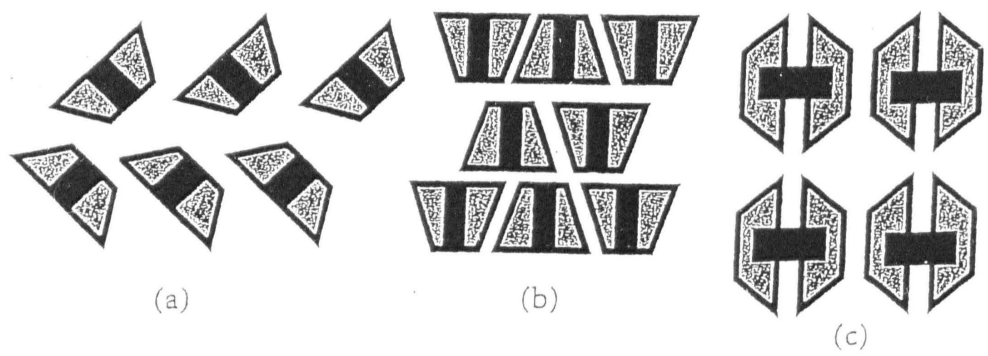

Figure 2: *Three different crystal forms, of cyclodextrine inclusion complexes (a) Herringbone-type cage; (b) Brick-type cage and (c) Channel-type with head-to-head arrangement of CD molecules.*

Consequently the host-guest interaction between the apolar CD cavity and apolar guest molecule is mainly ruled by Van der Waals forces. The effect of guest-guest interaction is important in case of an excessively strong cohesive forces between the guest molecules. The strong guest-guest interactions obstruct their separation, which is a precondition for the inclusion. Consequently the crystals with the melting point higher than 200°C cannot be complexed.

Crystal packing of inclusion complexes in case of α-CD with small guests like iodine, methanol to 1-butanol is cage-type with herringbone motif. With larger guests α-CD prefers channel type crystal structure; α-CDs complexes with small aromatic guests have slightly distorted baskets due to the benzene ring inside the cavity packed in the Brick-type cage structure. β-CD forms herringbone-type cage complexes with small guests. Larger guests are located within double baskets formed between two CD molecules. These CD dimers can be stacked either collinearly to form channel-type structure, or can be displaced sideways to different degrees. γ-CD forms herringbone cage-type structure only with water. γ-CD complexes with other guests crystallize in channel-type structures.

Modeling in structure analysis and prediction

Molecular modeling is a method of optimization of the structure and bonding geometry using minimization of the total potential energy of the crystal or molecular system. The energy of the system in molecular mechanics is described by the empirical force field. That means the total potential energy of system is expressed as the sum of bond interaction energy E_{bond} and nonbonding interaction energy $E_{nonbond}$: $E_{tot} = E_{bond} + E_{nonbond}$. The bond term describes the covalent bonding geometry for two, three and four atoms by bond stretching E_{bs}, bond angle E_{ang} and torsion angle E_{tor} deformations and departure from planarity E_{inv} (inversion terms).

$$E_{bond} = E_{bs} + E_{ang} + E_{tor} + E_{inv} \qquad (1)$$

In empirical force field all energy terms are expressed by simple analytical expressions using bond distances, bond angles and torsion angles etc..., where the force constants for individual atoms are empirical force field parameters. The nonbonding energy $E_{nonbond}$ comprises the Coulombic, Van der Waals and hydrogen bond contributions.

$$E_{nonbond} = E_{Coul} + E_{VDW} + (E_{HB}) \qquad (2)$$

Van der Waals interactions are described using Lennard-Jones potential

$$E_{VDW} = A\, r_{ij}^{-12} - B r_{ij}^{-6} \qquad (3)$$

or the exponential term:

$$E_{VDW} = A \exp(-Br_{ij}) - C r_{ij}^{-6} \quad (4)$$

Hydrogen bonds are modeled by similar way:

$$E_{HB} = Fd_{ij}^{-12} - Gd_{ij}^{-10} \quad (5)$$

Where A,B,C, are empirical parameters, d_{ij} is the distance donor-acceptor.

This simplified description of the crystal energy enables us to model large supra-molecular systems, which cannot be treated using *ab-initio* calculations. The energy terms describing the valence interactions and force field parameters may differ in various force fields and it is evident that the choice and test of the force field belong to the most important part of the modeling strategy.

Classical molecular dynamics calculates the dynamic trajectory of the system solving the classical equations of motion for a system of interacting atoms. The temperature and the distribution of atomic velocities in the system are related through the Maxwell-Boltzmann equation. The use of temperature and pressure controlled molecular dynamics enables to study temperature dependent processes and to explore the local conformational space.

Host-guest complementarity, complex formation and crystal structure

The host-guest complementarity in case of cyclodextrine inclusion complexes is mainly given by the size factors, i.e. mutual relationship between the size of the guest molecule and CD cavity. This is the first task for molecular modeling in prediction of complex formation. In order to reach the global minimum of potential energy we use the grid search strategy creating the series of initial models with systematic rotation and translation of the guest molecule in CD basket. An example of the lowest energy structure for the benzyl alcohol-β-CD inclusion complex is in the figure 3. The total host-guest interaction energy, i.e. the intermolecular interaction energy between the guest molecule - benzyl alcohol and the host

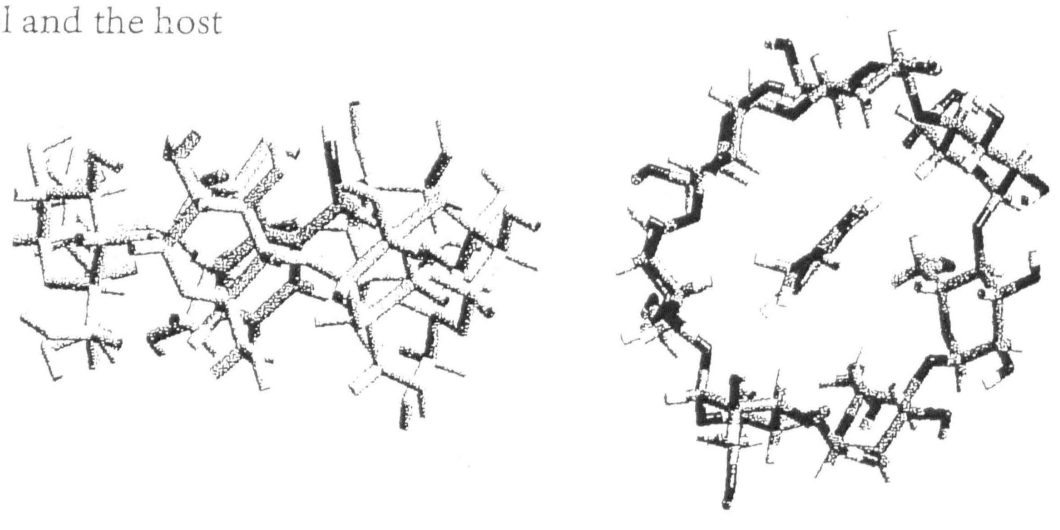

Figure 3: *The side and top view of the lowest energy structure of the benzyl alcohol-β-CD complex.*

molecule - β-CD is –19.4 kcal/mol. The Van der Waals contribution to the total host-guest interaction energy is predominant, as one can see in the table 1. The inclusion of benzyl alcohol in β-CD is energetically favored. Anyway in general the value of the host-guest interaction energy cannot be used as the universal criterion of the complex ability, as the second important factor ruling the complexation is the guest-guest interaction energy, which can prevent the guest molecules separation.

Total H-G interaction (kcal/mol)	*VDW (kcal/mol)*	*Coulombic (kcal/mol)*
-20.2	*-19.4*	*-0.8*

Table 1: *The total host-guest interaction energy and its Van der Waals (VDW) and Coulombic components for the benzyl alcohol-β-CD complex, i.e. the interaction energy between one benzyl alcohol and one β-CD basket.*

CD complexes with small guest molecules can be arranged in the same crystal structure as the original host structure of cyclodextrine. The large guest molecules and guests, which are not very deeply included in the CD basket, cause the rearrangement of the CD crystal structure. Figure 4 shows two guest molecules of different size and the two crystal structures of their CD complexes. In upper layer of the fig.4 (right corner) is the view of the crystal structure of β-CD (monoclinic, space group $P2_1$). The large guests with less favorable shape for inclusion form the dimeric structure of CD complexes (see fig. 4a lower layer).

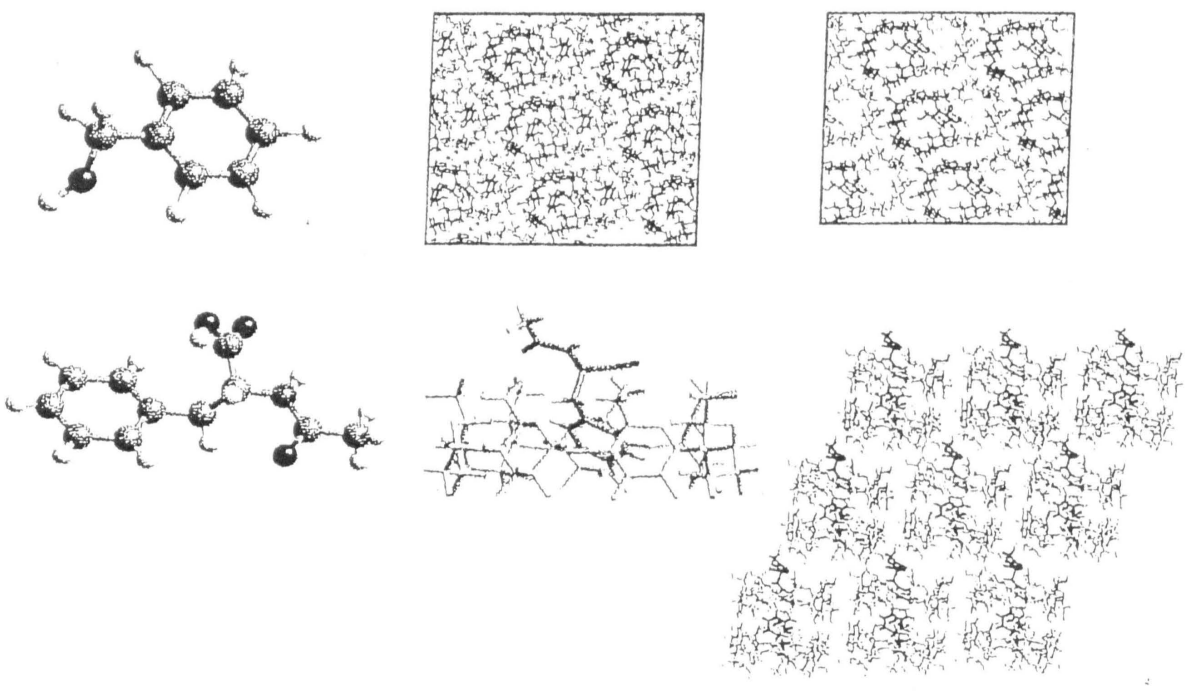

Figure 4: *Two guest molecules of different size and crystal structure of their β-CD complexes. Host structure β-CD is in the upper right corner.*

Molecular modelling is very useful tool in prediction of complexation, analyzing the sterical conditions and energy characteristics. In addition modeling is very helpful in structure analysis of CD complexes. These structures are very often more or less disordered and then the conventional diffraction analysis fails. In such a case modeling provides us with the structure model including the character and degree of disorder and with energy characteristics describing the structure stability.

It is evident that by the use of empirical force field one has to pay special attention to the modeling strategy. That includes the choice and test of the force field using a known related structure. Table 2 shows the comparison of experimental and calculated structure parameters for benzyl alcohol-β-CD. Anyway, it should be especially emphasized, that modeling strategy must be based on the available experimental data, usually the comparison of diffraction patterns and IR spectra for inclusion complex, host and guest structures.

parameter	*a (Å)*	*b(Å)*	*c(Å)*	*γ*
experiment	*15.36*	*10.10*	*21.29*	*112.8*
calculated	*15.67*	*10.38*	*21.26*	*112.7*

Table 2: *Experimental structure parameters (overtaken from databaze) and calculated using empirical force field cff 91 (from Cerius² force field library [7]) for benzyl alcohol-β-CD.*

References:

1. Saenger W., Steiner T., (1989). *Acta Cryst.* **A54,** 798-805.
2. Frömming K. H., Szejtli J., (1994). *Cyclodextrines in Pharmacy*, In *Topics in Inclusion Science*, Vol. 5, pp. 1-82.
3. Saenger W., (1984). *Inclusion compounds,* Vol. 2, edited by J.L. Atwood, J.E.D. Davies & D.D. MacNicol, pp.231-260. London: Academic Press.
4. Saenger W., (1985). *Isr. J. Chem.* **25**, 43-50.
5. Comba P., and Hambley T.W.,: *Molecular Modeling of Inorganic Compounds*, VCH, Weinheim, New York, Basel, Cambridge, Tokyo, (1995), p. 4.
6. *Cerius²* Forcefield-Based Simulations, Software Manual (1997) Molecular Simulations Inc., San Diego
7. Maple R. J., Dinur U., Hagler A.T., *Proc. Nat. Acad. Sci. USA* (1988) **85**, 5305-5354

APPENDIX 2

Miroslava Fraňová: Determining the crystal structure and conformational behaviour of tibolone, its metabolites and tibolone-β-cyclodextrin (TB-β-CD) complex using molecular simulations, Pharmaceutical Sciences Fair & Exhibition, 2005

Following abstract was admitted to the conference "Pharmaceutical Sciences Fair & Exhibition" as a short communication. The quotation of the acceptance letter is written below.

Determining the crystal structure and conformational behaviour of tibolone, its metabolites and tibolone-β-cyclodextrin (TB-β-CD) complex using molecular simulations

Franova, M[1]; Capkova, P[1]; Petrickova, H[2]; Dohnal, J[2]
[1]Charles University, Faculty of Mathematics and Physics, Prague, Czech Republic; [2]Zentiva, Prague, Czech Republic

New compound containing tibolone (TB) and β-CD in ratio 1:20 was experimentally prepared. Its structure could not be determined from X-ray diffraction pattern itself. With the help of molecular simulations we found that the new entity is TB-β-CD complex and that TB can be immersed into the β-CD cavity in two ways, OH group inside and outside the basket, and that the host-guest interaction energy is in both cases nearly the same. We used classical molecular dynamic simulations in NVT ensemble and cff91 force field to study the stability of tibolone versus isotibolone at room temperature and at temperature of 340K. Molecular dynamics showed that isotibolone is more stabile than tibolone and that tibolone prefers the conformation with negative inversion angle (angle between the bond C2-C4 and the plane defined by atoms C1, C2 and C5). Stability of inclusion complex TB-β-CD was studied for TB being immersed into the CD with OH group inside and outside the basket. Model with C2-C4 bond inside the basket (OH group outside the basket) was found to be stabile whereas the model with C2-C4 bond outside the basket was found not stable, that means jumps between two torsion angles have been observed during dynamics trajectory.

Frömming KH, Szejtli J. 1994. Cyclodextrins in pharmacy.Kluwer Academic Publishers

Cerius2 User Guide, Molecular Simulations Inc., San Diego

"Dear Dr / Professor Miroslava Franova ,

On behalf of the PharmSciFair Planning Team we are pleased to inform you that your abstract entitled:

Determining the crystal structure and conformational behaviour of tibolone, its metabolites and tibolone-<beta>-cyclodextrin (TB-<beta>-CD) complex using molecular simulations

has been accepted for a short communication presentation at the Pharmaceutical Sciences Fair & Exhibition, on June 12-17, 2005 in Nice. The abstract will be published on a CD, circulated at the PharmSciFair and on the PharmSciFair Online, two weeks prior to and two weeks after the event. In addition, some of the PharmSciFair Programme Providing Partner Societies indicated that they might make a selection of abstracts submitted under their domain for publication in their (own) scientific Journal. If your abstract would be selected for such publication, they will approach you."